

---

---

## Chapter 9: POWDER PANEL AND PROPELLANT DISCHARGE TECHNOLOGIES

---

---

William L. Grosshandler  
National Institute of Standards and  
Technology

### TABLE OF CONTENTS

9.1	Introduction.....	925
9.2	Enhanced Powder Panels.....	927
9.2.1	NGP Objectives.....	927
9.2.2	Background on Powder Panel Technology.....	928
9.2.3	Operating Principle.....	929
9.2.4	Technical Issues.....	931
9.2.5	Survey of Powder Panel Applications.....	932
9.2.6	Powder Dispersion Screening Experiments.....	935
9.2.7	Live-fire Proof-of-concept Demonstrations.....	945
9.2.8	Optimization Program.....	949
9.2.9	Live-fire Demonstration Testing of Optimized Enhanced Powder Panels.....	955
9.2.10	Mass-trade Comparison Analysis.....	968
9.2.11	Summary of Powder Panel Research Program.....	972
9.3	Solid Propellant Gas Generators”.....	974
9.3.1	Brief History.....	974
9.3.2	Operating Principles.....	975
9.3.3	Experimental Techniques.....	976
9.3.4	Results: General Behavior of Propellants.....	988
9.3.5	Results: Cooled Propellant Formulations.....	992
9.3.6	Results: Chemically Active Fire Suppressants.....	1001
9.3.7	Results: Hybrid Fire Extinguishers.....	1011
9.3.8	Summary of Solid Propellant Gas Generator Research.....	1018
9.4	References.....	1021

### 9.1 INTRODUCTION

Halon 1301 has a vapor pressure high enough to propel it from a storage bottle and through distribution piping rapidly enough to suppress even fast growing fires. Nitrogen gas is used to pressurize halon 1301 storage bottles to ensure that even at temperatures as low as -40 °C, where the halon 1301 vapor pressure has dropped considerably, the total pressure is sufficient for rapid discharge of the fire suppressing fluid.

Hydrofluorocarbon alternatives to halon 1301, such as HFC-125, are discharged in a similar manner, but because around three times the amount of agent is required to ensure the fire is extinguished, a larger

pressure vessel is needed, and the total system is considerably bulkier and heavier than the halon 1301 system.

Two technologies were explored in the Next Generation Fire Suppression Technology Program (NGP) that avoid the need for, and the attendant bulk and safety issues of, a high pressure storage vessel to operate effectively. These technologies are (1) powder panels, and (2) solid propellant gas generators. Both of these technologies have the ability to discharge fire fighting agent in less than 100 ms, which makes them suitable for protecting aircraft dry bays (enclosed spaces adjacent to a fuel cell). The solid propellant gas generator can be adapted to aircraft engine nacelles, as well.

Powder panels consist of powdered fire extinguishing agents sandwiched, unpressurized, between two rigid membranes that, as a unit, can be attached to or used in place of the skin of the aircraft confining a dry bay. The powder is released and dispersed into the dry bay when the panel is pierced by a projectile, forming an aerosol cloud sufficiently dense to prevent ignition or suppress a fire resulting from the rupture of the adjacent fuel tank. The system is entirely passive.

The powder panel designs that existed prior to the NGP were inefficient. The research conducted as part of the NGP was aimed at enhancing the powder panel in three ways:

- using more chemically active fire suppressant materials,
- enhancing the dispersion of the powder, and
- decreasing the system mass.

Solid propellant gas generators (SPGGs, alternatively referred to as SPFEs, solid propellant fire extinguishers, for the current application) contain no fluids and are at atmospheric pressure prior to activation. The propellant within a chamber is activated by an initiator and burns rapidly to produce large quantities of gases. These materials either can be dispersed directly into the volume being protected or through a manifold of piping similar to what is used for halon 1301. Prior to the advent of the NGP, the primary application for SPGGs was for automotive airbags and aircraft inflatable escape slides. As first mentioned in Chapter 2 of this book, the gas mixture is very hot upon exit from the SPGG but cools rapidly as it expands within the compartment into which it is discharged. During testing on the F-22 program, distribution lines from the generators to the nacelle would become white hot during discharge and for a brief period thereafter. In testing performed by the U.S. Navy using a “single grain” inert gas generator, the same effect of heating of the distribution line during discharge was also noted. Placing inert gas generators within a nacelle and thus eliminating the need for distribution lines previously had been considered impractical due the potential degrading affect of the nacelle operating temperature environment on the life of the solid propellant. Inconel distribution lines were demonstrated to not melt, but would still become white hot.

The focus of the NGP research was to develop upgraded SPGG technology for aircraft fire protection by finding ways (1) to reduce the temperature of the gases dispersed by the generator, and (2) to increase the suppression effectiveness of the products (including finely dispersed particulates). The latter involved changing the chemical reactants, their stoichiometry and morphology, the geometry of the containment vessel, and incorporating various additives thought to be adept at retarding ignition or at quenching the combustion process. In addition, the concept of a hybrid fire extinguisher (HFE) was studied, with a

SPGG used as a compact source of high pressure gas to propel a liquid hydrofluorocarbon or aqueous mixture.

## 9.2 ENHANCED POWDER PANELS

### 9.2.1 NGP Objectives

The combat environment for military aircraft or even a terrorist environment for civilian aircraft poses a significant fire hazard when a ballistic threat is introduced. These threats are designed to act as ignition sources upon penetration of onboard flammable fluid containers. As previous combat experience and vulnerability analyses have shown, fire is the most significant vulnerability faced by an aircraft subjected to ballistic threat impact.

One area of focus for the NGP has been improved storage and delivery of fire extinguishing agents. One such technology, the powder panel, passively stores and then delivers agent upon the impact of a ballistic projectile. Powder panels have most often been applied to the lining of aircraft dry bays to provide passive, light mass, effective fire protection against ballistic impact. Projectile penetration of the dry bay and adjacent fuel tank releases agent from the powder panel into the fire zone to inert the space before or as the adjoining fuel spills into the space and is ignited by incendiaries. The recognition of ballistic threat-induced fires as a major contributor to aircraft vulnerability and a need to avoid active halon fire extinguishing systems has led to a renewed interest in powder panels as a fire protection device.

Despite the potential for powder panels, commercial units are of roughly the same design that has existed for decades, and their limited range of effectiveness has prevented further implementation in production aircraft. In 2001, the NGP embarked on an effort to use current technology and new ideas to examine the feasibility of enhanced powder panel designs and demonstrate proofs-of-concept. This section details a two-phase effort to accomplish this work.<sup>1,2,3,i</sup>

The objective of the NGP research was to identify concepts for powder panel enhancement (relative to current capability and to halon 1301) and demonstrate their performance. The basis for this advanced protection consisted of characterization of current powder panel technology and assessment of recently developed improvements in powder panel materials and construction. The expected outcome of this work was enhanced powder panel concepts that are competitive with halon 1301 in critical parameters such as mass, volume occupied, and fire extinguishing capability, and, thus, are candidates for use in its place.

NGP research into enhanced powder panels was performed by Cyphers and co-workers at Skyward, Ltd. The Aerospace Survivability and Safety Flight (46 OG/OGM/OL-AC) was the managing laboratory. In Phase I of the work, background information was gathered on the state of current powder panels, initial concepts for enhanced powder panels were examined, and the feasibility of improved powder panel features was demonstrated. In Phase II, the examination was widened to study whether enhanced powder panels could become practical, while maintaining improved performance. Optimized powder panels were examined for their potential to meet production requirements and their benefits were examined against other fire protection alternatives. The program concluded with live fire demonstration tests of the optimized powder panels.

---

<sup>i</sup> Large portions of the text of Section 9.2, as well as all the figures, have been used from Reference 1 without further attribution. The reader should consult the original document for additional details.

### 9.2.2 Background on Powder Panel Technology

Powder panels are passive fire protection devices for discharging dry chemical agents to prevent or extinguish combat-induced fires in military vehicles. They consist of two walls, an internal rib or core structure, and a fire extinguishing agent, typically a dry chemical powder, that fills the interior space. Historically, commercial powder panels have consisted of thin walls of aluminum foil or composite sheets, with an aluminum or Nomex honeycomb core. Typical thicknesses for commercial powder panels have been reduced to just over 2.5 mm. Powder panels are typically arranged along the walls of a void area in a military vehicle (called a dry bay in an aircraft) adjacent to or on the walls of a flammable fluid container (fuel tank, fuel line, hydraulic fluid reservoir, etc.). Figure 9–1 depicts the typical arrangements of powder panels. They are typically attached directly to the wall of the flammable fluid container by an epoxy adhesive. Testing has shown this arrangement to be more effective than mounting on the walls of the dry bay separated from the fluid container.<sup>4</sup> Upon penetration by a ballistic projectile, powder panels release powder into the fire zone before or as the adjoining fuel spills into the space and is ignited by incendiaries or other ignition sources.

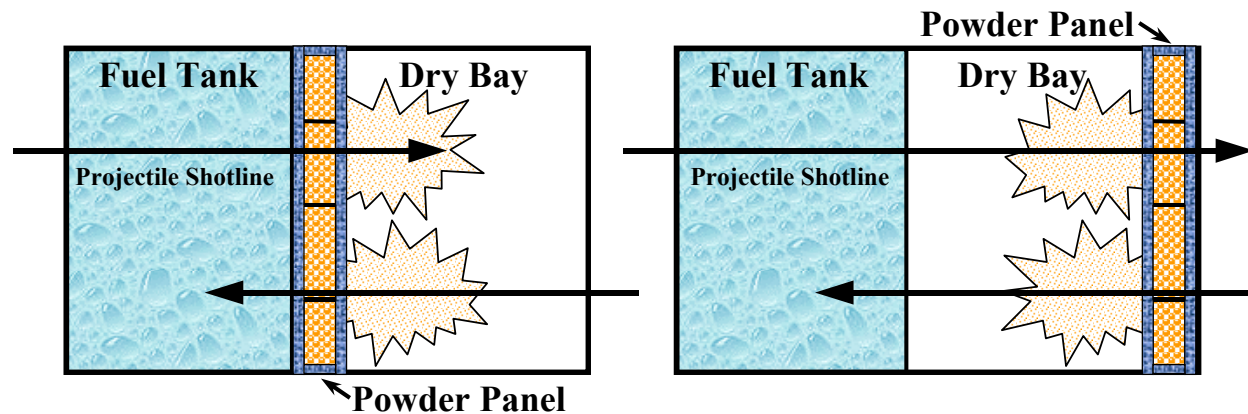


**Figure 9–1. Typical Powder Panel Arrangements.**

The design and acceptability criteria for these devices are different from conventional active fluid suppressant systems. Powder panels add mass based upon the surface area of the fuel wall/fire zone interface, as opposed to the volume of the fire zone, so the relative benefit of the panels is dependent upon the configuration of the particular bay. Typical areal densities (mass/surface area) for commercial powder panels are on the order of 1.95 kg/m<sup>2</sup> to 2.44 kg/m<sup>2</sup>.

Powder panels are not a new concept for extinguishing ballistic threat-induced fires in aircraft, as discussed previously. Powder panels around aircraft fuel tanks were first developed and used by the Royal Aircraft Establishment in England. Some U.S. military helicopters (e.g., the AH-1W/Z and the UH-1N/Y) and the V-22 aircraft have implemented powder panels in their vulnerability reduction designs. Powder panels have also been widely examined for military combat land vehicles, such as tanks and armored personnel carriers, but have been applied in limited circumstances.

Nonetheless, despite testing which has demonstrated the effectiveness of these devices, powder panels have seen limited use in aircraft for several reasons. False discharges do not occur with these passive fire protection devices, but cleanup following a fire or inadvertent damage has been a concern. This concern,

primarily in aircraft, stems from the possibility of corrosion by the contact of chemical powders with vehicle structure. As a result, current powder panels often use an inert fire extinguishing powder, such as aluminum oxide ( $\text{Al}_2\text{O}_3$ ), to prevent reaction with the metal. In military ground vehicles, wide application of powder panels has been limited due to the potential ill, albeit limited, effects on crew members or obscuration of the crew compartment upon activation. Although non-toxic agents can be used, during the period of time the powder particles are suspended in crew areas, the crew may have difficulty breathing and operational effectiveness may be limited. Several other reasons cited for their limited use overall include concerns over durability, potential adverse effects on electromechanical components and optics, their ability to protect highly cluttered areas, airflow influences, and a lack of protection from accidental fires.

Although powder panels have been examined for years, current commercial powder panel designs are in essence very similar to those that have existed for decades. However, a number of factors have renewed interest in powder panel technology. First, the banned production of halon 1301 has created a demand for new techniques to fill its role. Also, new materials, powders, and construction techniques have been developed, which may allow for improved powder panel performance, in terms of both system mass and fire extinguishing capability.

Systems that have used halon 1301 for ballistic threat-induced fire protection in fire zones eventually may require some substitute technique. Powder panel technologies are viable alternatives for some of these applications. They don't require detectors, plumbing, wiring or bottles, and they are false-discharge resistant. Current designs have limitations, particularly limited powder dispersion ability, and problems providing protection against relatively small caliber threats. As a result, most don't compare favorably against halon 1301 in trade-off studies.

Improved powder panels could expand use of this fire protection technology for additional vulnerable fire zones on our critical weapons systems. New powder panel concepts with enhanced characteristics have been proposed recently. These include frangible materials to optimize dispersion, single-piece construction technology, modular designs, pre-dosed sections, lighter mass materials, and lower cost materials. These enhanced powder panels could be used in applications as halon 1301 or other fire extinguishing system replacements, or they could replace existing powder panels with superior technology.

### 9.2.3 Operating Principle

Powder panels work through the release of fire extinguishing powder into the mixing zone of a flammable fluid and an ignition source to essentially inert the zone and prevent a fire from igniting. To assist in the discussion of powder panels and their effectiveness, it is helpful to discuss fire ignition as it relates to an onboard aircraft fire due to ballistic projectile penetration.

For any fire to initiate, the interaction of a flammable fluid, oxidant, and ignition source is required.<sup>5</sup> However, the simple mixing of these three ingredients does not ensure fluid ignition or the initiation of a sustained fire. Fire initiation by a ballistic threat is a complex phenomenon involving a process that sequentially brings together the three ingredients at the right time, in sufficient and properly proportional quantities, and with the needed intensity. The process begins when the ballistic threat penetrates the vehicle, generates an ignition source, and traverses the vehicle penetrating the fluid container, thereby

releasing fluid into the open volume of the vehicle. This open volume is referred to as a dry bay in aircraft. While each threat type is inherently different, the result is the same, i.e., deposition of thermal energy into a volume of air in front of the impact hole and the raising of the temperature of this volume. If the threat impacts a flammable fluid container within the vehicle and releases fluid, the fluid will be injected into the dry bay some distance by the threat/container impact and the container pressure. As the fluid is injected into the dry bay, it atomizes (i.e., breaks up into droplets). As the droplets penetrate into the heated air, they begin to vaporize, and the fluid vapor mixes with the surrounding air and produces a flammable fluid/air mixture. As the fluid/air mixture is heated, a chemical reaction will commence.

As the reaction proceeds, heat is lost to the surrounding air by conduction. If the rate of heat produced by the reaction exceeds the rate of heat lost, the chemical reaction will accelerate until all the oxygen (for fuel rich conditions) within this volume is consumed; a flash is seen more or less simultaneously throughout this volume as ignition occurs. If the rate of heat lost exceeds the rate of heat produced, then the temperature of the volume will begin to decrease, and the rate of reaction will decline as well. Eventually the reaction will cease and ignition will not occur. As such, ignition is simply a reaction that proceeds to consume the available flammable fluid/air mixture contained within the volume encompassed by the ignition source, resulting in a flame visible within this volume. If, after ignition occurs, sufficient oxygen and flammable fluid are available, a sustained fire may result that could lead to a loss of the aircraft.

Fire extinguishing powder introduced into this volume immediately upon impact by the ballistic projectile has the potential to reduce the probability of a fire ignition. The powder must render the fuel/air mixture nonflammable so the chemical reaction does not continue. The powder can do this in two ways. According to Finnerty et al.<sup>6</sup> (and further citations in Reference 6), it is widely believed that fire extinguishing powders can function as both energy-absorbing materials and as solid surfaces on which free radicals can be destroyed. Heat may be absorbed by the heat capacity of the solid, the heat of fusion at the melting point, the heat capacity of the liquid, heat of dissociation from breaking of chemical bonds, and heat of vaporization. These all contribute to the total energy absorbing capability (endothermicity) of the fire extinguishing powder.<sup>7</sup>

From a chemical aspect, it has been found that there is a catalytic path for the destruction of free radicals, especially O, OH and H, by certain fire extinguishing powders that contain alkali metals, such as sodium and potassium.<sup>8,9</sup> Potassium salts have been shown to be more effective than sodium salts, and iodide anions are more effective than chloride anions. Any powder that has a chemical fire extinguishing capability will also have the heat-absorbing capability.<sup>10</sup>

Testing has shown that, for a fixed total mass of powder, smaller and more numerous powder particles, through the increased surface area available, are more effective at reducing the chance of ignition than fewer, larger particles.<sup>7,11</sup> A large total surface area of the powder is important in both heat absorption and chemical interference mechanisms. The former is why even an inert material like aluminum oxide can be effective if it is sufficiently finely divided. Conversely, large particles may actually pass through the flame zone before they can reach flame temperature, further reducing their ability to absorb as much heat as an equivalent mass of finer particles.

The effectiveness of the powder panel can, therefore, be enhanced through the proper use of a fire extinguishing powder (type and particle size), and by maximizing the amount of powder released into the mixing zone consisting of the flammable fluid and the ignition source. The objective of the enhanced

powder panels is to appropriately select a powder and maximize the mass of powder released into the mixing zone.

#### 9.2.4 Technical Issues

In order to become a viable concept for combat fire protection in aircraft, two major technical attributes of powder panels needed to be addressed. These attributes, performance and practicality, are intertwined. Previous testing evaluated a number of different powder panel designs and materials and showed limited ranges of effectiveness.

One consistent factor in many of these designs was the use of a honeycomb structural material as the rib or core material. Honeycomb provides several benefits to powder panels. First, it adds structural integrity to the panel, much as honeycomb has proven valuable for structural design in aircraft construction. Honeycomb also allows for even distribution of the fire extinguishing powder throughout the panel, minimizing concerns over powder settling. It also can be constructed of very light mass materials such as Nomex or aramid fibers. The limiting factor for honeycomb has been its performance. Only cells in the direct path of projectile penetration, and perhaps those just around the penetration area, are torn and allow powder to escape.

Different faces for the powder panel have been tested, focusing on materials such as aluminum foil and several different composites. Many of these efforts have focused on durability in the aircraft environment. However, performance, as quantified through surface area removal or fracturing, has been limited. This is true despite techniques to enhance opening of the powder panel walls, such as weak or selective bonding of the panels to the core, particularly for the front or open face to the fire zone. Very thin sheets or films have also been tried to promote surface removal and allow powder to escape.

Consequently, the NGP needed to demonstrate the feasibility of completely re-designing a powder panel so that it could release a more effective amount of powder. However, production and qualification requirements levied on fire protection methods, such as powder panels, might show these designs to be impractical for aircraft applications. Therefore, additional work was required to optimize these panels for attaining potential design requirements. For example, with aircraft mass restrictions being very demanding, powder panel mass needs to be minimized before it can even be considered competitive as a fire protection solution for a particular aircraft application. This goal involves proper material selection and powder panel thickness determinations. Another key aircraft requirement is durability in the aircraft's harsh operating environment. This includes an ability to survive under extreme (both hot and cold) temperature, vibration, g-loading, and exposure to a variety of chemicals (jet fuel, hydraulic fluid, etc.). These environmental restrictions further reduce the set of materials and design concepts that can be used. Other production requirements may be related to such items as toxicity, maintainability and reliability. Thus, the problem becomes one of developing a powder panel that is competitive with other fire extinguishing technologies by releasing sufficient powder when penetrated by a ballistic projectile to prevent fire ignition, while still remaining acceptable under tightly controlled aircraft environment requirements.

### 9.2.5 Survey of Powder Panel Applications

Cyphers and co-workers began with a survey of powder panel applications in operational U.S. aircraft and investigations of previous powder panel testing. The purpose of the survey was to identify powder panel materials and designs that have been previously evaluated and those that have actually been integrated into aircraft designs. The survey included the collection of all available data; however, it focused on more recent test programs and on testing related to U.S. aircraft applications. Using this information as a baseline, it was then possible to explore potential improvements in powder panel designs.

Powder panels around aircraft fuel tanks were first developed and used by the Royal Aircraft Establishment in England.<sup>12</sup> They have also been examined widely for military combat land vehicles, such as tanks and armored personnel carriers.<sup>13,14,15,16</sup> An example of the integration of powder panels into a U.S. aircraft design is the use of these fire extinguishing devices in the V-22 Osprey. The widest use of powder panels has been in helicopters, for which a number of test programs have been conducted to evaluate powder panel applications. A significant effort was conducted, for example, to evaluate both parasitic (attached to existing structure) and structural (panels themselves function as structure) powder panels in Army AH-1S Cobra helicopters.<sup>12,17,18,19</sup> Although powder panels were never integrated into the AH-1S, they did find their way into the Navy UH-1N Huey and AH-1W Super Cobra.<sup>20</sup> These legacy aircraft are being upgraded to UH-1Y and AH-1Z configurations, both of which also will use powder panels for dry bay protection. Testing was conducted at Boeing to evaluate powder panel applications in the AH-64 Apache. This evaluation examined the use of powder panels along various fuel tank walls. Powder panels have also been evaluated recently for the RAH-66 Comanche helicopter.

The powder panel application survey indicated that no U.S. fixed wing aircraft currently employ powder panels. A number of reasons have been offered for this:

- Powder panels do not assist with accidental fires.
- Low-tech approaches are difficult to sell.
- There are concerns over accidental leakage that could lead to corrosion, durability, volume-filling capability with clutter involved, and detrimental airflow influences.

There have been powder panel test programs relating to U.S. applications extending back to at least the late 1970s.<sup>16</sup> Many of the test programs included evaluations of the fire extinguishing effectiveness of various powder panel designs and various dry powders contained within the panels.<sup>3,21,22</sup> Standard designs included the use of thin aluminum foil, Nomex, or composite panels sandwiching an aluminum or Nomex honeycomb core, which contained the fire extinguishing powder. Typical powders included aluminum oxide ( $\text{Al}_2\text{O}_3$ ), Purple K ( $\text{KHCO}_3$ ), and Monnex ( $\text{KC}_2\text{N}_2\text{H}_3\text{O}_3$ ).  $\text{Al}_2\text{O}_3$  has been extensively used in powder panel testing and is the only powder identified in U.S. aircraft applications, primarily due to its low corrosiveness compared to the other powders.<sup>5,13</sup> A summary of some previously tested powder panel materials is included in Table 9–1.

The literature review revealed some unique powder panel designs and configurations evaluated in previous testing,<sup>23,24</sup> but also more common powder panel materials and designs. Very thin aluminum or aluminum foil and composite materials have most often been evaluated for the front face or the face toward an open dry bay. Similar materials have been evaluated for the back face or the face attached to or directly adjacent to the flammable fluid container. As Table 9–1 indicates and the literature search showed, the most commonly evaluated rib structural design by far has been honeycomb. The honeycomb

has been composed of various materials, but it has most often been evaluated on its ability for even distribution of powder and for its structural rigidity.

**Table 9–1. Examples of Previously Tested Powder Panel Materials.**

Front Face	Rib Structure	Back Face	Panel Thickness (mm)	Powder
0.025 mm 8111-0 aluminum (Al) alloy foil	2024-T2 Al honeycomb	0.025 mm 8111-0 alloy Al foil	1.3	Monnex
0.10 mm Al	fiberglass	0.33 mm Al	1.8	KDKI
0.51 mm 2024-T3 Al	honeycomb	0.51 mm 2024-T3 Al	2.3	Al <sub>2</sub> O <sub>3</sub>
0.025 mm stainless steel	Al foil bags	4.06 mm 2024-T3 Al	2.5	Al <sub>2</sub> O <sub>3</sub> +10 % KI
5.1 mm titanium	Nomex	2-ply fiberglass/ epoxy	3.0	Al <sub>2</sub> O <sub>3</sub> with 1 % silicon oxide
2-ply graphite-epoxy tape	honeycomb	2-ply graphite/ epoxy tape	3.0	silicon oxide
3-ply (0/90/0) graphite epoxy		3-ply (0/90/0) graphite/epoxy	6.4	Purple K
2-ply Kevlar-epoxy cloth polyethylene		2-ply Kevlar/epoxy cloth polyethylene	9.5	potassium bicarbonate
Pro-Seal coated ballistic nylon bags		Pro-Seal coated nylon	12.7	10 % acetate in water
			25.4	

In addition to examining military-specific powder panel testing, an examination of recent powder panel work for non-ballistic applications was performed. Data were obtained for powder panel evaluations using a much wider variety of materials with potential for greater fire extinguishing effectiveness. Drawing upon data from the powder panel survey, a baseline set of materials and designs was established for examination in the first phase of this project.

The second phase of the NGP research involved an expanded survey and investigation that included the identification of aircraft using active halon systems for fire protection, particularly in areas where powder panels could be used. This research was to be used for later comparisons of potential powder panel fire protection systems with current halon systems. The expanded survey also included the identification of design issues for integrating enhanced powder panels into production aircraft and the identification of any necessary qualification testing required before implementation.

The examination of aircraft fire protection systems in the expanded survey revealed that halon systems are infrequently used in dry bay areas.<sup>25</sup> Conversely, powder panels have been demonstrated to be effective almost exclusively in these areas. Active halon fire extinguishing systems are prevalent in engine nacelles or auxiliary power unit compartments for fire protection (e.g., in the A-10, B-2, C-12, C-130, F-14, F-22, P-3 and many other aircraft) or for inerting in fuel tank ullage areas to protect against ullage explosion (e.g., in the A-6, F-16, and F-117). Powder panels have typically been evaluated in aircraft dry bay areas and have only been integrated into production aircraft in these areas (e.g., in the V-22 and AH-1W). Therefore, as a part of the cost-benefit or return-on-investment analysis presented later, a direct comparison of an existing halon fire extinguishing system with an enhanced powder panel system proved to be difficult.

There are only a few potential examples of halon fire protection systems that could provide direct comparisons for a dry bay area. Most of these examples, however, do not offer likely replacement possibilities and are not applicable across a wide range of aircraft. For example, the C-5 aircraft has a center wing leading edge dry bay which is protected by a halon fire extinguishing system. However, this

system was incorporated to protect against overheat or safety-related fires from hydraulic components, not ballistic impact. It is located above the fuselage and would be difficult to hit in most reasonable combat scenarios. Replacement with a passive powder panel fire protection system may not prove practical in this case. As in this example, some of the current halon systems are focused on protecting flammable fluid lines or electronics, which has not been a focus for integrated powder panels thus far. The C-5 has two other dry bay-type areas with halon protection, focusing on electronics protection, not flammable fluid container protection. The B-1 also has an overwing fairing protection system, meant for protection of a hydraulic line and fuel line. It is not an ideal area for comparison with powder panels, either, for the same reasons discussed for the C-5 aircraft. Data were gathered during this survey for other aircraft areas that provide a more practical application for enhanced powder panels.

Discussions were held with various aircraft manufacturers to examine production design requirements or issues, and to provide data to them, which could allow for the consideration of enhanced powder panels in design trade studies. The manufacturers included Bell Helicopter-Textron, Inc., The Boeing Company, Sikorsky Aircraft Corporation, and Lockheed Martin Corporation. The specific aircraft discussed were the V-22, RAH-66, and F-35.

Specific production aircraft requirements were considered proprietary in most cases, but general design requirements were not and are notable. Among the key design criteria often mentioned in the discussions were powder panel thickness, areal density (mass per unit area), and temperature environment. As with any other aircraft component, particularly a forward-fit component, size and mass are big factors. The powder panel must not interfere with existing equipment and cannot create a significant mass penalty. Since design values associated with specific military aircraft are part of the technical specifications for the respective aircraft, these values will not be discussed herein.

However, these values along with current commercial powder panel thicknesses and mass were used as design goals for the Phase II optimization effort. Commercial powder panels used for testing had thicknesses greater than 2.54 mm. The core was composed of a honeycomb design and the face sheets were constructed of a composite material. These panels had areal densities of around 2 kg/m<sup>2</sup>. In repeated conversations with aircraft manufacturers, the temperature range most often quoted as a potential extreme requirement for powder panels was from -40 °C to 104 °C. In many aircraft areas, continuous service temperature would not reach these extremes, but for purposes of the optimization design effort, these temperatures were considered important.

The aircraft prime contractors were also asked if enhanced powder panels would have to undergo any qualification tests such as thermal cycling, impact resistance, vibration or other durability testing, chemical resistance examinations, and moisture absorption evaluations, for example. Based upon their responses, data suggest that commercially available powder panels may have used individual material data to support such qualification, but the assembled powder panels did not appear to be subjected to many of these tests for production qualification. This is not to imply that future powder panel applications may be relieved of such requirements. Some limited production design criteria were considered for the fully assembled enhanced powder panel, such as panel thickness, areal density, and temperature environment, as mentioned above. However, resources in this program did not permit a full examination of many of these other potential production requirements.

## 9.2.6 Powder Dispersion Screening Experiments

### Experimental Setup

Phase I experimental testing was conducted at the Air Force 46<sup>th</sup> Test Wing Aerospace Survivability and Safety Flight's Aerospace Vehicle Survivability Facility (AVSF) at Wright-Patterson Air Force Base (WPAFB), Ohio. An experimental test device (dry bay/fuel tank simulator) was designed and fabricated to enable a direct comparison of powder panel materials and designs, both existing and improved concepts. Through an impact dynamics study, various characteristics critical to the fire extinguishing effectiveness of powder panels were examined. The test device shown in Figure 9–2 allowed for the experimental screening of candidate powder panels by comparing these characteristics in a highly repeatable fashion. Among the characteristics examined were panel impact dynamics, including cracking and material removal, the amount of fire extinguishing powder released into the test article, the dispersion of this powder, and the time the powder remained suspended in the dry bay.

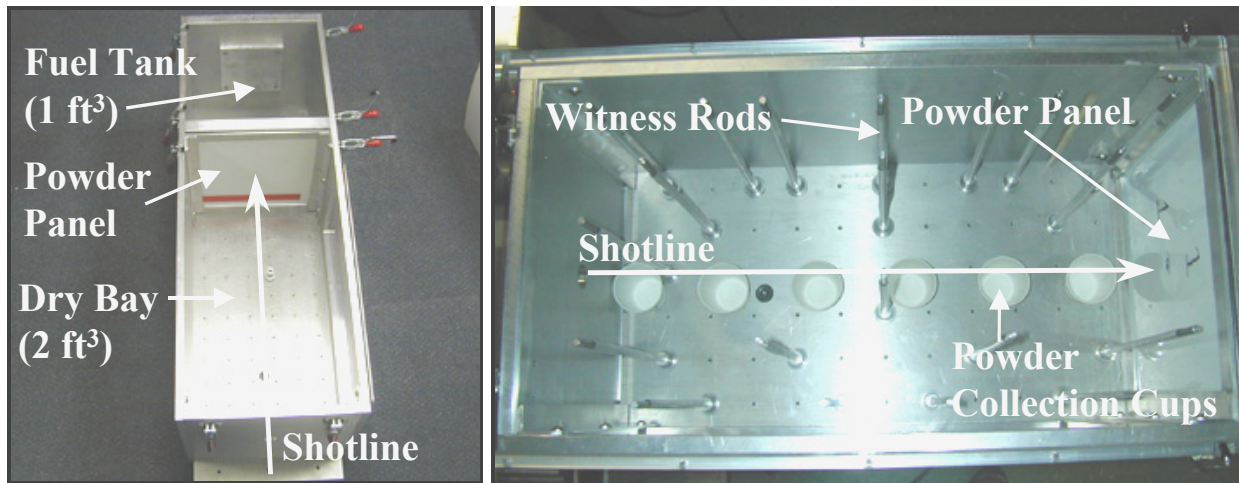


**Figure 9–2. Experimental Test Device and Powder Collection Methods.**

The test device simulates a 0.057 m<sup>3</sup> (2 ft<sup>3</sup>) aircraft dry bay and a 0.028 (1 ft<sup>3</sup>) m<sup>3</sup> fuel tank, with a dry-to-wet shotline. The fuel tank is capable of holding fluid, and the dry bay has Lexan windows to allow for visual observation of each test. Testing in Phase I did not involve fluid in the tank or airflow, to simplify the screening process. Replaceable 7075-T6 aluminum panels of 2.03 mm thickness were inserted to represent the fuel tank wall adjacent to the dry bay. In most of the tests, powder panels were secured directly in front of the fuel tank wall. This offered the worst-case scenario, without fluid in the tank, for evaluating the amount of powder released into the dry bay. The test device also allowed for the installation of powder panels directly behind the dry bay wall where the projectile enters the test article.

The test device was designed to capture powder dispersion information so a direct comparison between candidate powder panels could be made. Figure 9–2 (right side) shows the powder collection methods used in the dry bay. Witness rods are located throughout the dry bay. Plastic tubes are slid over the rods to capture released powder during each test. The rods are placed in a pattern to ensure that the powder dispersion characteristics throughout the dry bay are understood. The plastic tubes are qualitatively examined for signs of powder after each test. Powder collection cups are also located in the dry bay.

These cups are located along the shotline, where the powder concentration is most important during a ballistic projectile impact. The path of the projectile incendiary or impact flash is the location where the mixture of flammable fluid and ignition source is most likely to result in fire initiation. The collection cups were examined and weighed after each test to determine the amount of powder collected. In addition to these collection methods, each panel was weighed before and after each test to determine the amount of powder released. Panel components were also individually weighed to assist in determining the mass of powder loaded into each panel. The removed area of the front face (dry bay side) of the powder panel was also determined. This area was typically a direct correlation with the amount of powder released into the dry bay and provided another measure to compare the panels. The back face (fuel tank side) removed area of the powder panel was also determined for comparison with the front face and to examine the influence of one upon the other. Digital video was captured for each test to assist in determining characteristics related to powder suspension and dispersion.

Figure 9–3 shows the light-gas gun (compressed helium-filled bottle rated at 20.68 MPa) used to launch 0.50 caliber hard steel ball projectiles at velocities of approximately 671 m/s. The kinetic energy of these projectiles was roughly equivalent to a threat greater than a 7.62 mm armor piercing incendiary (API), but just less than a 12.7 mm API projectile.



**Figure 9–3. AVSF Range A Light-gas Gun.**

Testing during Phase I involved only one dry chemical fire extinguishing agent. The powder selected was Purple K ( $\text{KHCO}_3$ ) due to its non-toxic nature, visibility for post-test inspection, and fire extinguishing effectiveness. Corrosion from long-term exposure was not a concern in these tests.

### **Results of Powder Dispersion Screening Tests**

A total of 32 powder panel tests were conducted during the first phase of this program. These tests included components similar to those examined in previously tested powder panel programs to provide some baseline data. Among the materials tested were thin aluminum (0.41 mm thick) and aluminum foil panels. Also examined were 3.2 mm and 6.4 mm thicknesses of 5052 aluminum honeycomb, acting as the rib structure for various panels. A Nomex (aramid fiber paper) honeycomb core of 9.5 mm thickness was also tested. Table 9–2 is a compilation of all systems examined.

**Table 9–2. Phase I Powder Panel Configurations Tested.**

Test No.	Material Description	Total Thickness (mm)	Pretest Mass (g)
1	0.41 mm Al front, 5.3 mm corrugated polyallomer, 0.25 mm Al back	6.0	630
2	0.25 mm Al front, 5.2 mm corrugated polyallomer, 0.41 mm Al back	5.9	594
3	Double wall polypropylene	4.5	427
4	Double wall polycarbonate	6.6	561
5	Double wall polycarbonate, scored	6.6	704
6	1.52 mm ABS faces, 9.5 mm acrylic eggcrate rib	12.4	963
7	1.8 mm (peak) acrylic prismatic faces, 9.5 mm acrylic eggcrate rib	12.9	1038
8	2.0 mm clear acrylic faces, 9.5 mm acrylic tube ribs	13.5	1402
9	1.8 mm textured acrylic front, 1.5 mm ABS back, two ABS ribs (3.0 mm thick) at 102 mm and 203 mm	6.9	769
10	1.8 mm acrylic prismatic front, 1.5 mm ABS back, two ABS ribs (3.0 mm thick) at 102 mm and 203 mm	7.2	830
11	102 mm x 102 mm scored clear 1.5 mm acrylic front, 2.0 mm clear acrylic back, 3.2 mm polycarbonate honeycomb rib	6.9	574
12	51 mm x 51 mm scored clear acrylic, 2.0 mm clear acrylic back, 3.2 mm polycarbonate honeycomb rib	7.6	579
13	1.5 mm ABS faces, 9.5 mm Nomex rib (PN2-1/8-6.0)	13.5	1128
14	1.8 mm textured acrylic front, 2.0 mm clear acrylic back, 6.4 mm Al honeycomb rib (PAMG-XR1-8.1-1/8-002-5052)	10.5	832
15	1.5 mm ABS faces, 6.4 mm Al honeycomb rib (PAMG-XR1-8.1-1/8-00205052)	10.2	764
16	2.0 mm clear acrylic faces, 6.4 mm Al honeycomb rib (PAMG-XR1-8.1-1/8-002-5052)	10.8	942
17	1.5 mm ABS faces, 9.5 mm hollow acrylic tube ribs	13.3	1268
18	51 mm x 51 mm scored 2.03 mm clear acrylic front, 2.0 mm clear acrylic back, 3.2 mm Al honeycomb rib	7.2	638
19	0.08 mm epoxy primer sheet front, 1.5 mm ABS back, two ABS ribs (3.0 mm thick) at 102 mm and 203 mm	5.6	441
20	1.8 mm acrylic prismatic front, 1.5 mm ABS back, 1.6 mm Al corrugation	5.6	434
21	1.8 mm acrylic prismatic front, 1.5 mm ABS back, two ABS ribs (3.0 mm thick) at 102 mm and 203 mm	7.8	552
22	1.8 mm styrene prismatic front, 1.5 mm ABS back, 1.6 mm Al corrugation	5.4	328
23	1.8 mm styrene prismatic front, 1.5 mm ABS back, two ABS ribs (3.0 mm thick) at 102 mm and 203 mm	6.5	517
24	1.5 mm fiberglass polyester resin front, 1.5 mm ABS back, two ABS ribs (3.0 mm thick) at 102 mm and 203 mm	6.3	722
25	1.5 mm polyester resin front, 1.52 mm ABS back, two ABS ribs (3.0 mm thick) at 102 mm and 203 mm	6.5	746
26	Double wall polypropylene, scored, panel - on dry bay wall	4.3	402
27	2.5 mm polyester resin front, 1.5 mm ABS back, two ABS ribs (3.0 mm thick) at 102 mm and 203 mm	7.1	620
28	2.5 mm polyester resin front, 1.5 mm ABS back, two ABS ribs (3.0 mm thick) at 102 mm and 203 mm	7.4	876
29	2.5 mm epoxy resin front, 1.5mm ABS back, two ABS ribs (3.0 mm thick) at 102 mm and 203 mm	7.1	791
30	1.3 mm clear acrylic front, 1.5 mm ABS back, two ABS ribs (3.0 mm thick) at 102 mm and 203 mm	6.7	597
31	1.3 mm clear acrylic front, 1.5 mm ABS back, two ABS ribs (3.0 mm thick) at 102 mm and 203 mm, dry bay clutter	6.2	596

The majority of tests featured unique materials and designs not evaluated in previous powder panel ballistic testing. The goal was to find a front face material and powder panel design that results in significant front face material loss and powder release into the dry bay during a ballistic impact event. Thermoplastic and thermoset materials were the focus of most testing. For the front panel face (dry bay side), materials that exhibited brittle properties upon impact, but durability in handling, were of utmost interest. Front face materials evaluated included a polycarbonate (Lexan), polystyrene, polypropylene, and polymethylmethacrylate (acrylic, Plexiglas). These materials are cost-effective and easily obtainable in off-the-shelf forms. For example, off-the-shelf acrylic and polystyrene overhead fluorescent lighting panels in a variety of faceted designs were tested. These designs may enhance or degrade their brittle nature. The use of intentional surface scoring of flat acrylic panels was also examined using a couple of different scoring patterns and different techniques for implementing the scoring lines. The intent was to determine if surface scoring could be used to enhance the fracture characteristics of the material.

Thermoset polymers were also evaluated for the front face. Tested materials included two polyester resins, an epoxy resin, and a thin epoxy primer. The thin epoxy primer tested was only 0.076 mm (0.003 in.) thick. It is available commercially as a spray and requires a careful procedure for forming it and bonding it to the rib structure. The other thermoset materials are readily available in commercial form, requiring the mixing of a two-part liquid resin.

Plastics were also tested for the back face (fuel tank wall side) and in various configurations for the internal rib structure of the panel. The impetus for experimenting with the back panel was to determine if the fracture characteristics of the back panel influence the front panel in any way. For the dry bay/fuel tank configuration examined, there was a desire to inhibit the back panel hole size to reduce flammable fluid leakage, which could assist in reducing fire ignition probability in an actual production configuration.

Finally, a number of materials and designs were examined for the powder panel internal rib structure. The rib structure adds rigidity and strength to the panel, prevents settling of the powder, and must allow for easy release of as much powder as possible. Some of the panels examined in Phase I were single piece extruded materials that had front and back walls and internal channels. These panel designs were composed of polycarbonate and polypropylene. They were filled with powder in their production form, and the ends were sealed for testing.

As mentioned, honeycomb materials were also examined. One honeycomb material evaluated was 3.2 mm thick, composed of polycarbonate material, and featured a circular cell structure. The honeycomb materials maximized the amount of bonding area to the front panel, which typically inhibited front face cracking. Bonding areas could be reduced to allow for more cracking of the front face, however, the support of the honeycomb structure inhibits flexure, thereby working against crack propagation.

Several other rib designs were conceived to enhance powder release and yet prevent the settling of powder that might reduce its effectiveness to impacts in certain areas. One design included sections of hollow acrylic tubing aligned horizontally and spaced at vertical distances of one inch or less. Both the tubes and the spaces between the tubes were filled with powder to ensure total coverage to threat impact. This rib design provided significant panel stiffness due to the amount of bonding surface area and seemed to provide leverage for sections of the front face to flex and break out. Another design concept was to use strips of solid plastic oriented horizontally in a fashion similar to the tubes. In these trials, the width of the solid strips was minimized since powder would not be present in these locations during a projectile

impact. Tests were conducted with the number of these ribs minimized, the spacing maximized, and the overall panel thickness minimized. These panels were relatively stiff due to the strength of the panel face-to-rib bonds, but allowed for significant flexing of the front face due to the rib spacing. This rib arrangement required several tradeoffs. Ribs that formed channels too far apart allowed powder settling or bulging of the face sheets, but allowed for flexure of the front face during impact, which optimized cracking. Rib channels that were too close together prevented powder settling, but were more prone to function like honeycomb and provide too much support to the front face, reducing the likelihood of significant cracking. In these rib arrangements, powder along the length of the panel could be released from all open channels, which afforded greater performance than a honeycomb design. In a honeycomb design, only the cells penetrated or torn around the perimeter of the impact will release powder, unless significant cracking or area is removed from the front face.

A corrugated aluminum foil with 1.6 mm peak-to-peak height was also examined in some tests. The metal did not show a propensity to break up in these tests, so the front face would need to break up and separate for the panel to be effective. Some of the benefits of this design are similar to the channel design; however, the combination of metal and plastic in these trials may have some operational environment drawbacks, such as significantly different coefficients of thermal expansion. This design, the acrylic tube design, and variations of the horizontal plastic strip design allowed for filling of the powder panel after the panel was nearly assembled. Only the one edge had to be sealed after filling. This design variation could offer some improvement for assembly.

Phase I testing was able to identify novel powder panel designs with enhanced performance over more standard design concepts. Table 9–3 lists some of the more novel and effective designs, while Table 9–4 lists some designs that feature more baseline design concepts and less effective performance.

**Table 9–3. More Effective Powder Panel Designs in Experimental Testing.**

Test No.	Material Description	Thickness (mm)	Panel Mass (g)	Powder Release (g)	% Powder Released	Front Face Area Removed (cm <sup>2</sup> )
8	2.03 mm clear acrylic faces, 9.53 mm acrylic tube ribs	13.5	1402	48	6	32
9	1.78 mm cracked ice acrylic front, 1.52 mm ABS back, two ABS ribs (3.05 mm thick)	6.9	769	23	5	18
12	2.03 mm (50.8 mm x 50.8 mm scored) clear acrylic, 2.03 mm clear acrylic back, 3.18 mm polycarbonate honeycomb rib	7.6	579	9	5	23
21	1.78 mm acrylic prismatic front, 1.52 mm ABS back, two ABS ribs (3.05 mm thick)	7.8	552	30	13	20
23	1.78 mm styrene prismatic front, 1.52 mm ABS back, two ABS ribs (3.05 mm thick)	6.5	517	28	13	26
27	2.49 mm polyester resin front, 1.52 mm ABS back, two ABS ribs (3.05 mm thick)	7.1	620	8	4	25
28	2.49 mm polyester resin front, 1.52 mm ABS back, two ABS ribs (3.05 mm thick)	7.4	876	83	18	81

**Table 9–4. Less Effective Powder Panel Designs in Experimental Testing.**

Test No.	Material Description	Thickness (mm)	Panel Mass (g)	Powder Release (g)	% Powder Released	Front Face Area Removed (cm <sup>2</sup> )
1	0.41 mm Al front, 5.3 mm polyethylene corrugated rib, 0.25 mm Al foil back	6.0	630	0.6	0.2	1
2	0.25 mm Al foil front, 5.2 mm polyethylene corrugated rib, 0.41 mm Al back	5.9	594	0.04	0.01	1
13	1.5 mm ABS faces, 9.5 mm aramid rib	13.5	1128	1.5	0.2	1
14	1.8 mm textured acrylic front, 2.0 mm clear acrylic back, 6.4 mm Al honeycomb rib	10.5	832	1	0.2	1
15	1.5 mm ABS faces, 6.4 mm Al honeycomb rib	10.2	764	1	0.2	1
16	2.0 mm clear acrylic faces, 6.4 mm Al honeycomb rib	10.8	942	3	0.6	2
18	2.0 mm (5.1 cm x 5.1 cm scored) clear acrylic front, 2.0 mm clear acrylic back, 3.2 mm Al honeycomb rib	7.2	638	2	0.8	10

The tables indicate the mass of each powder panel, which were all about 302 mm square. Total powder-filled mass for panels tested in the first year of testing ranged from 428 g to 1,400 g. Most of the mass difference is due to varying thicknesses of the panels, with the mass of the powder contributing significantly because of increased panel internal volume. By contrast, commercial panels obtained during the NGP weighed between 175 g and 189 g for a similar size. Obviously, this was one design feature requiring optimization in Phase II testing.

Some measures of effectiveness are also noted in Table 9–3 and Table 9–4, including powder release or loss as a result of the ballistic test, percentage of the powder released, and the front face area removed. The estimate of the powder release is determined by comparing the panel mass before and after each test and weighing/estimating panel material lost. In cases where the panel was not effective at dispersing the powder, the hole on both faces of the panel may have been virtually the same size as the projectile (12.7 mm diameter). In other cases, a significant amount of the front face material may have been lost (Figure 9–4). Obviously, in these cases, a significant amount of powder was also released from the panel. The amount of powder released during testing varied from a fraction of a gram in some of the more standard designs to over 100 g.

A review of the Phase I test data indicated a wide disparity in the reaction of the panels. In some tests, the powder release was negligible, i.e., no powder was detected on the witness rods and no powder deposited in the cups. In these ineffective powder panel tests, more powder is actually observed exiting the back of the panel, along with the projectile, versus entering the dry bay. In other tests (Figure 9–5), the cloud of powder in the dry bay engulfed the entire dry bay and remained for a matter of minutes. Many tests resulted in some minute residue in the cups that was more likely spall from the powder panel front face and/or ribs, rather than the powder. In tests of effective powder panel concepts, powder was observed on all the witness rods and measurable powder mass was observed in all six cups. The amount of powder deposited in the collection cups varied during testing from no trace to over seven grams by mass.



**Figure 9–4. Test Example of Significant Panel Fracture and Material Loss.**

Typically, 0.05 g or less was captured in any single cup, with the highest concentration of the powder being closest to the powder panel, as expected. Twenty different witness rods were placed throughout the dry bay and visible powder was noticed in more effective tests on all of the witness rods. To further verify the dispersion of the powder for effective designs, several panels were tested with dry bay clutter and powder was still observed on all witness rods, even those in isolated areas.

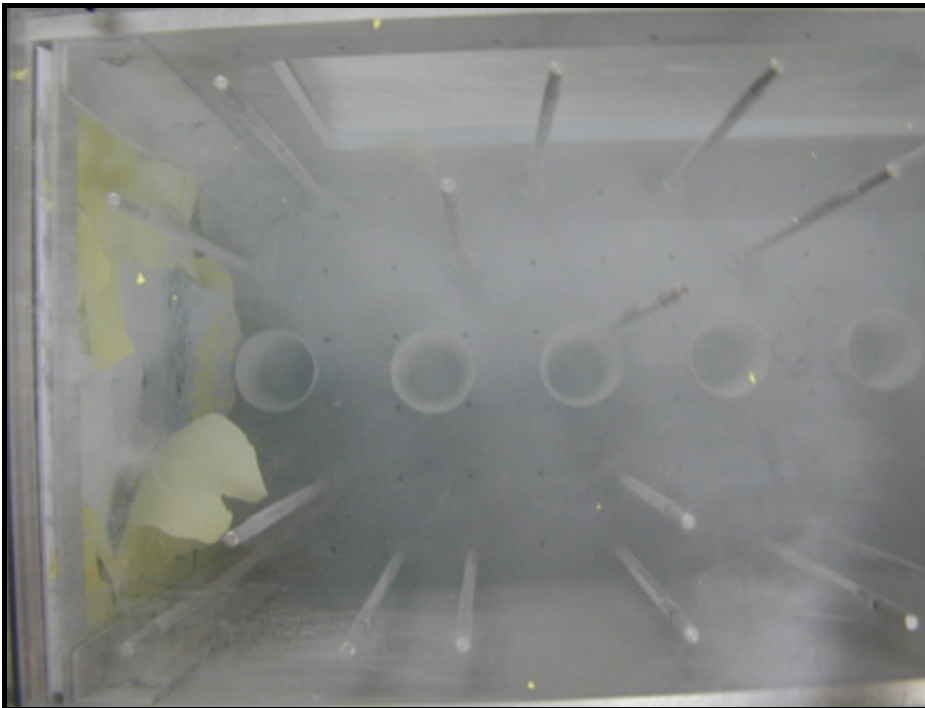


**Figure 9–5. Test Example of Effective Powder Release and Dispersion.**

The most promising of the new powder panel designs examined in this research offer the potential to be competitive with halon 1301 in a wider variety of dry bay designs. In one of these cases (epoxy primer front face), nearly 50 % of the front face area was removed, almost 60 % of the powder was released, and the powder remained suspended throughout the dry bay for over four minutes. This occurred despite the fact that this was one of the thinnest panels tested. This compares with testing of other powder panel designs integrated into operational aircraft, where the powder disperses only along the shotline, dissipates in tenths of a second, and the amount of dispersed powder was limited to the region of projectile penetration (approximate powder release of a few percent).<sup>26</sup>

Figure 9–6 and Figure 9–7 show major performance benefits achievable with some of the enhanced design concepts listed in Table 9–3 (by test number) over more standard powder panel designs (Table 9–4). Results indicated the powder panel front face area removed could be increased by 15 to 20 times over more standard designs (Figure 9–6). Testing also revealed the amount of powder released into a dry bay could be increased 5 to 10 times with an enhanced powder panel design (Figure 9–7). Testing also indicated that powder dispersion could be enhanced, even with dry bay clutter, ensuring the prevention of fire ignition over a wider area (Figure 9-8). In this figure, the number of witness rods with detectable powder residue is indicated for each test. Effective designs resulted in powder being suspended in the dry bay for much longer periods of time than standard powder panels (as much as four minutes in one test compared to one second or less). Finally, the design and fabrication effort revealed enhanced powder panels afforded greater design flexibility, which can be utilized to target mass, durability, and other application-specific design goals. These findings revealed that new powder panel concepts could significantly enhance the fire extinguishing effectiveness of this vulnerability reduction method, thereby demonstrating the feasibility of enhanced powder panels.

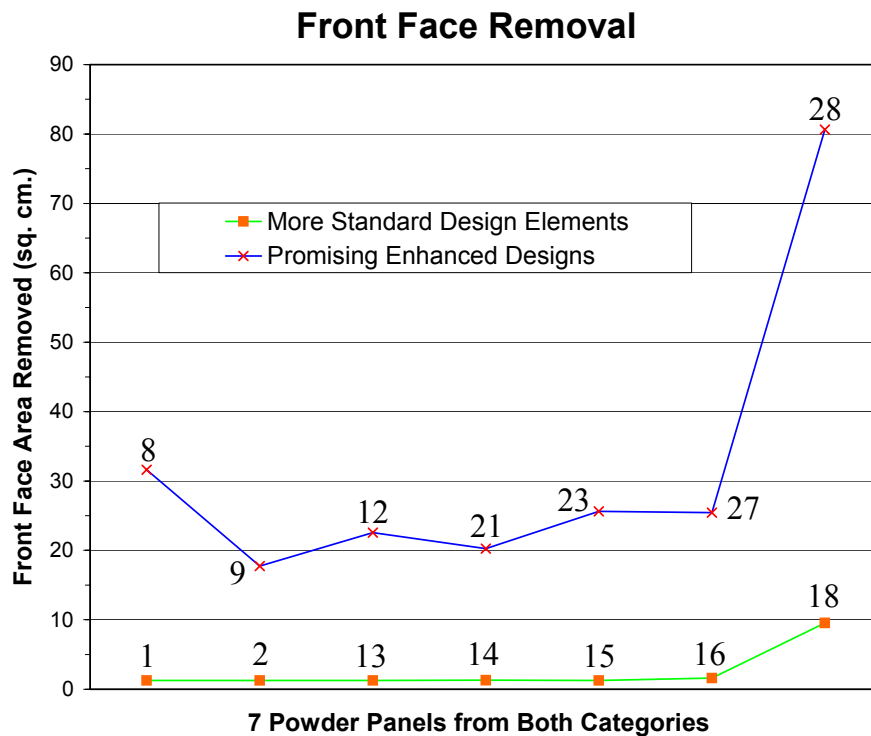


**Figure 9–6. Effect on Powder Panel Fracture Area of Standard Design Features and Enhanced Designs.**

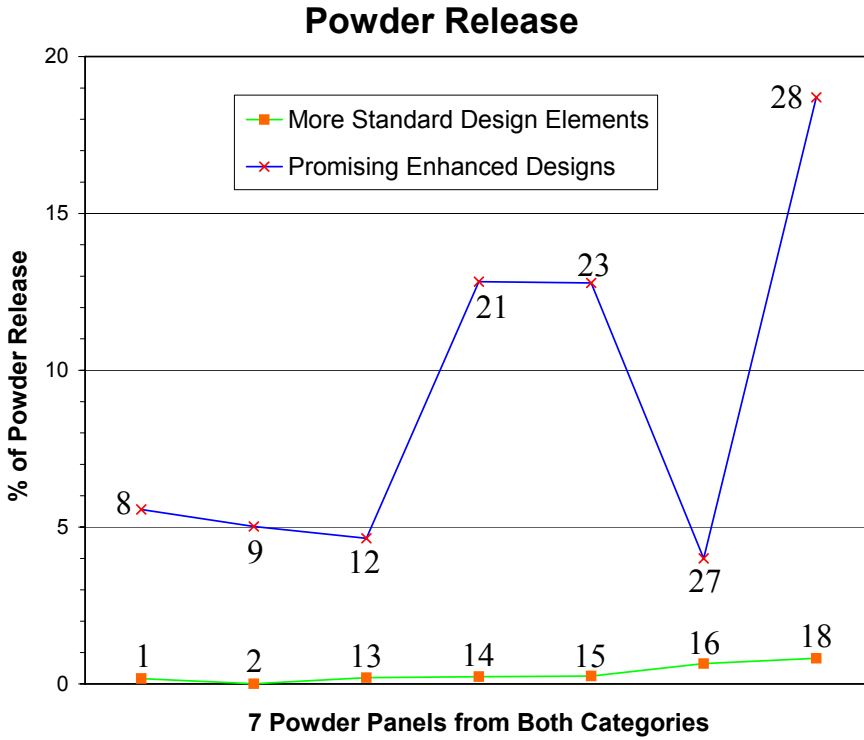


**Figure 9–7. Effect on Powder Delivery of Standard Design Features and Enhanced Designs.**

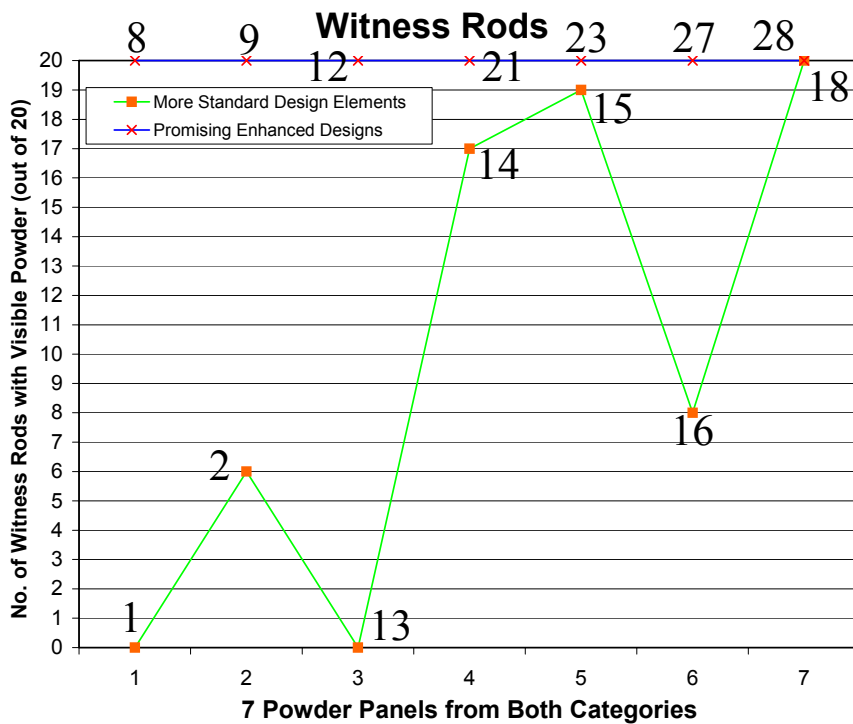


**Figure 9–8. Effect on Powder Dispersion of Standard Design Features and Enhanced Designs.**

Experimental observations indicate, as predicted, that the front face material properties are of utmost importance. More brittle materials outperformed ductile materials (that resist fracturing) by releasing more powder into the dry bay. The projectile seemed to melt its way through polycarbonate and

polypropylene materials, and even some polystyrene materials, resulting in little or no powder released into the dry bay. Acrylic front face panels and faceted acrylic and styrene materials reacted in a much more brittle nature, resulting in lost material or cracking that more effectively released powder into the dry bay. One acrylic panel with a prismatic square pattern actually did not perform very well. It appears that the pattern on the panel inhibited crack growth. Mixed results were found during testing of scored acrylic panels. Some cracking seemed to follow scoring lines in the vicinity of the impact that may have contributed to more material loss. However, comparisons between 5.1 cm and 10.2 cm scoring patterns showed that cracks emanating from the hole area, created directly by the projectile impact, were actually prevented from growing longer, i.e., scoring lines acted as crack stoppers. With appropriate scoring designs, though, it appears crack growth optimization techniques could be used to enhance performance.

A strong synergism was found between the rib structure and the front face. Increasing the bond surface area between the front face and ribs inhibited powder dispersion for the designs tested. Results indicated that standard honeycomb ribs resisted greater front face cracking because of the increased number of bond sites. Experiments on bonding honeycomb materials to the front face in a reduced number of selected areas, such as the panel perimeter, proved effective for polycarbonate honeycomb, but not necessarily for the aluminum honeycomb. It was reasonable to conclude from the testing, weaker and fewer bonding sites would allow both designs to function more effectively, as previous work has shown. Multiple explanations were plausible for the more effective polycarbonate tests. It is probable there was a contribution from the more brittle properties of the polycarbonate, which did fracture in some locations, and the design of the aluminum honeycomb likely distributed the impact energy over a greater surface area without allowing critical flexure of the front face. Design concepts using channels or horizontal ribs proved to be associated with the most effective powder panels, particularly when a more frangible front face was used. Channel designs allowed more powder to be released from the impact location than more segmented or cellular designs. Tradeoffs would be necessary for these designs between rib spacing and powder loading, as sufficient powder must be available at all potential impact sites, but more powder translates to greater mass. Testing indicated three-piece powder panel designs outperformed easy-to-assemble double-wall extrusion designs, as built-in rib channels inhibited cracking.

Variation in the powder panel back face had much less effect on powder panel performance than the front face or rib design. A number of tests involved less brittle ABS material for the back face, since it is postulated that a smaller hole in the back face may actually mitigate the chance of a dry bay fire by reducing fuel leakage and confining it to an area along which most of the powder is released. This would provide a second means to increase powder panel effectiveness. The first being the use of a more brittle front face to maximize fire extinguishing powder release, while the flammable fluid leakage is minimized. Experimental testing did reveal that the front face of the powder panel can be designed to fracture and release large amounts of powder, while minimizing the damage to the panel back face. Phase I testing did not involve a fluid-filled tank, thereby eliminating hydrodynamic ram pressures on the fuel tank wall and reducing the chance of damage to the back face. In the tests involving ABS, the damage sustained by the back face was a hole just larger than the diameter of the 12.7 mm diameter ball projectile.

## 9.2.7 Live-fire Proof-of-concept Demonstrations

### China Lake Testing Facilities

Following Phase I experimental testing, Skyward, Ltd. was afforded the opportunity to participate in several live fire demonstration tests of enhanced powder panels. These proof-of-concept tests were conducted in two different test series simulating aircraft dry bays and involving the potential ignition of a fuel fire. These tests provided Skyward with an opportunity to select some of the more effective enhanced powder panel design features identified in Phase I, perform some quick optimization, add some unique design features not previously evaluated, and perform live fire testing, all in advance of the initiation of Phase II. The promising results of these demonstration tests provided a leap forward for the initiation of Phase II.

#### *JTCG/AS Demonstration Testing*

The ability of enhanced powder panels to prevent fire ignition was first demonstrated in a Joint Technical Coordinating Group on Aircraft Survivability (JTCG/AS), since renamed Joint Aircraft Survivability Program Office (JASPO), test program examining reactive powder panel concepts, which is a method of using a reactive energetic backing with any powder panel design to enhance powder delivery effectiveness.<sup>27</sup> These tests were conducted at the Naval Air Warfare Center-Weapons Division Weapons Survivability Laboratory in China Lake, California. Four tests of enhanced powder panels without reactive backing were conducted. These tests involved the firing of 12.7 mm API projectiles into a dry bay/fuel tank simulator containing JP-8 fuel. Projectiles were fired at approximately 757 m/s at a 0° angle into the dry bay, impacting an aluminum striker plate, which was separated from the powder panel/fuel tank by approximately 0.30 m. The projectiles then continued through the powder panel, penetrating the fuel tank and releasing JP-8 fuel. A 0.46 m wide x 0.61 m high x 1.22 m long dry bay (right side of Figure 9–9) was connected to a 1.22 m x 1.22 m x 1.22 m fuel tank (left side of Figure 9–9).

A 3.18 mm thick 2024-T3 simulated fuel tank bulkhead was positioned on the front or initial impact side of the fuel tank. The powder panel was attached to this removable bulkhead panel with a 2-part epoxy adhesive. Tests were also conducted with commercial powder panels in this test series to provide a basis of comparison with the enhanced powder panel tests, as well as to tests with no protection.

#### *FAA Demonstration Testing*

A second demonstration test series of an enhanced powder panel was conducted in a Federal Aviation Administration (FAA) program.<sup>28</sup> This test series was also conducted at China Lake, just after the JTCG/AS series. This test examined the feasibility of powder panels in preventing fuselage fires in commercial aircraft caused by the release and impact of an uncontained engine rotor blade with flammable fluid lines. Figure 9-10 shows a schematic of the test article. A simulated rotor blade was fired through the lower bay and into the luggage compartment and an ignitor initiated a fire in the presence of leaking fuel as the rotor blade penetrated the lower bay. An enhanced powder panel successfully prevented a fire from igniting in one of the tests. A second test was invalidated due to problems with the timing sequence, but unrelated to the powder panel. Two commercial powder panel tests were also conducted during this test series to evaluate their effectiveness and allow comparison of the results with those of the enhanced powder panel test.

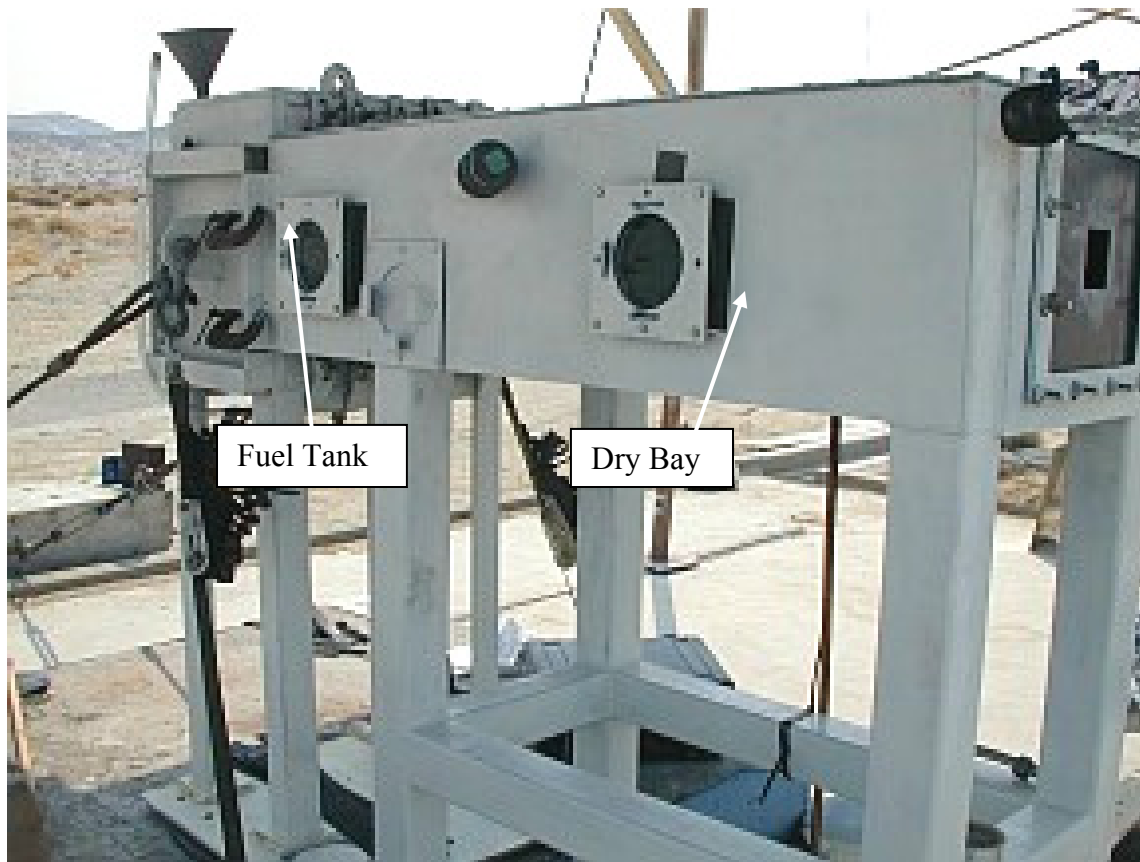


Figure 9–9. JTCG/AS Test Article.

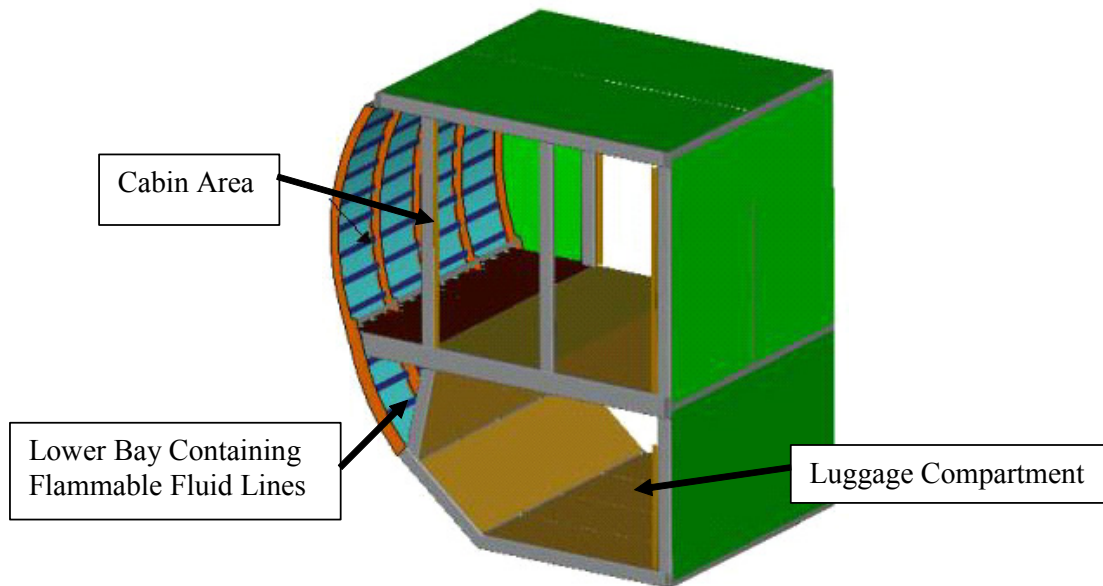


Figure 9–10. Schematic of the FAA Test Article.

**Live Fire Test Results**

Following the experimental testing of Phase I, the opportunity for demonstrating enhanced powder panels arose at the Navy’s Weapons Survivability Laboratory. Lessons learned from the NGP Phase I experimental testing were used to design and fabricate some new, slightly more optimized powder panels. These panels again incorporated thermoplastic materials. However, thinner panels and reduced powder loading resulted in reduced mass, and new panel designs were utilized. Masses were decreased on average 100 g to 200 g from those designs evaluated in experimental testing for 30.2 cm x 30.2 cm panels. The mass of the panels tested at China Lake varied from 320 g to 422 g, and the thicknesses ranged from 2.4 mm to 3.3 mm. In both the JTCG/AS and FAA test programs, the enhanced powder panels showed solid improvement over current powder panel designs. Fire ignition was prevented in all five valid tests involving enhanced powder panels (four JTCG/AS tests and one FAA test). Conversely, fires resulted in all four valid commercial powder panel tests (two JTCG/AS and two FAA tests).

The powder releases from both the commercial and enhanced panel designs in the China Lake tests were as much as ten times those experienced in the light gun tests conducted at WPAFB due to a number of significant differences in the two facilities and test protocols: the energy of the projectile used at China Lake was about 17% larger; the striker plate at China Lake caused the projectile to spall and yaw; and, most significantly, fuel was present in the China Lake tests that applied extra pressures from the hydraulic ram effect, distorting the wall and imparting additional forces on the panel.

Figure 9–11 shows some images captured from high-speed video in JTCG/AS testing demonstrating the fire mitigation capability of enhanced powder panel designs. Powder discharge was estimated to be at least 90 % of the pretest powder loading for the enhanced powder panels, compared to 5 % to 10 % for commercial powder panels. Greater powder dispersion throughout the dry bays was also evident for the enhanced powder panels. Figure 9–12 compares the amount of fire extinguishing powder released from an enhanced powder panel with a commercially available powder panel in the JTCG/AS tests.

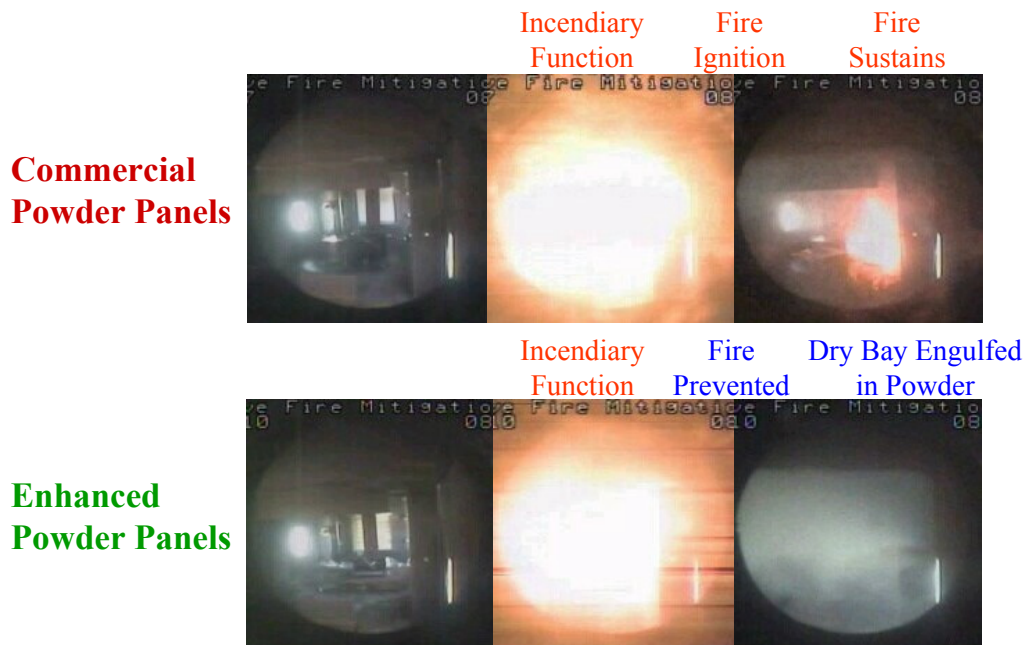


**Figure 9–11. Enhanced Powder Panel Fire Mitigation Capability.**

Figure 9–13 shows that impact of the enhanced powder panel by a rotor blade in the FAA test resulted in release of all the fire extinguishing agent, as it prevented fire ignition. Baseline testing showed that unprotected fuselage areas did indeed result in sustained fires.

**Commercial Powder Panel  
~5-10% Powder Release**



**Enhanced Powder Panel  
~90% Powder Release**



**Figure 9–12.  
Comparison of  
Commercial  
and Enhanced  
Powder Panel  
Agent Release  
in JTCG/AS  
Dry Bay Fire  
Extinguishing  
Testing.**



**Figure 9–13. Entire Contents of Enhanced Powder Panel Released During FAA Test in Which the Fire Was Prevented.**

## 9.2.8 Optimization Program

### Optimization Testing Methodology

In Phase II, Skyward continued their impact dynamics research, with a focus on optimizing the enhanced powder panels, parametrically examining design variations, and then demonstrating the optimized panels. Panel materials, thickness, and construction techniques were optimized to reduce the panel mass and thickness, while maintaining effective powder release and dispersion.

Testing was conducted in the same simulated dry bay experimental device used for concept evaluations in Phase I, and with the same light gas gun launching 12.7 mm diameter ball projectiles. Optimization test variables included panel materials and thicknesses, fire extinguishing powder loading (mass of powder inserted into a given panel size), rib designs, and the assembly process. Optimization testing focused on three primary areas of investigation:

- effectiveness optimization (maximize front face fracture and powder release);
- practicality enhancement (reduce mass, decrease panel thickness, address production issues); and
- reliability improvement (quantify reliability of measures of effectiveness, increase durability, and reduce risk of accidental leakage).

Maximizing powder release into the dry bay continued to be the defining goal, but other requirements were levied on the design effort to ensure that the enhanced powder panels were as practical and reliable as possible. Mass was reduced, panel thickness was minimized, and other potential production requirements were considered. An areal density (mass per unit area) target was provided by one of the vehicle manufacturers for the design effort.

Phase II testing primarily involved the use of aluminum oxide ( $\text{Al}_2\text{O}_3$ ) over Purple K ( $\text{KHCO}_3$ ) or other powders, even though these other powders have been demonstrated to be more effective as fire extinguishing agents. At least two of the aircraft manufacturers in the powder panel survey expressed doubt that any potentially corrosive chemical powder would be acceptable by their aircraft, so there was a conscious effort made to demonstrate the effectiveness of  $\text{Al}_2\text{O}_3$  during the optimization testing.  $\text{Al}_2\text{O}_3$  is the only known powder panel agent to be incorporated into an aircraft due to its lack of reactivity with aircraft structure. Additionally, since  $\text{Al}_2\text{O}_3$  has a much higher specific gravity than  $\text{KHCO}_3$  (3.95 compared to 0.88), it was thought to be worst-case and would help with determining success in mass reduction efforts. The  $\text{Al}_2\text{O}_3$  tested was 5  $\mu\text{m}$  in average particle diameter, compared to an average of approximately 30  $\mu\text{m}$  for the  $\text{KHCO}_3$ , which may also mean the former could pack more tightly.

Certain front face materials evaluated in Phase I testing proved to be effective and remained a focus in Phase II. These materials included thermoplastics with brittle material properties and some thermoset resins. Other unique materials were also examined that more appropriately targeted optimization requirements. Efforts were made to minimize front face and overall thickness and yet maintain sufficient strength to avoid accidental fracture. Lower density materials were compared to more dense materials.

Various new and unique designs were examined for the rib structure in Phase II, including the thickness of the ribs and attachment methods to the front and back faces. The rib design was examined in detail because it directly affects the potential fire extinguishing powder loading, which can be the primary mass

driver in the overall design. Various rib materials were examined for influence on powder panel performance, including some materials evaluated in the more effective Phase I designs.

Phase II testing also included examinations of back face materials and thicknesses and their influence on powder panel effectiveness. Materials examined in Phase I were once again tested along with some materials not previously evaluated. Testing included designs where the front and rear faces and the rib materials were the same and others where dissimilar materials were used.

Bonding techniques were also examined, with an emphasis on ensuring a robust overall design that reduced the risk of accidental leakage. In addition, rib-to-face bonding was examined for its influence on the performance of the powder panel. This influence was noted in Phase I testing and further examined in Phase II. Bonding materials were examined, as well as bonding patterns or techniques.

### Parametric/Optimization Experimental Results

A total of 25 tests were conducted in Phase II optimization tests in Range A at the AVSF. Table 9–5 lists the panels tested and includes pretest panel masses and areal densities, along with the mass of powder released, the percentage of powder released, and the estimated front face area removed. The panels are listed in descending order by the mass of powder released in each test.

**Table 9–5. Phase II Optimization Tests.**

Test No.	Material Description	Total Thickness (mm)	Pretest Mass (g)	Areal Density (kg/m <sup>2</sup> )	Powder Release (g)	% Powder Released	Face Area Removed (cm <sup>2</sup> )
5	0.64 mm polystyrene front 1.3 mm polycarbonate ribs 0.51 mm polycarbonate back	2.4	295	3.24	5.2	3.2	11
22	0.76 mm acrylic front 0.76 mm polycarbonate ribs 0.76 mm polycarbonate back	2.3	215	2.37	4.0	8.4	6
24	0.51 mm composite front 0.76 mm polycarbonate ribs 0.38 mm polycarbonate back	1.6	141	1.55	3.0	6.3	1
8	0.76 mm acrylic front 1.3 mm polycarbonate ribs 0.76 mm polycarbonate back	3.0	348	3.82	3.0	1.8	12
18	0.64 mm polystyrene front 0.76 mm polycarbonate ribs 0.51 mm polycarbonate back	1.9	332	3.65	2.5	1.2	2
14	0.64 mm polystyrene front 1.3 mm polycarbonate ribs 0.76 mm polycarbonate back	2.7	368	4.05	2.2	1.9	10
2	0.64 mm polystyrene front 0.76 mm polycarbonate ribs 0.51 mm polycarbonate back	2.4	252	2.77	2.2	1.8	5
10	0.76 mm acrylic front 1.3 mm polycarbonate ribs 0.76 mm polycarbonate back	2.8	453	4.98	2.1	0.7	1

Test No.	Material Description	Total Thickness (mm)	Pretest Mass (g)	Areal Density (kg/m <sup>2</sup> )	Powder Release (g)	% Powder Released	Face Area Removed (cm <sup>2</sup> )
4	0.64 mm polystyrene front 1.3 mm polycarbonate ribs 0.51 mm polycarbonate back	2.4	330	3.63	1.7	0.8	24
23	0.51 mm composite front 0.76 mm polycarbonate ribs 0.38 mm polycarbonate back	1.6	140	1.54	1.6	2.8	2
17	0.64 mm polystyrene front 0.76 mm polycarbonate ribs 0.51 mm polycarbonate back	1.9	330	3.63	1.5	0.8	2
6	0.64 mm polystyrene front 0.76 mm ABS ribs 0.76 mm ABS back	2.2	201	2.21	1.4	1.5	10
11	0.64 mm polystyrene front 1.3 mm polycarbonate ribs 0.76 mm polycarbonate back	2.7	404	4.44	1.0	0.7	7
13	0.64 mm polystyrene front 1.3 mm polycarbonate ribs 0.76 mm polycarbonate back	2.7	410	4.51	0.8	0.5	3
16	0.64 mm polystyrene front 0.76 mm polycarbonate ribs 0.51 mm polycarbonate back	1.9	306	3.37	0.8	0.4	2
7	0.64 mm polystyrene front 0.76 mm ABS ribs 0.76 mm ABS back	2.2	194	2.13	0.8	0.9	6
21	0.64 mm polystyrene front 0.76 mm polycarbonate ribs 0.76 mm polycarbonate back	2.2	192	2.10	0.6	1.2	1
9#	0.08 mm glass epoxy front 0.1" Nomex honeycomb ribs 0.08 mm glass epoxy back	2.7	175	1.92	0.3	0.2	1
15#	0.08 mm glass epoxy front 2.5 cm Nomex honeycomb ribs 0.08 mm glass epoxy back	2.7	175	1.92	0.2	0.2	0.5
19	1.0 mm polycarbonate front 0.76 mm polycarbonate ribs 0.76 mm polycarbonate back	2.5	270	2.96	0.1	0.3	0.7
20*	1.0 mm polycarbonate front 0.76 mm polycarbonate ribs 0.76 mm polycarbonate back	2.5	261	2.87	N/A	N/A	0.7
25*	0.51 mm composite front 0.76 mm polycarbonate ribs 0.38 mm polycarbonate back	1.6	124	1.36	N/A	N/A	19

# Existing powder panel designs.

\*Tests conducted with water in fuel tank; not able to accurately determine powder release.

A summary of the designs is also provided in Table 9–5, listing the front and back face materials and the material thickness. Effective front face materials tested in Phase I were evaluated, including a textured polystyrene. Some other materials were also examined, including other thermoplastics and some composite materials not evaluated in Phase I. Materials used for the back face concentrated on polycarbonate, which proved to be effective in Phase I, although some tests were conducted with ABS, a more ductile material. Table 9–5 also shows the rib materials tested and the thicknesses of the internal section of the panel. Different rib designs and manufacturing processes were examined in the optimization testing. Rib materials most often mirrored the back face material.

Optimization testing indicated significant decreases in mass were possible from Phase I test panels, while maintaining improved powder release. Panel masses were reduced as much as 57 % from the lightest panel tested in the first phase, with an increase in powder release. Figure 9–14 compares the lightest Phase II panel with the lightest Phase I panel and a commercial powder panel. Two of the lightest pretest filled panel masses were 124 g and 140 g. By comparison, commercial powder panels tested in Phase II weighed approximately 175 g. Therefore, the enhanced powder panels were reduced as much as 29 % below the commercial panel mass. Enhanced powder panel thicknesses ranged between 1.6 mm and 3.0 mm in optimization evaluations. This was a reduction of more than 60 % from the thinnest panel tested in Phase I. Commercial panels evaluated in Phase II were 2.7 mm in thickness. The enhanced powder panels were, therefore, reduced about 39 % in thickness below the commercial powder panel.

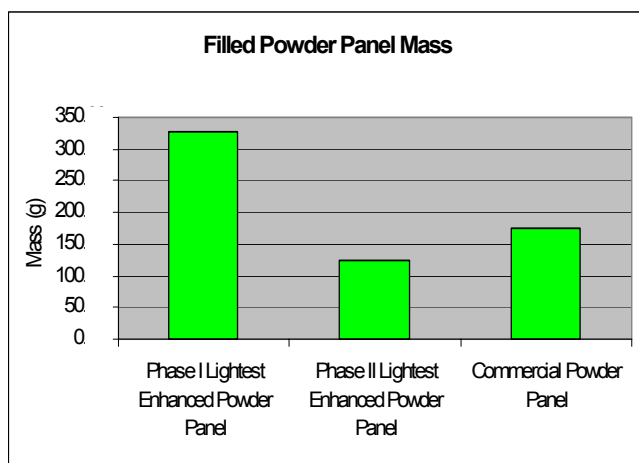


**Figure 9–14. Enhanced Powder Panel Mass Reduction.**

Figure 9–15 compares the thinnest panels tested in Phase I and Phase II with the commercial powder panels. Reductions in thickness reduce the amount of powder in the panel, which is the significant mass consideration. However, a thicker panel along the shotline also reduces the potential powder release, which obviously affects powder panel effectiveness. Therefore, there is a balance necessary between panel thickness, which affects panel mass, and the effectiveness of the panel, as measured by powder release or loss. Front and back face materials and the rib structure design were other variables examined to increase performance without increasing mass.

Powder release is an important factor in the testing because the greater the amount of powder dispersed in the dry bay, particularly along the shotline, the lower the chance of an ignited fire. The amount of powder released in Phase II testing ranged from as low as 0.1 g to as much as 5.2 g. This powder release or loss is not as much as the most effective panels in Phase I testing, but the panel thickness and available powder has been significantly reduced to meet likely design goals. Powder release for the commercial

powder panel tests was 0.2 g and 0.3 g. Figure 9–16 compares the best performing Phase II enhanced powder panel (no water in the tank) with the best performing commercial powder panel. These data show the amount of powder released from the enhanced powder panels was as much as 21 times greater than the commercial powder panels.

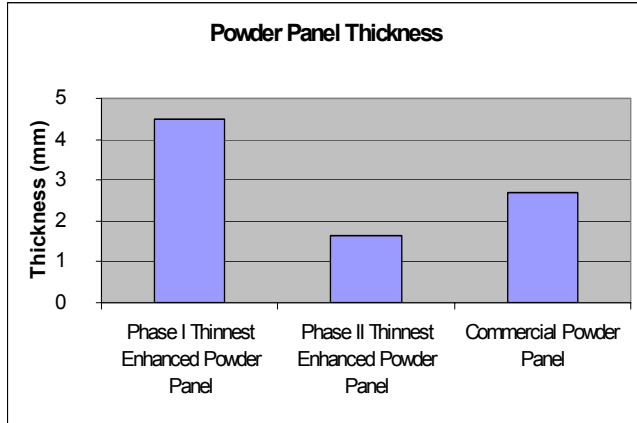


**Figure 9–15. Enhanced Powder Panel Thickness Reduction.**

The percentage of powder released (powder released or lost divided by pretest total powder loading multiplied by 100) has also been used as a measure of powder release effectiveness. The enhanced panel design attempts to maximize the release of the available powder in the panel. Optimized panels tested ranged from 0.3 % to 8 % of the total powder released. The commercial panels released approximately 0.2 % of the total powder contained.

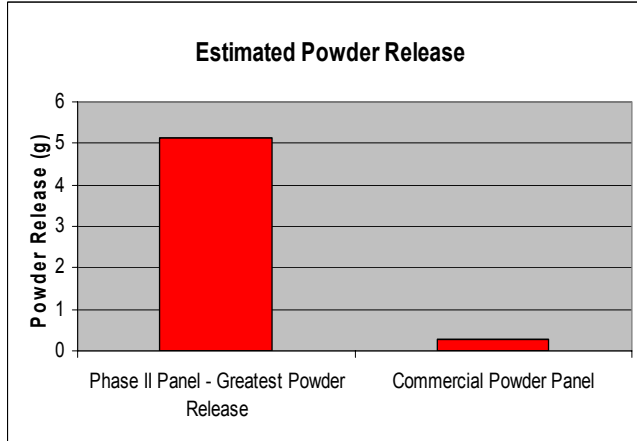


**Figure 9–16. Comparison of Enhanced and Commercial Panel Powder Released.**

Figure 9–17 compares the best performing Phase II enhanced panel (no water in the tank) with the best performing commercial panel. These data show the enhanced panels could increase the percentage of total powder released by as much as 42 times. A ranking of the panels using percentage of powder released does not track directly with a ranking of the panels by total powder released, since there was some considerable variance in overall pretest panel mass.

Tests 9 and 15 in Table 9–5 were conducted on the commercially available powder panels. As mentioned previously, these panels are composed of a honeycomb core and two thin composite face sheets. The commercial powder panels were among the lighter panels tested (empty mass and with powder), but also released nearly the least amount of powder and the smallest percentage of powder. Except for one test

examining a ductile front face, the powder release and percentage of powder released for the commercial panels is less than half the next enhanced powder panel. As discovered in previous testing with Nomex honeycomb cores, powder is released from those cells directly penetrated by the projectile and those torn on the perimeter of the penetration either by the penetrating projectile or hydrodynamic ram forces acting on the fuel tank panel. However, the damage area is relatively well contained and powder is not able to escape from the rest of the panel. Enhanced powder panels offer the potential for a much greater percentage of the panel's contents to be released. It was anticipated at this point in the program that the effects of hydrodynamic ram on the powder panel will only increase the amount of improvement an enhanced powder panel can offer. Further testing would verify this assertion.

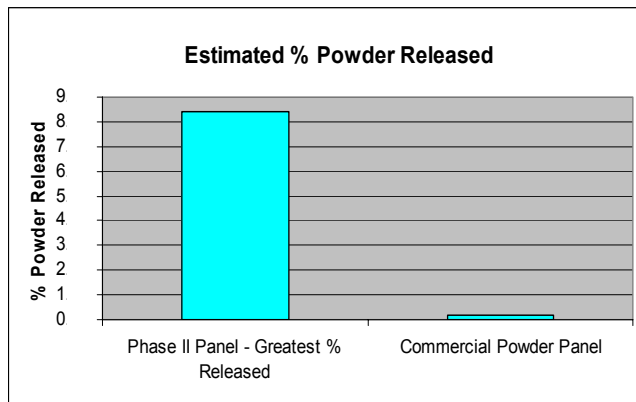


**Figure 9–17. Comparison of Enhanced and Commercial Panel Percent Powder Released.**

The outlier enhanced powder panel (Test 19) utilized polycarbonate throughout the design, including the front face. In this test, the entrance hole in the front face and exit hole in the rear face essentially self-sealed together and prevented virtually any powder from escaping, except through the penetration area alone. This design was also examined in Test 20 with water in the fuel tank and yielded the same damage. The front face area removed for these tests was approximately  $0.7 \text{ cm}^2$ , the least effective performance by an enhanced powder panel. By contrast, Test 4 resulted in almost  $25 \text{ cm}^2$  of the front face removed and Test 25, with water, resulted in over  $19 \text{ cm}^2$  being removed.

Figure 9–18 compares the enhanced powder panel experiencing the greatest front face area removal (no water in the tank) with the better performing commercial powder panel ( $1.1 \text{ cm}^2$ ). An improvement of over 22 times is shown with this enhanced powder panel.

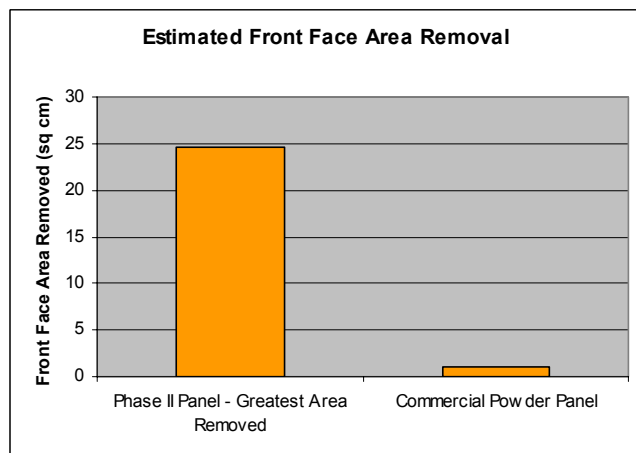


**Figure 9–18. Comparison of Enhanced and Commercial Panel Front Face Area Removal.**

For Tests 20 and 25, conducted with water in the fuel tank, a post-test mass of the panel to determine powder release or loss was not practical. The powder in both panels absorbed water as a result of the test. These two tests, however, demonstrated that hydrodynamic ram would significantly enhance front face fracture for a more brittle front face, leading to greater powder release, but would not likely assist fracture for a ductile front face. Front face area removal was increased for the same panel design by as much as 12 times (comparing Test 24 to Test 25) due to the additional forces and fuel tank panel deformation associated with hydrodynamic ram. This result demonstrated that in cases where the powder panel will be attached to a flammable fluid container, and hydrodynamic ram is expected when the container is punctured, the powder panel can be designed to take advantage of the expected hydrodynamic ram event.

In summary, the Phase II data showed that an enhanced powder panel (Test 24) can be 19 % lighter and 39 % thinner than a commercial powder panel, yet release over 10 times more powder mass, 30 times greater the percentage of powder originally contained in the panel, and sustain at least 32 % greater front face area removal. The data also showed that the effects of hydrodynamic ram would further increase the performance of an enhanced powder panel.

### **9.2.9 Live-fire Demonstration Testing of Optimized Enhanced Powder Panels**

#### **Testing Objective**

At the end of Phase II, a series of live fire demonstration tests was conducted of the optimized designs. These tests were to demonstrate (a) that the most promising enhanced powder panel designs could prevent fire ignition and be competitive with commercial powder panels in vital design criteria such as mass and thickness; and (b) that powder dispersion and fracture mechanics results shown in the small experimental test article could be extrapolated to a larger, more realistic test article. They also examined attachment techniques for the panels, the effectiveness of  $\text{Al}_2\text{O}_3$  (historically the preferred dry chemical powder in aircraft applications), and the effect of certain variables on enhanced powder panel effectiveness.

#### **Wright-Patterson AFB Facility**

Phase II live fire demonstration testing was conducted by the Air Force 46<sup>th</sup> Test Wing Aerospace Survivability and Safety Flight. The tests were conducted in outdoor Range 2 at their Aerospace Vehicle Survivability Facility, Wright-Patterson Air Force Base (WPAFB), Ohio (Figure 9–19).

Baseline testing was conducted to ensure that fire could be ignited when a powder panel was not present. One test was conducted with a standard commercial powder panel to evaluate its effectiveness for the same test variables. Finally, six enhanced powder panel tests were conducted. Figure 9–20 shows the test article setup.



**Figure 9–19. Range 2 at the WPAFB Aerospace Vehicle Survivability Facility.**

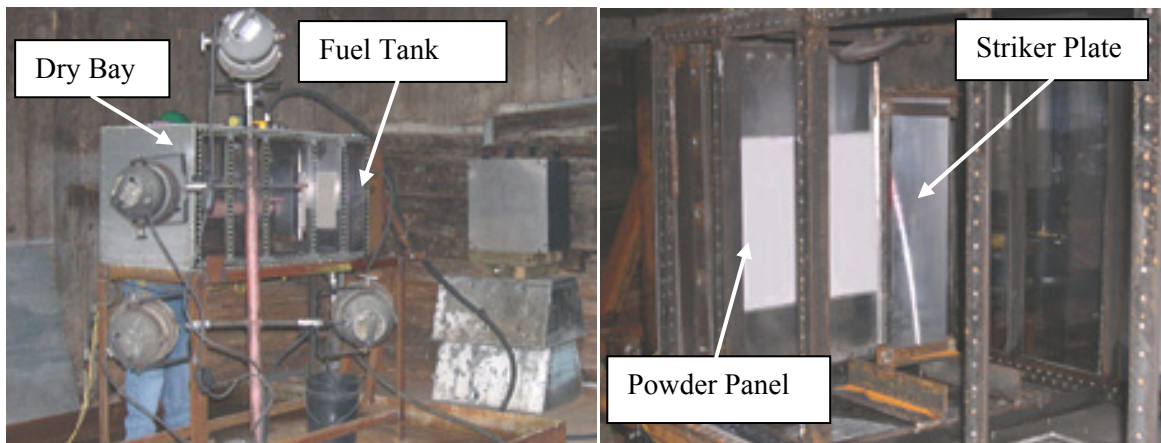


**Figure 9–20. Test Article.**

### ***Instrumentation***

Threat Velocity Measurement Equipment - The projectile velocity at impact was calculated for each test by measuring the elapsed time required to travel from the gun barrel muzzle to the striker plate. A gun break wire was installed in a small hole drilled in the side of the barrel near the exit end. The wire was

severed as the projectile exited the muzzle. A break-paper grid was located at the intended impact point on the striker plate, and was broken when the projectile impacted the target. With the break wire and break paper time increments determined and the standoff distance known, the impact velocity could be calculated. If the paper grid and strain gage failed before impact, the projectile velocity could still be estimated using the gun break signal and the pressure transducer signal recorded on the Nicolet data acquisition system.

**Thermocouples** - Temperature-time histories were collected to obtain a temperature profile for the dry bay test article. Thermocouples were located within the dry bay. All thermocouples operated in the  $-18^{\circ}\text{C}$  to  $1330^{\circ}\text{C}$  range with a 1 kHz sampling rate. One thermocouple was located on the back side of the striker plate below the target location and the other near the fuel tank wall above the powder panel.

**Optical Records** - A high-speed video camera (approximately 500 frames/s) was mounted beside the test article to record the view looking through a Lexan panel on the side of the test device. Skyward provided a digital video camera (approximately 30 frames/s) that also recorded the event through the Lexan panel. Both cameras were aimed toward the powder panel, but covered as much of the dry bay as possible. A standard video camera (30 frames/s) was positioned more distant to focus on the overall test article and capture the entire event.

### **Test Article and Procedures**

Nine ballistic tests were conducted, including unprotected and powder panel-protected configurations of the dry bay/fuel tank simulator. The test article and test setup were similar to the enhanced powder panel demonstration tests conducted at the Weapons Survivability Laboratory at China Lake, California. A simulated dry bay/fuel tank test article (Figure 9–21) was used of a larger size than the experimental test device. The dry bay measured 0.61 m wide x 0.61 m high x 1.22 m long. The fuel tank attached to one end of the dry bay measured 0.36 m wide x 1.22 m high x 0.61 m long. The powder panels were connected to a simulated fuel tank wall composed of 1.8 mm thick 2024-T3 for most tests. A striker plate was located 0.30 m in front of the powder panel/fuel tank wall to ensure projectile functioning. Lexan panels in the test article allowed test results to be observed directly.

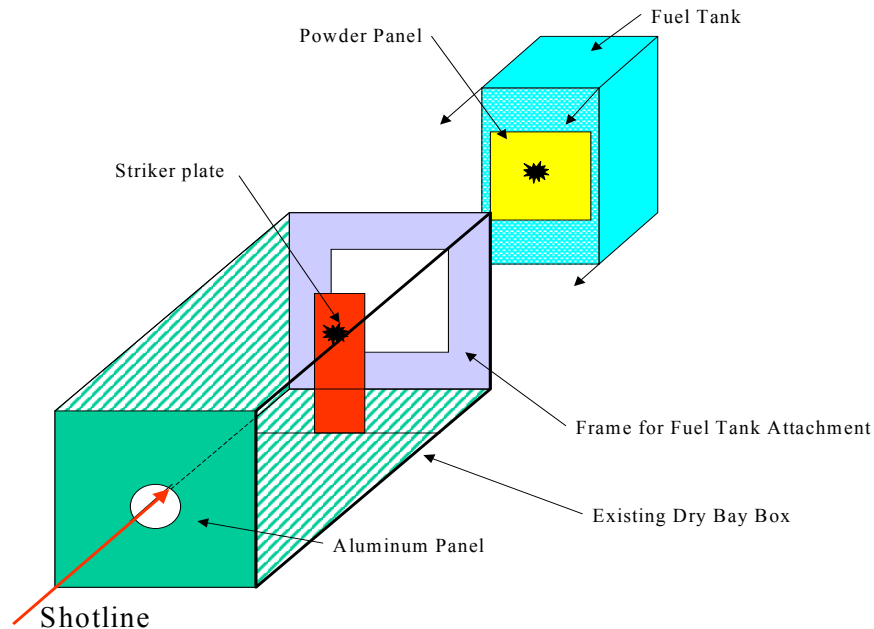


**Figure 9–21.**  
**Schematic of Test**  
**Article. (Top and Lexan**  
**Side Removed for**  
**Clarity)**

The test article was placed near the east wall of AVSF Range 2, with the fuel tank on the east side. The gun was positioned to the west of the test article, and fired from the west toward the east wall of the range. This configuration ensured projectiles did not leave the range enclosure. Figure 9–22 shows the relative position of the test article and gun setup.

A single threat type was used for each of the enhanced powder panel tests. The 12.7 mm API Type B-32 projectile was fired through the center of the test article at a velocity of approximately 760 m/s. A physical description of the projectile is provided in Figure 9–23. The projectiles were fired from Mann barrels at close range to minimize targeting error, and the projectile powder mass was modified, as necessary, to achieve the desired impact velocity.

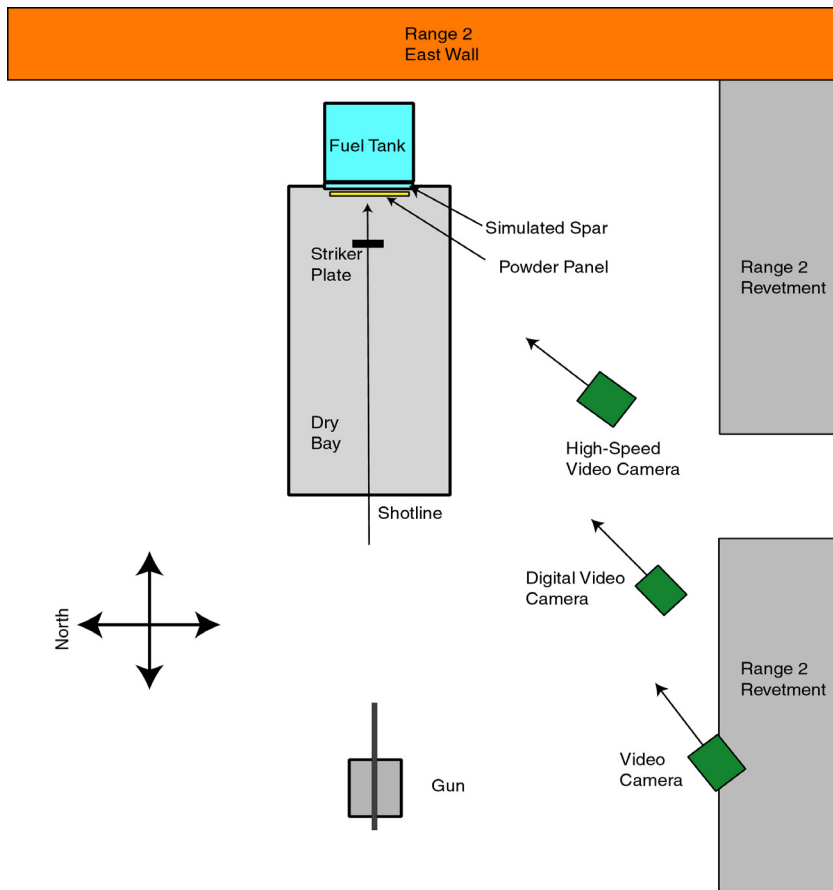


**Figure 9–22. Test Article Setup in Range 2.**

The setup was reviewed prior to each test to ensure that the appropriate powder panel was installed in the proper location, the fuel tank was filled, and the appropriate impact location on the striker plate was targeted. The principal safety issue with this testing was the safe containment of the ballistic threat. The principal method of stopping the threat was through a catch plate located on the back wall of the fuel tank test article. The east wall of Range 2 was behind the test article if the projectile were to escape. An external catch plate was positioned on this wall as well.

The powders that were used for testing were non-toxic; however, because the dry powder is a finely divided solid material, it can become suspended in the air causing a mild discomfort similar to that

experienced in any dust-laden atmosphere. To minimize the exposure to the dust, all participants used dust masks during test clean-up.

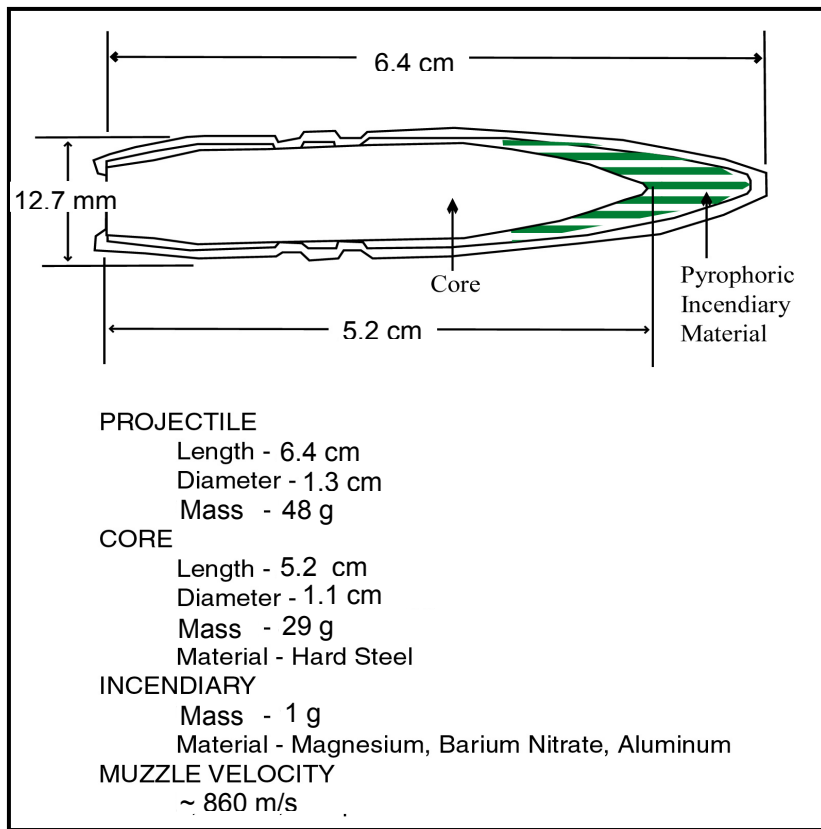


**Figure 9–23. 12.7 mm API Type B-32 Projectile Description.**

### Live Fire Demonstration Test Results of Optimized Enhanced Powder Panels

Some of the more practical, yet effective enhanced powder panels were evaluated in live fire demonstration tests conducted at the end of Phase II. This testing involved many of the same elements involved in proof-of-concept testing after Phase I. However, in these tests, the thinner and lower mass Phase II optimized panels were evaluated. A total of nine tests were conducted, as summarized in Table 9–6. The test was set up to ensure a threat function for each powder panel test. A successful powder panel test was considered to be one where no fire ignition occurred, assuming both fuel leakage and functioning of the ballistic threat. Estimates of the front face area removed and the percentage of powder released were made. Due to the presence of JP-8 fuel, it was not possible to weigh the precise amount of powder released or lost, so an estimate of the percentage of the original powder released was made. This was a rough estimate based upon a post-test examination of the panel and area calculations. It was impossible to determine the influence of leaking fuel on remaining powder in the panel immediately after the test, but the estimates do correlate well with powder dispersion evidence and fire ignition results.

Two different enhanced powder panel designs were evaluated in the demonstration tests, with the primary differences involving material composition. Enhanced Design 1, in Table 9–6, was lighter with potentially better thermal resistance capability. Enhanced Design 2 was heavier, with features to make it

more durable. Test EPP-08 varied in design somewhat from the Enhanced Design 1, utilizing a self-sealing back face material, but was essentially the same in other respects.

**Table 9–6. Phase II Enhanced Powder Panel Live Fire Demonstration Tests.**

	<b>Powder Panel</b>	<b>Panel Mass (g)</b>	<b>Panel Thickness (mm)</b>	<b>Powder</b>	<b>Threat Function?</b>	<b>Fire Ignition?</b>	<b>Front Face Area Removed (cm<sup>2</sup>)</b>	<b>Estimated % Powder Released</b>
EPP-01	No Panel - Baseline	N/A	N/A	N/A	Yes	No	N/A	N/A
EPP-02	No Panel - Baseline	N/A	N/A	N/A	Yes	Yes	N/A	N/A
EPP-03	Commercial	189.0	2.69	Al <sub>2</sub> O <sub>3</sub>	Yes	Yes*	50	8
EPP-04	Enhanced Design 1	145.4	1.90	Al <sub>2</sub> O <sub>3</sub>	Yes	No	156	70
EPP-05	Enhanced Design 1	140.8	1.90	Al <sub>2</sub> O <sub>3</sub>	Yes	Yes*	146	83
EPP-06	Enhanced Design 2	186.5	1.90	Al <sub>2</sub> O <sub>3</sub>	Yes	No	309	88
EPP-07	Enhanced Design 2	227.0	1.90	KHCO <sub>3</sub>	Yes	Yes, but powder extinguished fire	329	83
EPP-08	Enhanced Design 1	157.1	2.13	Al <sub>2</sub> O <sub>3</sub>	Yes	No	54	61
EPP-09	Enhanced Design 2	226.3	2.16	KHCO <sub>3</sub>	Yes	No	252	62

\* Panel dislodged from fuel tank wall during test

Two baseline tests were conducted at the beginning of the test program. The purpose of these tests was to ensure threat functioning and the ignition of a fire in an unprotected or inadequately protected dry bay. For these conditions, a successful powder panel would prevent fire ignition, despite the functioning threat, and an unsuccessful powder panel would not prevent fire ignition. In the first baseline test, the fuel tank panel was a 2.0 mm thick 7075-T6 plate. This was the same material and thickness used as the simulated fuel tank panel in all Range A experimental tests. In EPP-01 a fire was not ignited, as a large deluge of fuel was seen engulfing the dry bay almost immediately, creating an extremely fuel rich environment. The threat did function, but the fuel tank panel resisted the significant hydrodynamic ram pressures and peeled away from the fasteners attaching it to the fuel tank. The fuel tank panel deformed significantly before its edges at the fastener locations tore through, but the impact hole was not significantly larger than the threat size. The toughness of this material was also evident in the Range A tests, where hydrodynamic ram was most often not a variable and worst-case conditions were desired. In these demonstration tests, it was desired to allow hydrodynamic ram damage to occur. Without hydrodynamic ram forces and minimized fuel spurting, it is possible an inaccurate judgment could be made regarding powder panel effectiveness. In this first baseline test, the panel resisted hydrodynamic ram forces such that the weakest failure point was the fuel tank panel attachment mechanism.

Since a fire was not ignited in this first test (and the potential for fire was essential for the powder panel evaluations), modifications were made to the test article and setup to better ensure fire ignition. For the second baseline test, the fuel tank material was changed to 1.8 mm thick 2024-T3 and a structural frame

was used to hold the fuel tank panel to the fuel tank without interfering with the powder panel positioned between its boundaries. In addition, the planned projectile velocity was lowered to 762 m/s to mirror proof-of-concept testing after Phase I and to reduce energy somewhat. The fuel level was lowered from completely full (about 64 l) to about three-fourths full (49 l) to permit pressure relief in an ullage area and reduce the amount of fuel that might immediately spill out into the ignition zone and create another over-rich condition. These modifications proved worthwhile, as EPP-02 did result in a fire. The fire was visible for about 4 s, but appeared to be self-extinguishing near that time. This would provide an adequate burn time for an evaluation of the powder panels, but an alteration to the test article was envisioned to be necessary.

The third test (EPP-03) involved a commercial powder panel, as Table 9-6 indicates. The threat functioned as planned, however a fire was ignited. The fire only lasted a short duration, as the fire appeared to be and seeking oxygen. A long jet of flame actually shot out of the entrance hole at the front of the dry bay. The fire lasted over 1 s, but thick black smoke from the combustion filled the dry bay and lasted for many minutes afterward. The temperature in the dry bay climbed about 49 °C. The conclusion was that the panel was not successful in inhibiting fire ignition or preventing a sustained fire, rather a self-extinguishing fire occurred due to a lack of oxygen. Closer inspection of the dry bay and the high-speed video revealed the commercial powder panel did not remain adhered to the fuel tank panel with the two-part epoxy used. The panel was dislodged after the threat flash and started coming loose as the fire was ignited below and almost behind the panel as it flew off. The powder release was not sufficient to allow powder to remain suspended in the dry bay; however, its effectiveness could remain in question since it did not adhere properly. Black markings evident of not only a flash, but of an ignited fire, were present in the dry bay. No powder residue was found in the dry bay following the test, although the panel did break up better than in non-fluid tests in Range. The damage area was approximately 10.2 cm high x 6.4 cm wide. It is estimated from an inspection of the panel that the front face area removed was approximately 50 cm<sup>2</sup> and about 8 % of the powder was released.



**Figure 9–24. Post-Test Damage Image of EPP-03 Commercial Powder Panel.**

The fourth test (EPP-04) involved an enhanced powder panel. For this test, modifications to the test article were considered to allow more venting or fresh oxygen to be available to the combustion process. However, since more enhanced powder panel tests were to be conducted, it was desired to conduct at least

one with the exact same conditions as the commercial powder panel for a direct comparison. In this test, the threat functioned as expected, with the high-speed video indicating a flash duration of approximately 0.008 seconds or more, which was comparable to the previous two tests. However in this test, as soon as the flash dissipated, the dry bay was engulfed in fire extinguishing powder, and no fire ignition occurred. The temperature in the dry bay around the flash climbed only about 10 °C. A review of the video confirmed that no combustion occurred after the threat function. Powder was visible on the walls of the dry bay, with powder on the Lexan window all the way to the end of the 1.2 m long dry bay. A significant amount of powder also covered the striker panel on the surface facing the powder panel. Powder was also visible in the dry bay for a number of minutes after the test. The panel was adhered with a two-part, fast curing epoxy, which was the same adhesive used in the commercial panel test. However, in this case the panel held fairly well, although some loss of adhesion occurred. Figure 9–25 shows a post-test image of the powder panel, demonstrating the front face fracture. The damage area was approximately 14 cm high x 18 cm wide. It is estimated from an inspection of the panel that the front face area removed was approximately 156 cm<sup>2</sup> and about 70 % of the powder was released.



**Figure 9–25. Post-Test Damage Image of EPP-04 Enhanced Powder Panel.**

In preparation for EPP-05, the dry bay test article was modified to allow for more fresh air to vent into the fire zone. A 7.62 cm diameter hole was drilled into the aluminum side wall of the dry bay. It was centered along the length of the dry bay, 0.61 m from the fuel tank wall and down about 13.3 cm from the top of the dry bay. In this test, a double-sided adhesive tape was used to adhere the powder panel, versus a two-part epoxy. The threat functioned in the test, as planned, and the high-speed video showed a fire ignited about 0.02 seconds after the flash dissipated. The fire lasted several seconds and the temperature climbed about 194 °C in the dry bay near the fuel tank. In the real-time and high-speed video, the powder panel was visible being dislodged from the fuel tank and slamming into the side Lexan panel. The fire started behind the powder panel in the corner opposite the direction the powder panel flew off. Powder was visible in the video emanating from the panel into the Lexan and down onto the floor. As the panel lay against the Lexan, continued powder leakage was visible onto the floor, and it suspended in the vicinity of the dry bay. It is unclear if the continued release of powder was responsible for the fire extinguishing later or if the fire self-extinguished. Inspection of the test article did indicate some black residue around the new dry bay opening, so the extra vent did provide an oxygen source to the fire. In this test, the powder panel design was exactly the same as in EPP-04. In addition, the powder panel broke

up at least as effectively as in EPP-04, so it was surmised that if the panel had not dislodged from the fuel tank wall, it would likely have prevented a fire. However, further tests were required to determine if the additional oxygen available would hinder the effectiveness of the enhanced powder panels. The post-test damaged powder panel is shown in Figure 9–26. The front face damage area was approximately 18 cm high x 15 cm wide. The front face area removed was approximately 145 cm<sup>2</sup>. About 83 % of the powder was released, but as described, much of this may have exited the panel as it flew into the Lexan side panel and then rested against it.



**Figure 9–26. Post-Test Damage Image of EPP-05 Enhanced Powder Panel.**

Test EPP-06 involved a different enhanced powder panel design, primarily involving a change to the front face material. It also marked the first test using MIL-S-8802 aircraft sealant, rather than a faster curing epoxy sealant, as the adhesive to attach the powder panel to the fuel tank wall. All tests conducted after EPP-05 used this adhesive. This powder panel and all the panels utilizing this sealant remained well adhered to the fuel tank during testing. In this test, the flash was visible in the high-speed video, and then powder was seen once again engulfing the dry bay with no fire ignition occurring. The temperature in the dry bay climbed no more than about 14 °C near the flash. Powder seemed to distribute well and quickly.

Powder was still lingering in the dry bay nearly fifteen minutes after the test, when the side panel was removed (Figure 9–27). Upon inspection of the fuel tank, powder was visible along the length of the Lexan window and across the surface of the striker plate facing the powder panel (Figure 9–28).

Some large pieces of the powder panel front surface were actually stuck to the striker plate along with the powder. Powder was also detected on the aluminum side panel nearly the length of the dry bay. Powder was also visible on the structural framework of the dry bay. In all of the powder panel tests, sufficient fuel leaked into the dry bay to make visible powder on the surface of the fuel very difficult to distinguish.

As shown in Figure 9–29, the powder panel was fractured in EPP-06 similar to the previous enhanced powder panel tests. The front face damage area extended nearly to the edges of the panel, measuring approximately 30 cm high by 27 cm wide. The front face area removed was approximately 309 cm<sup>2</sup> and about 88 % of the powder was released.

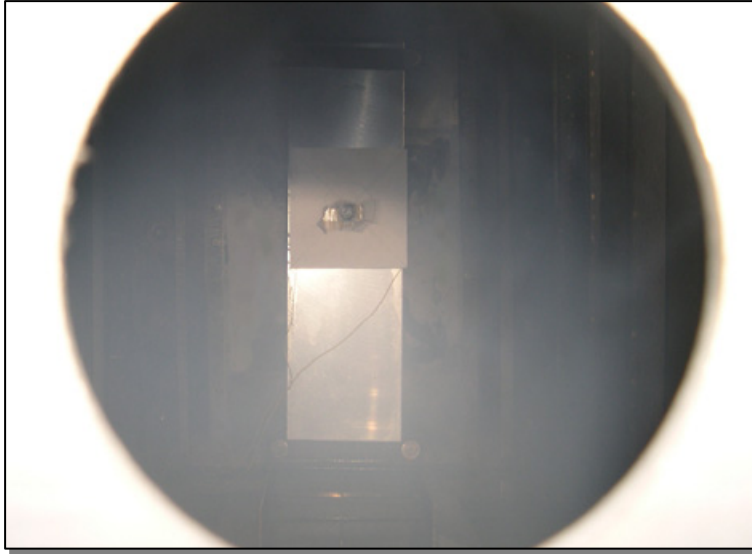


**Figure 9–27. Powder Suspension in the Dry Bay Well After the Test.**

In Test EPP-07,  $\text{KHCO}_3$  was used as the fire extinguishing powder, rather than  $\text{Al}_2\text{O}_3$ , to examine any difference in powder release or powder dispersion and suspension within the dry bay. The panel design was the same as in EPP-06. In this test, however, powder loading was increased and the panel weighed approximately 22 % more. In this test, the threat functioned as planned for a duration of less than 0.016 s.

**Figure 9–28. Powder Dispersion on Striker Plate and Side Lexan Panel.**



After the flash dissipated, the powder was seen in the video beginning to engulf the dry bay. However, a fire was ignited in the lower corner of the dry bay near the fuel tank panel and Lexan panel. It lasted only about 0.28 s as the powder was seen reaching this area about the time it was extinguished. The temperature in the dry bay climbed no more than 17 °C near the fuel tank. A small leak was evident from the fuel tank in pretest preparations and it occurred in this corner. It is plausible that some fuel remained in this corner of the dry bay after the leak was fixed. This likely allowed for an ignition of fuel already present in the dry bay, before fuel from the threat penetration hole fully began to spray into the dry bay. Based upon the evidence provided, this powder panel was considered successful, despite the brief ignition of a fire, because the powder was considered responsible for extinguishing the fire. Upon inspection of the test article, powder was evident on the Lexan panel and aluminum side panel similar to the previous

test. Powder was also evident on the dry bay structural framework, top panel, and striker plate. As expected, the  $\text{KHCO}_3$  was somewhat easier to distinguish than the  $\text{Al}_2\text{O}_3$ . The powder panel front face fracture was similar to EPP-06, as shown in Figure 9–30. The front face damage area extended nearly to edges of the panel again, measuring approximately 30 cm high x 27 cm wide. The front face area removed was approximately 329  $\text{cm}^2$  and about 83 % of the powder was released.



**Figure 9–29. Post-Test Damage Image of EPP-06 Enhanced Powder Panel.**

Test EPP-08 utilized  $\text{Al}_2\text{O}_3$  and used the same front face material evaluated in Tests EPP-04 and EPP-05. This panel had a slightly larger total thickness (2.1 mm) than these previously tested enhanced powder panels, but still weighed less than the commercial powder panel tested. This test also involved the use of a self-sealing material for the back face. In this test, the threat functioned as planned and no fire was ignited. The cloud of powder quickly moved throughout the dry bay. The temperature in the dry bay climbed no more than 13 °C. Powder was evident along the length of the Lexan panel and the other aluminum side panel. It was also found on the striker plate facing the powder panel and the dry bay top wall and back wall. The front face area removal was somewhat reduced from previous panels using the same front face, but cracking was extensive, allowing large flaps of material to easily release powder (Figure 9–31). The damage area extended about 29 cm high x 24 cm wide. The front face area removed was approximately 54  $\text{cm}^2$  and about 61 % of the powder was released. The hole in the back face of the powder panel was approximately 1.3 cm x 1.3 cm, resulting in an area removal about 66 % less than any of the other enhanced powder panel tests. It is, therefore, likely that less fuel was immediately available for fire ignition than in tests without a self-sealing back face. It is believed the thickness of the back face could be increased for such a design to improve self-sealing capability, while still maintaining an overall mass and thickness comparable to commercial powder panels. A test to verify this assertion was not possible during this test program.

The final Phase II live fire demonstration test (EPP-09) again involved  $\text{KHCO}_3$ . The same design used in Tests EPP-06 and EPP-07 was used, except the panel internal width was wider, and, therefore the overall panel was wider (2.16 mm). Despite the increased thickness, powder loading was such that it was very close in mass to EPP-07, which also examined  $\text{KHCO}_3$ . A large flash was evident in this test upon review of the high-speed video. However, no fire was ignited. The temperature in the dry bay near the flash climbed on average around 20 °C. A large cloud of powder enveloped the dry bay and powder was

visible striking the Lexan wall. Both side walls had visible powder deposits, as well as the top panel beyond the striker plate, and the striker plate itself. When the side wall was removed more than five minutes after the test, a large cloud of powder was still evident in the dry bay (Figure 9–32).



**Figure 9–30. Post-Test Damage Image of EPP-07 Enhanced Powder Panel.**

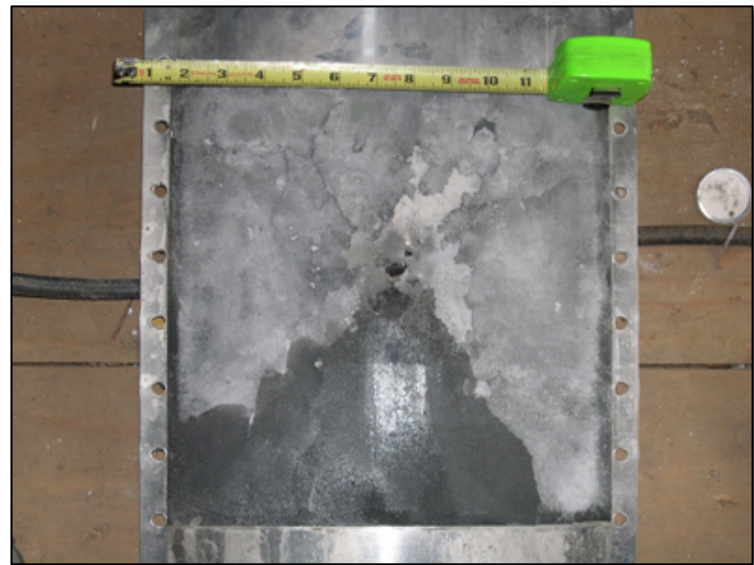


**Figure 9–31. Post-Test Damage Image of EPP-08 Enhanced Powder Panel.**

The damage to the enhanced powder panel front face was significant, as shown in Figure 9–33. The damage area extended about 30 cm high x 26 cm wide. The front face area removed was approximately 252 cm<sup>2</sup> and about 62 % of the powder was released.

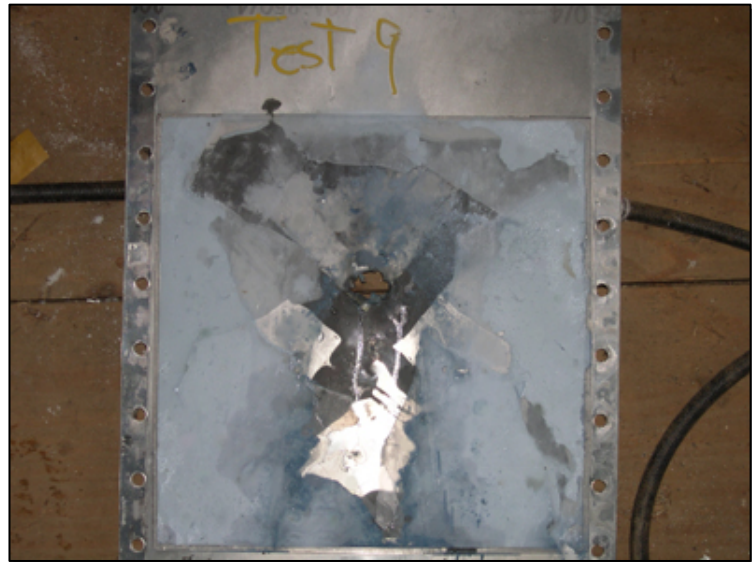
The results of the Phase II live fire demonstration tests were very promising. Out of six enhanced powder panel tests, only one test was considered unsuccessful, and it was likely due to the lack of adherence of the panel to the fuel tank. This problem was associated with the selection of adhesive for attaching the panel to the fuel tank, not the panel design itself. The same panel design was able to prevent fire ignition in two other tests. The commercial powder panel was unsuccessful in preventing fire ignition, but it too

failed to adhere to the fuel tank panel. Demonstration testing after Phase I at China Lake, with many of the same test conditions including the ballistic threat, showed these panels were not effective under these conditions. In these NGP demonstration tests, the enhanced powder panels released at least 87 % more powder than the commercial powder panel. Except for one enhanced powder panel, which still released significantly more powder, the size of the front face area removed was at least 34 % better for the enhanced powder panels compared to the commercial powder panel.



**Figure 9-32. Powder Evident in Dry Bay More Than 5 min after EPP-09 Test. (Side Wall Removed)**

**Figure 9-33. Post-Test Damage Image of EPP-09 Enhanced Powder Panel.**



Thinner enhanced powder panels appeared to release more of the total panel's powder content. However, they also likely contained less powder, so the total powder release may have been fairly close to the thicker panels. The powder panel utilizing a self-sealing back face (EPP-08) did appear to sustain less front face break-up than other enhanced powder panels. This could have been a result of this design variation. However, the reduction in the size of the back face hole, also likely contributed to the panel effectiveness by reducing immediate fuel leakage.

Both tests with  $\text{KHCO}_3$  resulted in successes, although Test EPP-07 did show evidence of a very brief fire ignition. It appeared the powder release did, however, result in the fire being extinguished.  $\text{KHCO}_3$  was expected to be at least as effective as  $\text{Al}_2\text{O}_3$ , however, the grain size of the  $\text{KHCO}_3$  was on average around 30  $\mu\text{m}$  compared to the 5  $\mu\text{m}$   $\text{Al}_2\text{O}_3$ . As previous testing has shown, a smaller grain size has proven to be more effective in fire extinguishing. It is inconclusive, however, in these few tests, whether or not grain size was even a factor.

It was conclusive that sufficient powder was released from each of the enhanced powder panels to significantly reduce the likelihood of a dry bay fire, regardless of the powder type. It was estimated that at least 40 g of powder was released in most of the enhanced powder panel tests, with as much as 70 g from the heavier panels. By contrast, it was estimated the commercial powder panel likely released less than 10 g of powder.

### 9.2.10 Mass-trade Comparison Analysis

Combat-related aircraft dry bay fires are a known vulnerability for many aircraft. However, the cost, mass, maintenance, and/or performance parameters have infrequently justified the installation of halon fire extinguishing systems for these areas. Other fire protection methods such as solid propellant gas generator systems, void space foam fillers, or even commercial powder panels have been implemented in some cases, but many dry bay areas still go unprotected. It is possible that a more effective powder panel could offer a justifiable option for previously unprotected dry bay areas or a well-supported alternative to areas protected by other means.

Cyphers and co-workers performed a comparison of an enhanced powder panel protection system with a halon fire extinguishing system to demonstrate its potential as a halon alternative. The powder panel survey had revealed that it was very difficult to find a practical example for which to perform a direct comparison. In addition, obtaining design information for certain areas that might provide a comparison was very difficult within the resources of this program. To further complicate this task, when information was obtained on a potential aircraft area or an alternative system used in trade studies, the information was often considered proprietary and was not releasable. Therefore, an emphasis was placed on generating some estimates for integrating powder panels into forward-fit or currently unprotected areas. When possible, active system information was estimated for possible integration into the same areas. It turned out that the most practical comparisons were with current powder panels and other currently-fielded active fire extinguishing systems, such as solid propellant gas generators (SPGGs) that generate a mixture of nitrogen, carbon dioxide and water vapor.

Comparisons with halon fire extinguishing systems in engine nacelles or APU compartments were considered, but rejected because significant additional work would be necessary to demonstrate that powder panels would even work in such an area, where airflow and hot surface ignition are concerns. Additionally, in these areas where accidental fires are of an equal or greater concern than ballistic threat-induced fires, powder panel protection is not currently a consideration due to the passive nature of powder panels. This eliminated some potential comparisons on the C-5 and B-1 aircraft, for example.

One forward-fit example explored was the C-130 Hercules aircraft. The C-130 outer wing leading edge is not currently protected by a fire extinguishing system. The wing is divided into two segments, the center wing section (CWS) and the outer wing section (OWS). Since the outer wing fuel tanks are vulnerable to

enemy fire, but currently have no fire protection, and because data were available (including wing geometry) for an estimated active fire extinguishing system, it was practical to use this example.

A preliminary analysis was conducted for the OWS leading edge dry bays circa 1996 to estimate the mass of an SPGG fire extinguishing system using then off-the-shelf components. The masses were estimated for the wing leading edge dry bays between engines #1 and #2 and between #3 and #4 (referred to as inboard leading edge dry bay) and outboard of the #1 and #4 engines (referred to as outboard leading edge dry bay). This analysis also included estimates for the engine area dry bays, but for purposes of this study, the comparison is limited to the leading edge dry bays. It was estimated one inboard leading edge dry bay would require about 1,070 g of agent and an outboard leading edge dry bay would require about 1,190 g. To provide this agent to each dry bay would require three 420 g unit generators each. The mass for each unit is about 1,300 g, for a total generator mass on one wing of 7,810 g. One controller would weigh about 1,920 g, which would be capable of controlling all the SPGGs in both wings. It is estimated both the inboard leading edge and the outboard leading edge would each require three optical sensors. Each sensor weighs approximately 177 g, for a total mass on one wing of 1,060 g. For purposes of this study, the cables and braces or mounting hardware required was arbitrarily assumed to weigh about 10 % of the SPGG and sensor mass for each dry bay. This mass could be more significant, depending upon where the controller is located, but should provide a slightly better estimate than ignoring this mass.

Feasibility and demonstration testing of SPGGs was conducted in the C-130 Vulnerability Reduction Program, as part of C-130J Live Fire Test & Evaluation, and determined that the mass of agent in the 1996 preliminary analysis was likely overestimated.<sup>29</sup> However, the estimates provided are the best available since a fully optimized system has not been examined. Table 9–7 provides mass estimates for each of the SPGG system components for the C-130 outer wing's leading edge dry bays.

Table 9–7 also provides estimates for enhanced powder panel fire protection systems. Estimates are shown for both a lower mass version (areal density of 1.60 kg/m<sup>2</sup>) and a heavier version (2.05 kg/m<sup>2</sup>), both of which have been demonstrated to be effective in this program. Areal densities for the commercial powder panels tested in this program ranged from 1.92 kg/m<sup>2</sup> to 2.08 kg/m<sup>2</sup>. An estimate using the lower mass 175 g commercial powder panel is shown. An estimate is also provided for the mass of adhesive to attach either enhanced or commercial powder panels. Finally, Table 9–7 shows estimated areas and volumes for the OWS wing leading edge dry bays. The SPGG agent requirements are estimated based upon volume, and the powder panel requirements are based upon wetted front spar area.

Table 9–8 summarizes total mass estimates for each wing leading edge fire extinguishing system for an entire C-130 aircraft (both wings). The data show that enhanced powder panels can be very competitive with SPGGs in terms of mass for such a system. For this example, the 1.60 kg/m<sup>2</sup> enhanced powder panel system would weigh about 0.8 kg more than the SPGG system for the entire aircraft. The lighter mass enhanced powder panel would obviously be a design objective, since for this application it could be as much as 5.6 kg lighter than its higher areal density counterpart. Future work will determine if further optimization is possible. The lighter commercial powder panel evaluated in this program was just under the mass of the heavier enhanced powder panel by 1.6 kg. The powder panel mass was calculated, as if they were applied across the entire surface area of the leading edge spar. With external stiffeners located across the surface of the spar, it is likely modular powder panel sections would be inserted between stiffeners. This would further reduce powder panel mass. Also, the mass of protective foam and tape typically used in the vicinity of SPGG discharge areas was not estimated, so the SPGG system mass would likely be higher. For a full analysis of this example, other issues such as cost and complexity

would also need to be examined. Obviously, the powder panel systems should be relatively simple to apply and maintenance free once applied. The complexity of integrating an active fire extinguishing system would be more complicated and involve some power requirements, safety concerns, and perhaps integration issues with other systems.

**Table 9–7. C-130 Wing Leading Edge Dry Bay Fire Extinguishing System Component Mass Estimates.**

Description	Inboard Leading Edge	Outboard Leading Edge
Volume	1.52 m <sup>3</sup>	1.68 m <sup>3</sup>
Area	2.73 m <sup>2</sup>	3.43 m <sup>2</sup>
SPGG Propellant Required	1,070 g	1,190 g
Number of SPGGs (420 g Units)	3	3
SPGG Mass (3)	3,910 g	3,910 g
Number of Optical Sensors	3	3
Optical Sensor Mass (3)	530 g	530 g
SPGG Controller Mass	1,920	-
Wiring, Brackets and Mounting Hardware (Estimate 10 % of SPGG/Sensor Mass)	444g	444g
Light Enhanced Powder Panel Mass - 1.60 kg/m <sup>2</sup>	4,370	5,490
Heavier Enhanced Powder Panel Mass - 2.05 kg/m <sup>2</sup>	5,600	7,030g
Commercial Powder Panel Mass - 1.92 kg/m <sup>2</sup>	5,240g	6,590
Adhesive Mass for Powder Panels (Estimate 10 % of Heaviest Panel Mass)	560 g	700 g

**Table 9–8. C-130 Wing Leading Edge Dry Bay Total Fire Extinguishing System Mass Estimates.**

Fire Extinguishing System	Total System Mass
Solid Propellant Gas Generator System Mass	21.4 kg
Lighter Enhanced Powder Panel Design 1 Mass - 1.60 kg/m <sup>2</sup> (0.327 lb/ft <sup>2</sup> )	22.2 kg
Heavier Enhanced Powder Panel Design 2 Mass - 2.05 kg/m <sup>2</sup> (0.420 lb/ft <sup>2</sup> )	27.8 kg
Commercial Powder Panel Mass - 1.92 kg/m <sup>2</sup> (0.394 lb/ft <sup>2</sup> )	26.2 kg

Data were available for a second comparison of enhanced powder panels, in this case with a current gas generator system on the V-22 aircraft. The outboard tip rib dry bay on this aircraft has a volume of approximately 0.260 m<sup>3</sup>. No airflow passes through this dry bay. Other relevant design details are part of the aircraft technical specifications and will not be described in detail. The active fire suppression system in this area consists of a 626 g inert SPGG, including 189 g of agent, and a 284 g sensor/detector. Testing was conducted on a larger inboard tip rib dry bay and this system was sized according to successful configurations in that area. The dry bay is monitored by a control box that currently monitors other areas of the aircraft, so no new mass was added for this equipment. Wiring and mounting hardware was added to the mass estimate, since this equipment is necessary specifically for this dry bay. The wiring would have to run to the control box in a central location. In the previous example, approximately 444 g was added for wiring and accessories. For this single generator and sensor, the mass for this estimate was reduced to 33 % of this estimate or 148 g for one wing, which is likely a favorable estimate. The total mass estimate for one wing would, therefore, be approximately 1060 g. For comparison, masses for both

enhanced powder panel designs discussed previously were estimated for this dry bay. The lighter mass powder panel, with an areal density of  $1.60 \text{ kg/m}^2$ , would weigh about 710 g per wing. Incorporation of the heavier enhanced powder panel, with an area density of  $2.05 \text{ kg/m}^2$ , would weigh about 910 g. The commercial powder panel by contrast, with an areal density of  $1.92 \text{ kg/m}^2$ , would weigh approximately 860 g. Table 9–9 summarizes these mass estimates.

**Table 9–9. V-22 Outboard Tip Rib Dry Bay Fire Extinguishing System Component Mass Estimates.**

Description	Outboard Tip Rib Dry Bay
Solid Propellant Gas Generator Mass(1)	630 g
Sensor/Detector Mass (1)	280 g
Wiring, Brackets and Mounting Hardware Mass (Estimate 33 % of Previous Example with 3 SPGGs)	150 g
Lighter Enhanced Powder Panel Design 1 Mass - $1.60 \text{ kg/m}^2$	710 g
Heavier Enhanced Powder Panel Design 2 Mass - $2.05 \text{ kg/m}^2$	910
Commercial Powder Panel Mass - $1.92 \text{ kg/m}^2$	860 g
Adhesive Mass for Powder Panels (Estimate 10 % of Heaviest Panel Mass)	90 g

Table 9–10 tabulates the total mass for the aircraft (both wings) for each of the fire protection systems. These data show the lightest enhanced powder panel weighs about 500 g less than the inert SPGG system. Even the heavier enhanced powder panel design would be very comparable, weighing about 100 g less than the inert SPGG system. The commercial powder panel system would weigh about 280 g more than the enhanced powder panel design, but still less than the SPGG system. Obviously, one major difference in this example was the existence of a controller on the aircraft for the active system, which did not add mass, but the overall active system still weighed a little more. Although the differences in mass for both comparisons are quite small, it is well known that aircraft mass increases carry large price tags. A judgment would need to be made based upon system cost and the savings in complexity, whether or not the mass differences (savings or cost) for the enhanced powder panel system would be worthwhile. Further optimization of these enhanced powder panel designs in subsequent programs may further reduce the mass differences between this passive fire extinguishing system and this active fire extinguishing system. Many other comparisons are possible between the enhanced powder panels and other fire protection methods. However, the purpose of the examples provided above was to simply demonstrate that enhanced powder panels, which have been demonstrated in live fire tests to be effective, have also been optimized to levels that make consideration of this vulnerability reduction technique valuable.

**Table 9–10. V-22 Outboard Tip Rib Dry Bay Total Fire Extinguishing System Mass Estimates.**

Fire Extinguishing System	Total System Mass
Solid Propellant Gas Generator System	2,120 g
Lighter Enhanced Powder Panel Design 1 Mass - $1.60 \text{ kg/m}^2$	1,610 g
Heavier Enhanced Powder Panel Design 2 Mass - $2.05 \text{ kg/m}^2$	2,010 g
Commercial Powder Panel Mass - $1.92 \text{ kg/m}^2$	1,900 g

### 9.2.11 Summary of Powder Panel Research Program

This NGP research has led to major gains in efficiency and effectiveness of powder panels, and has reached the point where there are alternatives to halon-like compressed systems suitable for controlling fires in aircraft dry bays. Although additional work is necessary to address manufacturing issues and ensure enhanced powder panels meet the requirements of individual aircraft programs, powder panel technology is a viable option for future fire protection of aircraft dry bays.

Findings from this research revealed that realistic powder panel concepts can significantly enhance the fire extinguishing effectiveness of this vulnerability reduction method. Enhanced powder panel designs can afford the following benefits over current commercial powder panel designs:

- greater front face area removal to allow more powder to escape,
- greater powder release into the dry bay,
- better dispersion of powder to prevent ignition off-shotline,
- longer powder suspension to prevent fire ignition for longer periods of time,
- design flexibility to target mass, durability, and application-specific design goals, and
- significantly improved fire extinguishing effectiveness over commercial powder panels, achieved at an equal or lighter mass and thickness.

Optimization goals were achieved for enhanced powder panels in this project. These goals were to lower enhanced powder panel mass and thickness to the levels of current commercial powder panels or below and to demonstrate greater performance in live fire testing. Enhanced powder panels evaluated in final demonstrations ranged in mass from 140 g to 230 g, with four of the six panels being lighter than the commercial powder panel evaluated (190 g). Thicknesses ranged from 1.9 mm to 2.2 mm, while the commercial powder panel thickness was 2.7 mm.

Live fire testing conducted in a dry bay of realistic size for an aircraft (0.45 m<sup>3</sup>), with an actual ballistic threat (12.7 mm API), and about 50 l of JP-8, resulted in the prevention of fire ignition in four out of six tests. In a fifth test, a fire starting from an existing pool of fuel was quickly extinguished (after only 0.28 s) by an enhanced powder panel. The cause of a lone unsuccessful test resulting in a fire was attributed to an inadequate attachment adhesive on the back of the enhanced powder panel. The test of a commercial powder panel resulted in a fire; however, the attachment adhesive again failed to hold. Although the commercial panel test was not conclusive, a further examination of the test results indicated a significant increase in vital performance characteristics for the enhanced powder panels. Despite being as much as 26 % lighter and 29 % thinner, the enhanced powder panel tests resulted in at least 34 % greater front face area removal and at least four times greater powder release. Powder was evident on surfaces throughout the dry bay following enhanced powder panel tests and was visibly suspended in the dry bay up to five minutes after some of the enhanced powder panel tests. No evidence was present of dispersed and/or suspended powder in the commercial powder panel test.

A number of lessons were learned about effective powder panel design. Some, previously discovered, were reaffirmed. Among the key lessons learned were:

- Brittle or frangible front face materials outperform ductile or tough materials.

- Front face crack growth optimization can be designed into the powder panel through the use of particular front face materials, thicknesses, rib designs, attachment methods to the ribs, and even surface scoring.
- A strong synergism exists between the rib structure and the front face design.
- The back face can be designed to aid in powder dispersion and/or reduce fluid leakage.

Another key finding in this program is that there are design features associated with enhanced powder panels that can make them very resistant to accidental leakage. With the use of plastics and certain composites, there are adhesives to attach the various elements of the panel that form extremely tight bonds. The selection of a front face material and thickness can take into account the likely harsh environment to which the powder panel will be exposed. Accidental leakage has been a significant concern for aircraft designers considering powder panels and is the primary reason that  $\text{Al}_2\text{O}_3$  has been the only chemical fire extinguishing powder finding production usage. With this resistance to accidental leakage in certain designs, perhaps other lighter mass and improved performance fire extinguishing agents can be considered. Not only are other powders lighter in mass, but improved effectiveness of these powders may lead to reduced requirements for powder loading.

To fully take advantage of the potential benefits from enhanced powder panels, further examination of the more promising designs should be performed for potential qualification test requirements. These may include, but are not limited to, operating temperature, chemical exposure, vibration, impact resistance, and moisture absorption. These issues were considered in the selection of materials for Phase II optimization testing, but qualification testing for these parameters was not conducted.

Despite significant increases in powder release for enhanced powder panels, a balance must be achieved between mass/thickness and effectiveness. For protection against larger threats, it may be warranted to consider higher powder loading, which is the significant mass driver. For strict mass restrictions, testing may be required for the given powder panel to determine the type and size of the threat for which protection is afforded.

As the previous section detailed, enhanced powder panels have been developed with increased effectiveness over current powder panel designs at equivalent or better mass and size. These enhanced powder panel designs can now be examined for various applications, particularly in military aircraft, as a trade-off with other fire extinguishing systems. Additional work will be required with the examination of production design requirements, which may cause some adjustments in the selection of materials or sizing, but the design principles should be in place. Some manufacturing concepts were developed and others conceived as a result of this work, which will need to be optimized for production application.

The potential of enhanced powder panel designs for increasing effectiveness without negatively impacting mass and other concerns has generated renewed interest by several aircraft programs. Among the programs inquiring about enhanced powder panel development are the F-35 Joint Strike Fighter, CH-53E Super Sea Stallion, RAH-66 Comanche, and the V-22 Osprey. Successful live-fire tests have been conducted on a production AH-1Z Super Cobra.

## 9.3 SOLID PROPELLANT GAS GENERATORS<sup>30,31,ii</sup>

### 9.3.1 Brief History

Solid propellant gas generators (SPGGs) are devices designed to produce gases of a desired composition (e.g., nitrogen, water vapor, and carbon dioxide) from condensed reactants similar to those used in solid rocket motors. SPGGs are compact, they can generate gases that are inert in fires, they do this quickly (fractions of a second) and on demand, and they produce gas temperatures that are very hot (greater than 1200 °C). The first three attributes (compactness, inert gases, and release on demand) are what make SPGGs attractive for fire suppression applications in aircraft; the fourth attribute (high exhaust temperature) is a limitation.

Prior to the advent of the NGP and its predecessor program to identify alternatives to halon 1301 for aircraft fire suppression applications, gas generators had been used primarily for automobile airbags and for inflatable slides for emergency evacuation of airplanes. In the early 1990s, development of the F/A-18 E/F and V-22 aircraft demanded a non-halon fire protection system to mitigate the hazard of fires due to equipment failures, accidents and enemy attack. Testing performed at the Weapons Survivability Lab of the Naval Air Warfare Center-Weapons Division (NAWCWD)-China Lake demonstrated that SPGGs could be integrated into a system that provided an effective alternative to halon 1301 for fire protection in military aircraft dry bays.<sup>32,33,34,35</sup>

Between 1993 and 1996, the Naval Air Systems Command (NAVAIR) sponsored live fire testing of SPGG systems develop by the Rocket Research Company (now Aerojet Redmond). The tests demonstrated the effectiveness of SPGGs in suppression of various fires in the F/A-18 E/F dry bays and the V-22 wing dry bays. Since the original F/A-18 E/F and V-22 programs, new propellants have been developed that implement some degree of chemical activity into the formulation.<sup>36,37,38,39</sup>

The SPGG program sponsored by the NGP was a collaborative effort between a group at Aerojet (that had been with its predecessor companies) and the Naval Air Warfare Center-Weapons Division. The objectives of this program were to develop new highly efficient, environmentally acceptable, chemically active fire suppressant capabilities based upon solid propellant gas generators; and to improve understanding of propellant and additive effectiveness in fire suppression. The program was designed to accomplish the following:

1. Establish baseline SPGG performance with Aerojet propellant designated FS-0140 (EPA SNAP-approved for use in normally occupied spaces).
2. Develop techniques for reducing the combustion temperature of the propellant, such as tailoring the propellant formulations, and for incorporating chemical additives (radical traps and re-light inhibitors).
3. Develop techniques for cooling the combustion products (e.g., coolant beds) to allay such problems as physical deformation or failure of distribution lines and threat to occupants.

---

<sup>ii</sup> Section 9.3 is based on References 30 and 31. Large portions of the text from these documents, along with the figures shown here (except as noted), have been used without further attribution.

4. Characterize the extinguishment mechanisms of solid propellant systems by examining the relative contributions of oxygen displacement, cooling and flame strain effects upon the SPGG-driven suppression event.
5. Modify existing hybrid extinguisher technology using additional gaseous and liquid suppressants, assuring operability at low ambient operating temperatures.
6. Measure the exhaust temperature, burning rates, and suppression effectiveness of the new propellants with and without additives.
7. Correlate laboratory- and mid-scale results.
8. Perform tests on real platforms defined by the weapon systems community (through JTCG/AS) on those agents that performed best in mid-scale tests.

### 9.3.2 Operating Principles

Conceptually, both SPGGs and pressure-bottle (blow-down) systems deliver agent according to the same analytical expression, whereby the rate of agent delivery  $m'_d$  is related to the discharge coefficient  $C_d$  of the agent, the throat area  $A_t$  and the pressure inside the delivery device  $P_c$ , i.e.

$$m'_d = C_d \times A_t \times P_c. \quad (9-1)$$

In a blow-down system, the initial bottle pressure is given by the sum of agent vapor pressure  $P_{vap}$  plus that of a pressuring gas (typically nitrogen)  $P_{pressurant}$ :

$$P_c = P_{vap} (\text{agent}) + P_{pressurant} \quad (9-2)$$

Here,  $P_c$  is at its maximum in the pre-discharge condition, and both  $P_c$  and  $m'_d$  decrease rapidly upon initiation of the discharge process. Where the SPGG differs from the blow-down bottle is its ability to store agent at zero internal pressure, and then to generate high pressures internally by the combustion of the solid propellant to form a blend of inert gases.

For solid propellants,  $P_c$  is directly related to the product of the burning surface area  $A_{surface}$  and the rate at which gas is generated from the propellant, referred to as the burn rate ( $BR$ , in units of cm/s), raised to a power. The logarithm of  $BR$  typically increases linearly with  $\log(P_c)$  with slope determined by the pressure exponent,  $n$ :

$$\log BR = n \log (P_c/A_{surface}) + \text{constant} \quad (9-3)$$

A pressure exponent less than one assures that high combustion-induced internal pressures can be maintained, translating into sustained high rates of agent discharge. Pressure exponents in the range of 1 to 2 result in extremely unstable combustion, with the relevant chemistry dominated by gas phase reactions.

Solid propellants are typically comprised of an intimate mixture of finely ground solid fuels and oxidizers, often blended together with a polymeric binder. The component fuel and oxidizer combine to create exhaust gases, with the generation of heat. For typical solid propellant reactions, exhaust temperatures are in the range of 1700 °C to 2200 °C.

Propellants used in SPGG fire extinguishers are designed to produce an inert gas blend of carbon dioxide, nitrogen and water vapor and to yield cooler exhaust temperatures. The Aerojet propellant FS-0140 used

as the baseline for the current study has  $\text{CH}_3\text{N}_5$  as its fuel and  $\text{Sr}(\text{NO}_3)_2$  as its oxidizer, with  $\text{MgCO}_3$  added to absorb heat and reduce the exhaust temperature. The exhaust product gases from FS-0140 consist of about 45 %  $\text{N}_2$ , 35 %  $\text{CO}_2$ , and 20 %  $\text{H}_2\text{O}$  by volume. The strontium and magnesium form solid oxides in the process. Peak chamber temperatures are around 1200 °C, and are reduced to about 775 °C in the exhaust stream.

Exhaust temperatures can be reduced further by mixing the fuel and oxidizer in off-stoichiometric proportions, by selecting less exothermic fuel/oxidizer combinations, or by adding materials that absorb heat through dilution, phase change, or endothermic decomposition. Propellant additives are also used to increase the radical scavenging propensity of the exhaust products, which, in turn, improve the efficiency by which the fire is suppressed. The temperature and chemical activity of an SPGG fire extinguisher can also be tailored through a hybrid arrangement (a so-called Hybrid Fire Extinguisher), with the propellant exhaust used to pressurize, disperse, and vaporize a liquid agent such as a hydrofluorocarbon or an aqueous solution.

While the mechanisms described above for controlling the exhaust temperatures and chemical activity of the effluent are easy to state on a theoretical basis, the effect of changing the propellant mixture is far from being predictable. This means that many combinations of propellants, additives, pressures and geometries need to be explored experimentally over a range of scales.

### 9.3.3 Experimental Techniques

#### Propellant Screening Tests

The developmental propellants described here were made up in batches less than 1 kg. In a typical process, individual ingredients were pulverized and then wet-mixed in an inert fluorocarbon medium with a polymeric binder. The solid was then collected, dried and compression molded into pellets. Larger batches of propellant were manufactured and pressed on an automated rotary press.

Propellant development for the Aerojet-NAWS China Lake effort generally took place according to (a) initial computational evaluation of candidate mixtures of fuel, oxidizer, processing additives and coolants, followed by (b) small-scale processing of compositions down-selected from (a), and then (c) scale-up of formulations down-selected from (b) in order to facilitate fire suppression effectiveness testing.

Computational evaluation consisted of thermodynamic analysis of the solid propellant compositions using the NAWC Propellant Evaluation Program (PEP)<sup>40</sup> augmented by the JANNAF Thermodynamic Database. PEP models the combustion process in a gas generator in two steps, the first determining equilibrium of the input mixture at a fixed combustion pressure, and the second calculating the equilibrium condition of that combustion chamber mixture upon expansion to atmospheric pressure. Computational inputs consisted of:

- chemical composition of individual ingredients
- enthalpy of individual ingredients
- density and mass fraction of individual ingredients in the mixture
- equilibrium chamber pressure (generally 6.9 MPa)

- equilibrium exhaust pressure (generally 101 kPa)

The outputs were:

- chemical constituents (and their respective fraction) at specified equilibrium conditions
- bulk adiabatic temperatures of combustion products formed at equilibrium at combustion chamber pressure (6.9 MPa) and exhaust pressure (101 kPa)

Preparations followed standard practices for any new propellant mixture, with initial preparation of small (1 g to 5 g) batches of propellant by hand grinding, to verify adequate safety properties (standard propellant testing includes sensitivity to impact, friction, and electrostatic discharge, ESD). Suitable mixtures were then scaled up to batches of 50 g to 1 kg for further evaluation.

New propellant formulations tested under the NGP were prepared by either dry or wet techniques. In a typical dry process, individual ingredients were weighed, combined with ceramic grinding media in a mechanical ball mill for dry-blending, and then dry-pressed into tablets for burn rate testing. Individual components were normally pre-ground to specific particle sizes and then added to the mixture for blending to a uniform composition, and then pressed on an automated rotary press. In a typical wet process, ingredients were weighed, pulverized and then wet-mixed in an inert fluorocarbon medium, where polymeric binder was deposited upon the powder and the mixture precipitated. The solid was then collected, dried and compression molded into pellets.

Preliminary characterization of the different propellant blends typically included analysis according to a burn rate test. Burn rate testing, when taken together with the gas output from PEP thermochemical calculations, provides a measure of the rate of gas/agent evolution from different solid propellant compositions. Most propellant burn rates were evaluated over a range of pressures between 3.4 MPa and 21 MPa.

Burn rate testing was performed by either a strand burner or a window bomb. In the strand burner technique, compression molded cylindrical grains (pills) of approximately 12.7 mm diameter and 12.7 mm thickness were prepared with a non-burning inhibitor (e.g., epoxy). The inhibitor was coated onto the outside circumference of the cylinder, as well as on one circular face. The inhibited grains were placed in a closed bomb, pressurized to a predetermined level (usually 6.9 MPa and 17.2 MPa). The uncoated face of the grain was ignited using an electric match and the time was measured from ignition to the end of the linear burn event. The burn distance/burn time yielded the burn rate.

Initial testing at China Lake was performed in a high pressure window bomb (Figure 9–34). This is a closed vessel, filled with an inert gas to a static pressure, and equipped with two optical windows. The full assembly is shown in the center, with the window for viewing and filming near the bottom. Single burn rate samples (e.g., single extruded grains) were ignited by a hot wire (seen on the left of Figure 9-34) and the rate at which the burning front advanced through the sample was recorded on film. For evaluating burn rate temperature sensitivity, a variable temperature stage was used, with a flow of liquid and gaseous nitrogen through the holes in the copper block surrounding the sample (right side of Figure 9–34) used to control temperature. This film was calibrated and analyzed to determine burn distance, burn time and hence burn rate. The pressure limit of this apparatus extends to 55 MPa, the higher end of nominal gas generator internal pressure maximum. More promising candidates were scaled up to larger batches, and the most promising up to several kilograms in size.

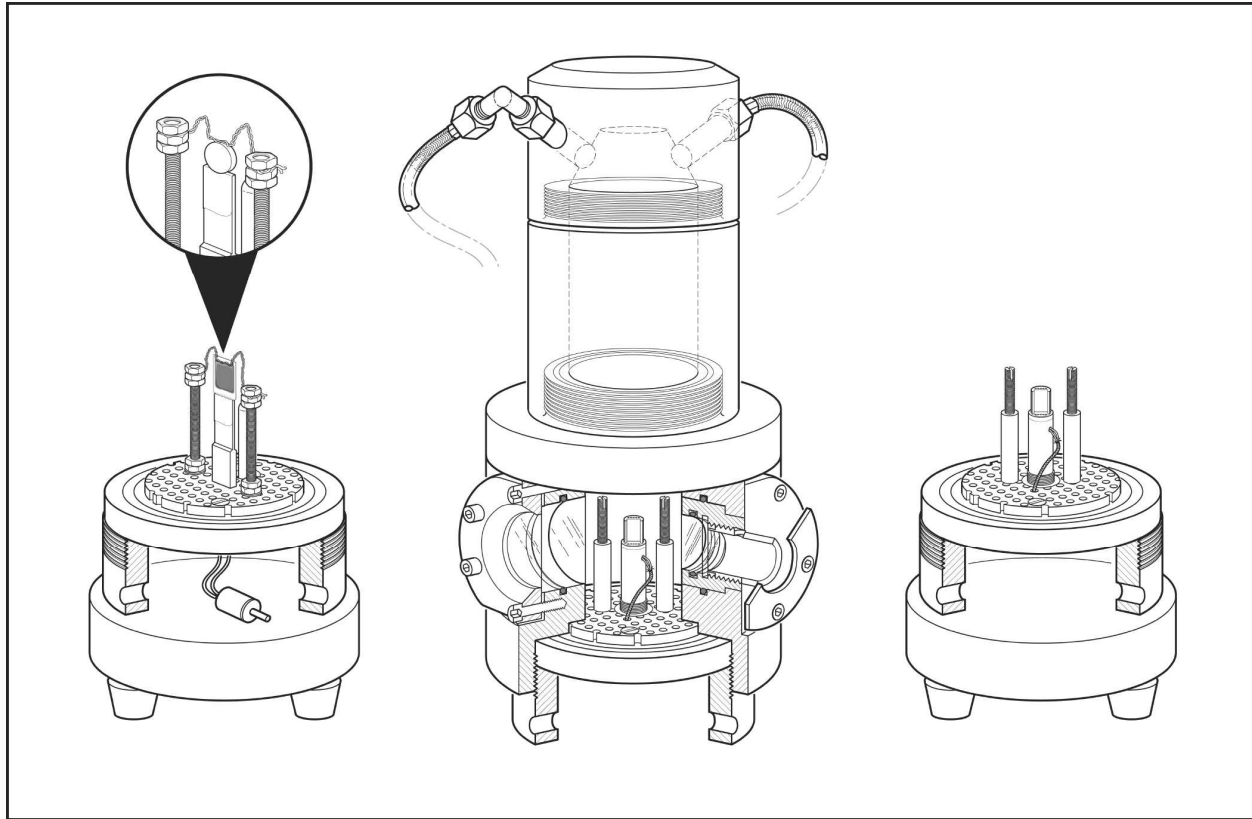


**Figure 9–34. NAWS-China Lake Propellant Burn Rate Apparatus.**

### Fire Test Fixture

The mid-scale Fire Test Fixture (FTF) developed by Aerojet was used to test the effectiveness of various agents under repeatable test conditions. The FTF fixture (shown in Figure 9–35 and Figure 9–36) is 1.87 m long x 0.61 m wide x 0.61 m high and is located in a concrete reinforced test cell with the floor coated with fuel-resistant, non-absorbing material. A schematic of the FTF test facility is shown in Figure 9–37. It consists of several major subsystems including:

- Main test chamber
- Air supply system
- Fuel supply system
- Ignition system
- Suppressant discharge system
- CO<sub>2</sub> emergency extinguishing system
- Control and data acquisition system

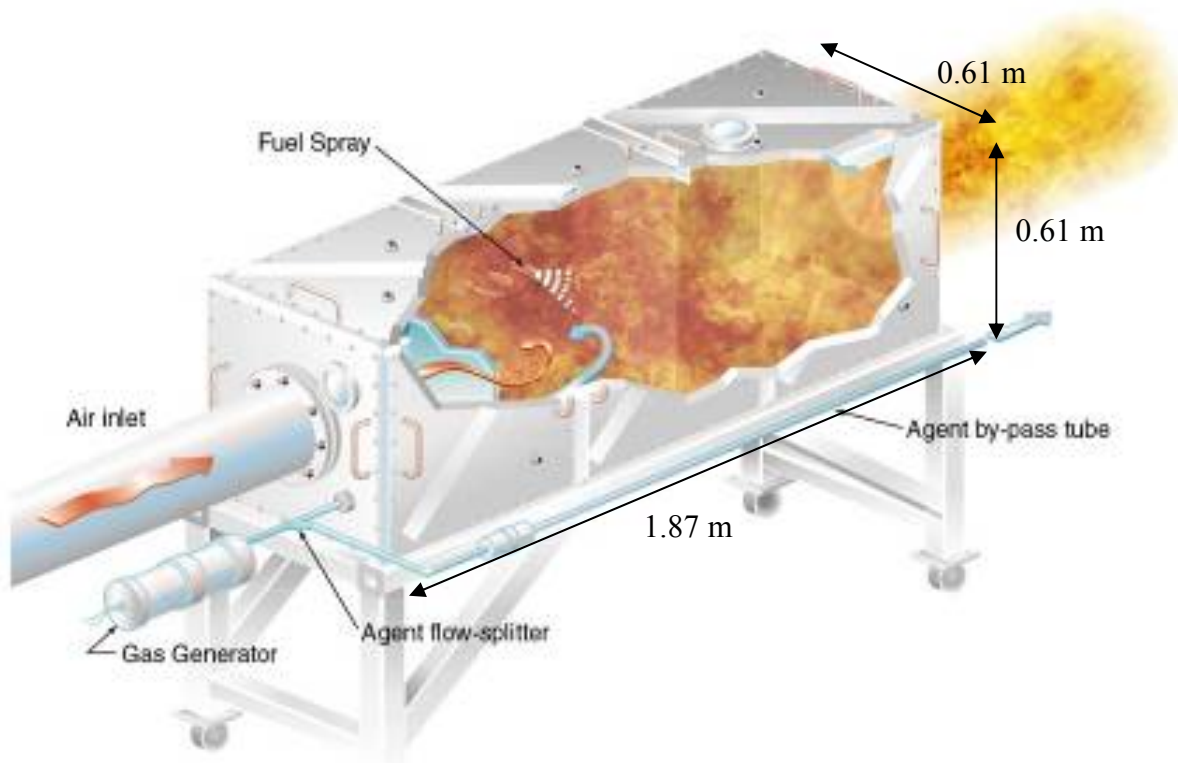


Figure 9–35. Aerojet Fire Test Fixture (FTF).

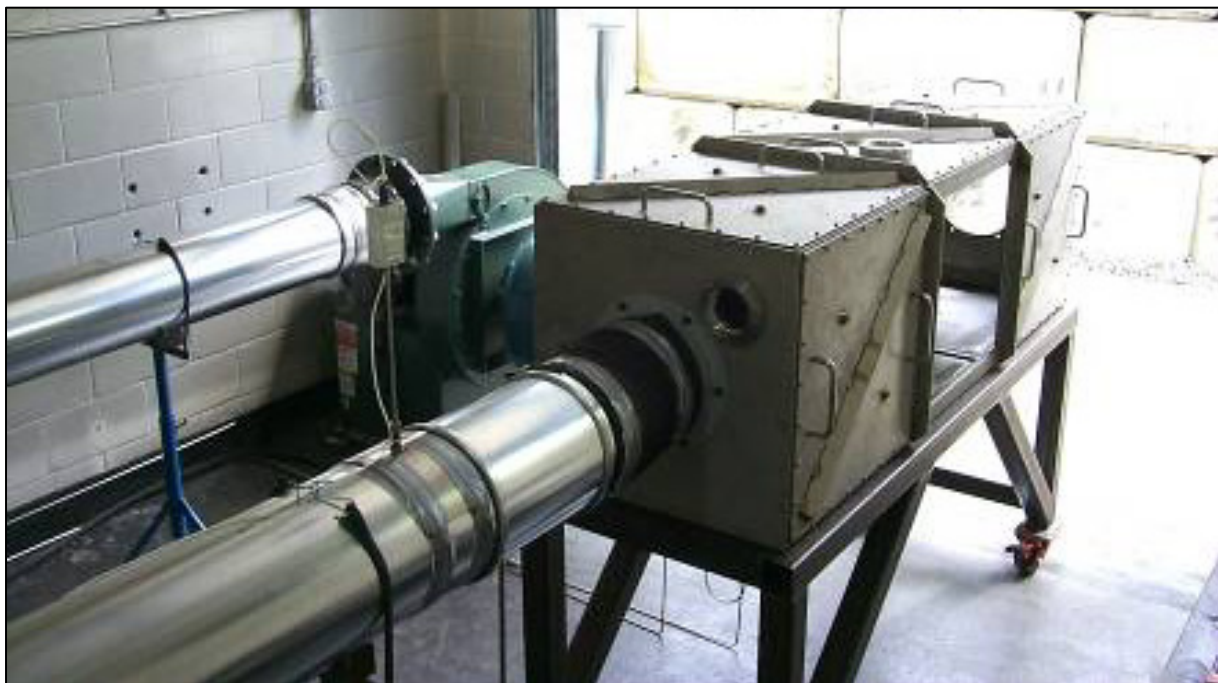


Figure 9–36. Photograph of Fire Test Fixture.

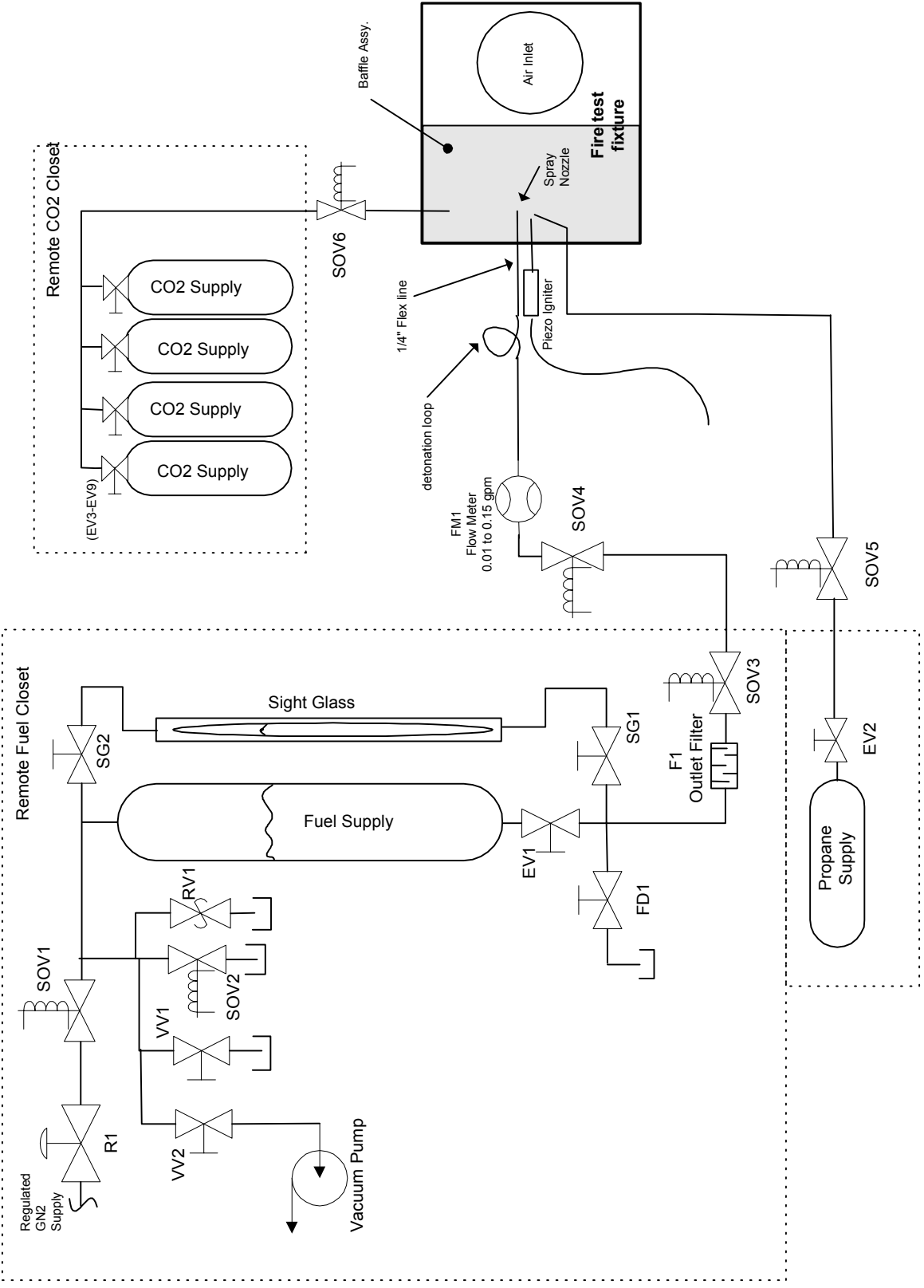
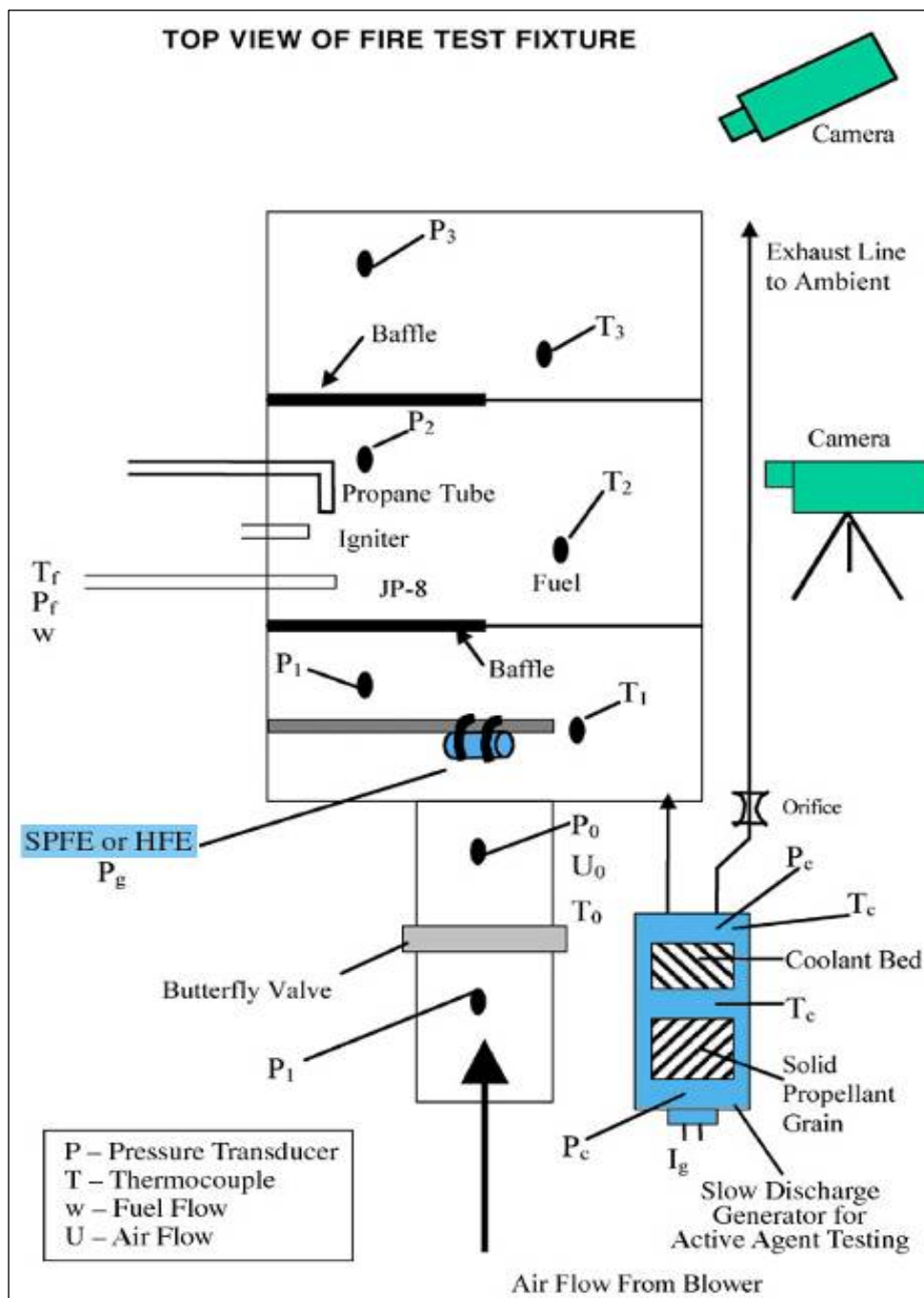


Figure 9-37. FTF Test Facility Schematic.

Various instruments were installed in the solid propellant fire extinguisher and FTF to monitor and control test variables, and to make sure they were in the similar ranges from test to test. These instruments included a pressure transducer in the hybrid fire extinguisher chamber, and thermocouples, pressure transducers, and flow meters in the FTF. The instrumentation layout is presented in Figure 9–38.



**Figure 9–38. Fire Test Fixture Operational Configurations.**

JP-8 was used as the fuel in all of the tests conducted in the FTF. The fuel mass flow was 20.3 g/s, which produced a nominal heat release rate of 1000 kW. The air mass flow was 385 g/s, producing a global

equivalence ratio of 0.80, if one assumes the stoichiometric air-to-fuel mass ratio for JP-8 is 15.18. Table 9–11 provides a summary of the operating conditions for the FTF and Table 9–12 compares these to the operating conditions of other fire test fixtures used in the NGP.

**Table 9–11. Fire Test Fixture Operating Conditions.**

Parameter		Value	
Flow Conditions		Air	JP-8
	Mass flow, m', g/s	385	20.3
	Volumetric Flow, L/s	316	25
	Linear Flow in pipe, cm/s	670	-
Stoichiometry			
	Air-fuel Ratio ( $m'_{\text{air}}/m'_{\text{fuel}}$ )	19	
	Equivalence Ratio	0.8	
Flame Zone Conditions			
	Flame Temperature, K	1200	
	Heat release rate, kW	1000	
	Length, cm	180	
	Cross-Sectional Area, cm <sup>2</sup>	3700	
	Volume, L	670	
	Residence time, s	0.27	
	Agent Injection Interval, ms	Up to 8000	

**Table 9–12. Comparison of Aerojet FTF to Other Fire Test Fixtures.**

Fixture 6	Turbulent Spray Burner <sup>41</sup>	Turbulent Spray Burner <sup>42</sup>	Baffle Stabilized Pool Fire <sup>43</sup>	Baffle Stabilized Pool Fire <sup>44</sup>	FTF
Characteristic					
Length (cm)	5.5	7.5	190	190	180
Cross-Sectional Area (cm <sup>2</sup> )	13.0	19.6	84.6	84.6	3716
Volume (L)	0.09	0.15	16.1	16.1	670
Air Mass Flow (g/s)	21.8	33.0	539	539	385
Residence Time (ms)	5	5	112	35	270
Fuel	JP-8	JP-8	Propane	Propane	JP-8
Fuel Mass Flow (g/s)	0.28	0.34	0.15	0.15	20.3
Equivalence Ratio	0.19	0.16	0.01	0.005	0.80
Fire Heat Release Rate (kW)	13	15.8	7	7	943

The nominal inlet air velocity in the FTF was 6.7 m/s, which, assuming a well-stirred model, leads to a characteristic residence time under cold conditions of about 1.3 s. The residence times when hot or along streamlines that pass by the baffles would be significantly shorter.

Once the desired SPGG device was mounted, the JP-8 spray was initiated and ignited with a propane pilot flame, and the air flow was set to the standard condition. Experience showed that a steady fire could be attained in about 4 s to 5 s. At that time the SPGG was fired, and the agent was discharged.

Depending upon the design, the gas generator device either was located within the FTF in the forward chamber (on a metal bar in the middle of the air flow, shielded from and upstream of the fire), or mounted outside of the FTF adjacent to the air inlet. Figure 9–38 illustrates the gas generator device placement within and outside of the FTF.

Tests were performed using two distinctly different configurations of suppressors mounted to the FTF. In the first configuration, the relative performance of several chemically active additives was determined. This testing utilized a slow discharge (5 s to 8 s) gas generator located outside the FTF; igniting this unit resulted in entrainment of candidate chemically-active agents into a SPGG exhaust stream for delivery to the fire. A neutral-burning solid-propellant gas generator, shown in Figure 9–39 and Figure 9–40, was mounted in the external location; the slow discharge was used in an attempt to minimize flame strain and mixing effects anticipated in rapid discharge tests, thereby emphasizing the performance difference among the various candidates. The discharge of the SPGG for these initial tests had a duration of approximately 5 s. Fine-grid metallic meshes and porous plates were used downstream of the agents to enhance the mixing between the SPGG exhaust and agents prior to entering a distribution tube. The distribution tube was split into two lines, one entered the test fixture, and the other discharged directly to ambient. (See Figure 9–38.) By varying the flow ratio between these two lines, the amount of agent entering the fire zone could be controlled. In the tests, the split ratio was fixed to be 50 %, and the initial agent quantity in the SPGG was varied.

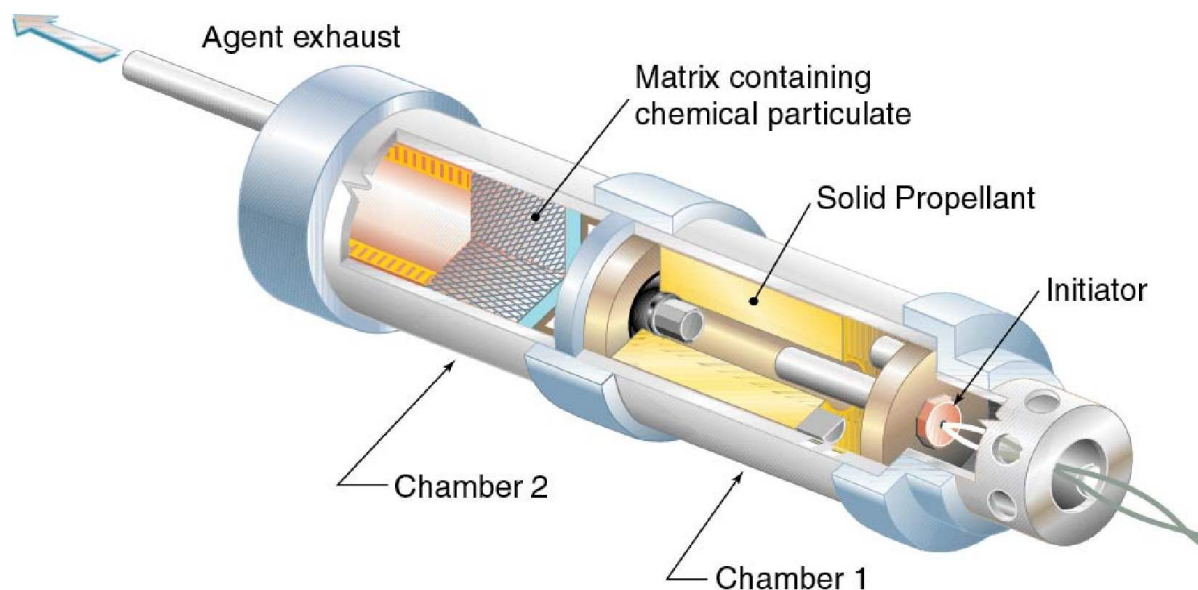


**Figure 9–39. Aerojet Slow Discharge Solid Propellant Gas Generator Test Unit.**



The second test configuration used the fire extinguisher mounted within the FTF in a chamber upstream of the fire. For this testing, the SPGG discharge times were generally maintained between 150 ms and 200 ms for ease of comparison with the original data. The SPGG used for this testing, shown in Figure 9–41, was mounted within the FTF and could be disassembled after a test, refurbished between runs, loaded with weighed quantities of test propellant, readily reassembled, and re-used for additional testing. For the hybrid extinguisher, the hybrid fluid typically surrounds the SPGG, resulting in a bottle within a bottle configuration, as shown in Figure 9–42.<sup>45</sup>

The relative efficiency of different suppressants was ranked based upon their threshold quantity. The threshold was defined as the amount of agent needed to extinguish the fire at least two out of three times. Typically three tests were conducted at the threshold amount and three additional tests were conducted at an agent load greater than the threshold amount. In the first (external SPGG) configuration, a “bleed” line with an orifice to ambient was used to adjust the percentage of agent delivered to the fire; the orifice in this line is gradually closed until testing yields a fire-out time of  $\approx 5$  s. In the second (internal SPGG/hybrid extinguisher) configuration, total agent loads were adjusted up (or down) until threshold levels were achieved. In Figure 9–43 are consecutive frames of a successful suppression event in the FTF.

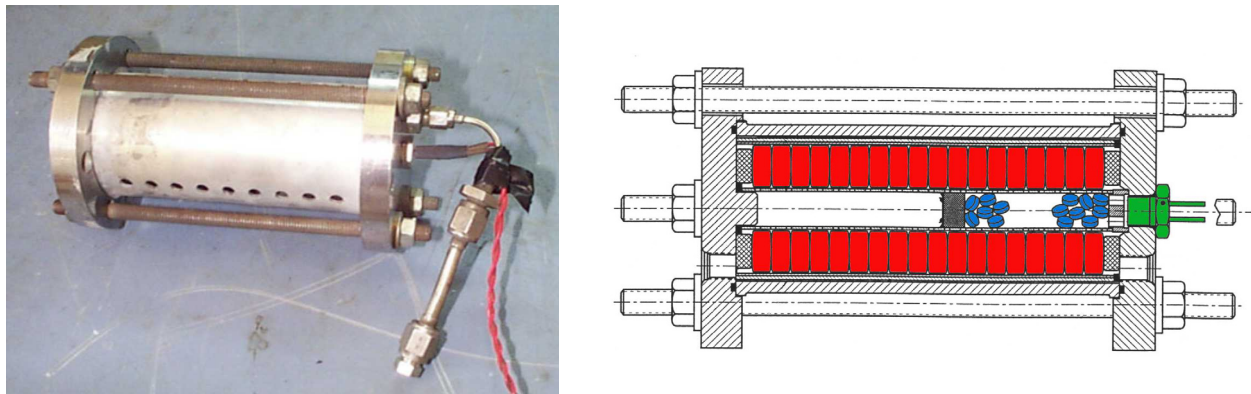


**Figure 9–41. Aerojet Reusable Rapid Discharge Solid Propellant Fire Extinguisher Unit.**

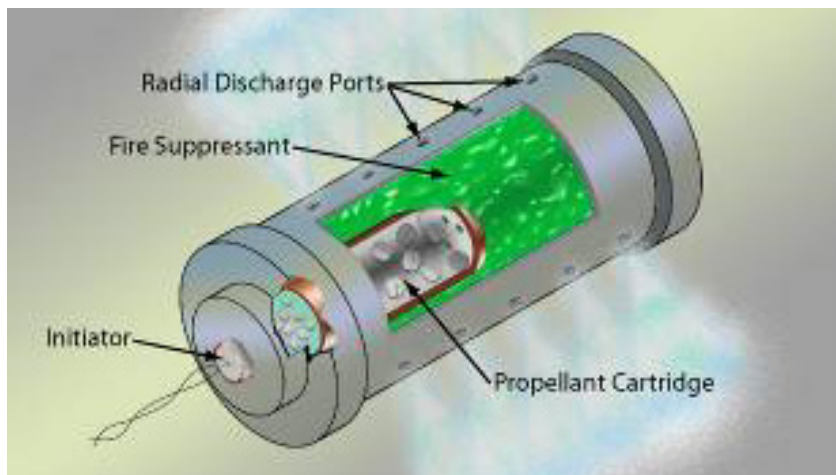


**Figure 9–42. Arrangement of a Typical Hybrid Fire Extinguisher.**

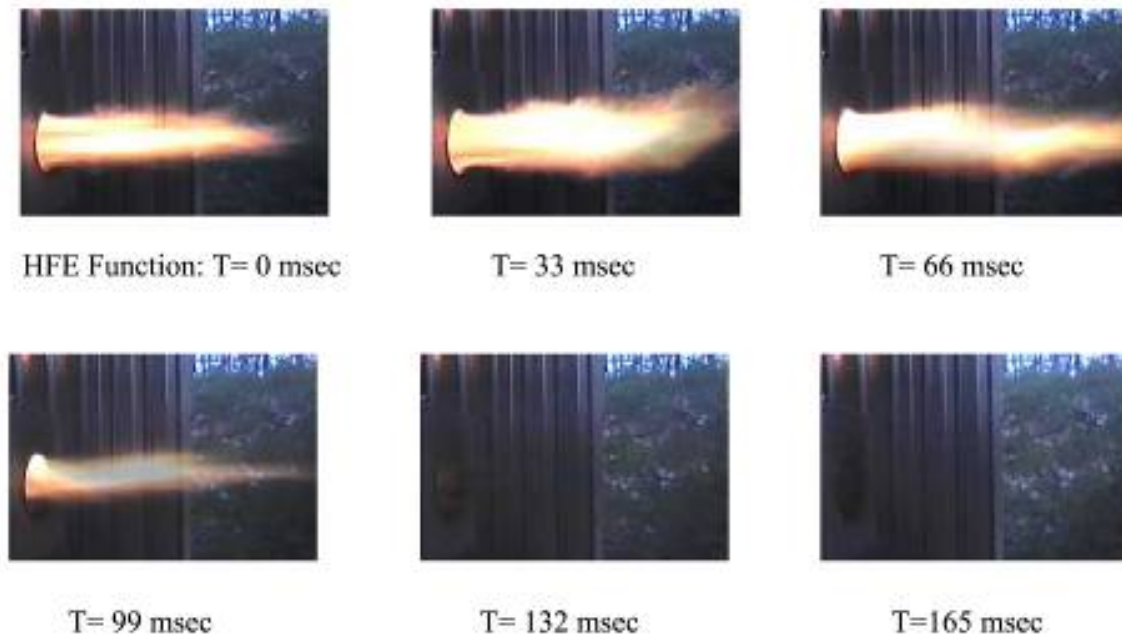


**Figure 9-43. Consecutive Frames during SPGG Suppression of a Fire in the FTF.**

#### **Full-scale Demonstration Tests at China Lake**

Although not included in the NGP-funded program, it is relevant to briefly describe the live-fire testing conducted by Aerojet for NAVAIR to demonstrate SPGG fire suppression technology on full-scale aircraft dry bays. The tests were conducted at China Lake on mid-wing sections and landing gear sponsons.

Figure 9-44 shows an SPGG fire extinguisher with 210 g of chemically active propellant mounted in the landing gear sponson test article. JP-8 filled the fuel line. The main landing gear door was either open or closed, and the external airflow was run up to about 120 m/s. The gun was then loaded, and fired. The projectile impacted the striker plate and fuel line, resulting in a fuel spray that immediately ignited. The SPGG extinguishers were initiated either automatically or following a set delay period after initial impact.

The intent of the mid-wing testing was to evaluate the potential for a common size gas generator for the entire aircraft. Testing evaluated the extinguishment performance of a common sized generator extinguisher at the most challenging fire location of the aircraft (the high airflow mid-wing compartment). The chemical gas generators were installed at various positions, with a typical installation shown in Figure 9-45.



**Figure 9–44. SPGG Installed in Sponson Test Article for Live-fire Demonstration.**<sup>46</sup>  
(Photograph reprinted with permission of the Naval Air Systems Command.)



**Figure 9–45. SPGGs Installed in Mid-wing Test Article for Live-fire Demonstration.**<sup>47</sup>  
(Photograph reprinted with permission of the Naval Air Systems Command.)

### 9.3.4 Results: General Behavior of Propellants

#### General

This research explored several complementary approaches directed toward identifying more effective solid propellant-based fire extinguishers. All of these approaches utilized a solid propellant gas generator to deliver the suppression agent to the fire, including:

- development and characterization of new, cooler solid propellant compositions
- development and characterization of new chemically active solid propellant compositions, and
- development and characterization of new hybrid fire extinguishers.

The benchmark by which all these improvements were measured was the first solid propellant composition manufactured by Aerojet and used on the F/A-18 E/F Dry Bay Fire Extinguisher and the V-22 Wing Fire Protection System. This propellant is referred to as FS01-40.

The thermodynamics, burn rate, and fire suppression effectiveness were studied using the techniques and apparatus described in the previous section, and the results of these studies are reported in this section for each of the three above approaches. The exhaust temperature and momentum, and the temperature of the propellant during discharge, are also important parameters that were examined.

#### SPGG Temperatures and Discharge Pressures

SPGG exhaust temperatures for different propellant compositions were measured at several points along the exit streamline. These measurements indicated gas temperatures varied widely with distance from the gas generator exit, with values near 600 °C directly outside the generator to below 200 °C at points ~ 30 cm from the gas generator. Temperature measurement of SPGG exhaust is complicated by the need for rapid (ms) response in the face of high velocity, high temperature gases. Fine wire thermocouples, while giving good response times, eroded/broke during testing near the gas generator exit; hence, no temperature data for this region are reported.

In a series of hybrid SPGG tests with propellant-to-liquid suppressant mass ratios ranging from about 1:10 to 1:5, exhaust temperatures were much lower than for the SPGG alone, dropping to values between 50 °C and 65 °C. The tests were conducted as “vise shots,” where a hybrid SPGG is mounted in a bench-top vise and held there for functioning (Figure 9–46).

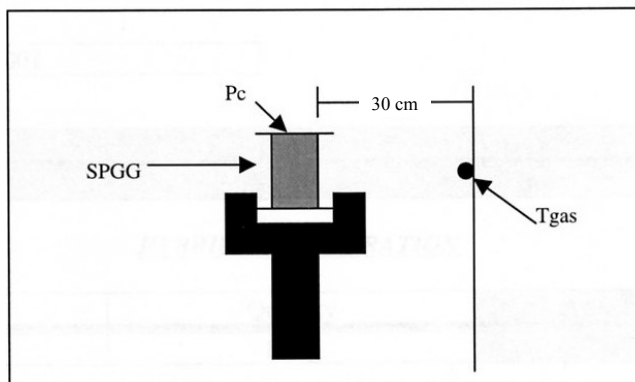


**Figure 9–46. Typical Setup of Preliminary Vise Shot for Hybrid Extinguisher.**

The hybrid configuration used a fixed mass (18 g) of inert solid propellant and different quantities of the HFE-1230 hybrid fluid. The quantity of hybrid fluid varied from 176 g (the standard 1:10 propellant:hybrid mass ratio) to 103 g (a 1:5 ratio).

For each of the tests, the following performance characteristics were recorded: chamber pressure ( $P_c$ ) and temperature of gas downstream of the discharge orifices ( $T_{\text{gas}}$ ). Type-K thermocouples were mounted on a screen  $\approx 30$  cm from the gas outlet (location was aligned with one set of gas outlet orifices) and data were collected at 100 Hz.

Temperatures recorded for the standard 1:10 propellant:hybrid mass ratio were reduced significantly as compared to all-SPGG configurations (55 °C to 60 °C vs.  $\approx 200$  °C, respectively). The recorded performance characteristics reveal that as the quantity of hybrid fluid is reduced (from 176 g to 103 g), the measured internal suppressor pressures are reduced proportionally (17.2 MPa to 9.9 MPa). Temperatures of the mixed air-suppressant exhaust blend, however, vary only slightly, with the reduced quantity of hybrid fluid yielding temperatures of  $\approx 65$  °C as compared to 57 °C for the 1:10 mass ratio.

Discharge rates were varied across a range to determine if this parameter played a role in suppression effectiveness. The rate of mass discharged from a gas generator is related to the internal pressure, which increases with the exposed area of the propellant. Different discharge rates were prepared by using a common propellant but varying the relative surface areas available for burning by making use of different sizes of tablets, while keeping the burning rate constant.

The three tablet sizes considered were small (9.5 mm diameter x 2.4 mm thick); standard or medium (12.7 mm diameter x 6.4 mm thick); and large (12.7 mm diameter x 12.7 mm thick). For the standard sized tablet (CA-04), internal pressures reached 12.4 MPa, and the device discharged the agent in about 0.2 s. For a fixed gas generator load (mass of propellant), the smaller pellet size had a larger total surface area, resulting in faster pressurization (peak pressure of 17.7 MPa) and a discharge time of 0.1 s, which can be seen in Figure 9–47. The large tablets had a smaller surface area (per unit mass) that produced a very uneven burn (yellow trace, Figure 9–47), and peak pressures reached only 5.5 MPa. In some cases the pressures were too low to rupture the burst disks, and when the disks did rupture, burn times stretched out to almost 1 s.

In an attempt to improve discharge characteristics of the larger tablet size, the gas generator orifice area was reduced by  $\approx 50\%$ . This reduction in area results in a less than two times higher internal pressure and a more regular and well-behaved pressurization curve, while retaining the longer discharge time desired. Even with the variations in peak pressures, all the SPGGs evaluated in Figure 9-46 were able to extinguish the fire in the FTF.

Figure 9–48 portrays the temperatures measured using Type K thermocouples tack-welded to the SPGG surface. Measured temperatures appear to peak at about 120 °C. While different tablet sizes do yield different performance times (as seen in the pressurization curve above), the heat output is expected to be unchanged with tablet size, which is approximately the case for the blue and yellow traces in Figure 9–48. The significantly different surface temperatures shown in the pink trace appear to be the result of differences in measurement location and thermocouple attachment quality.

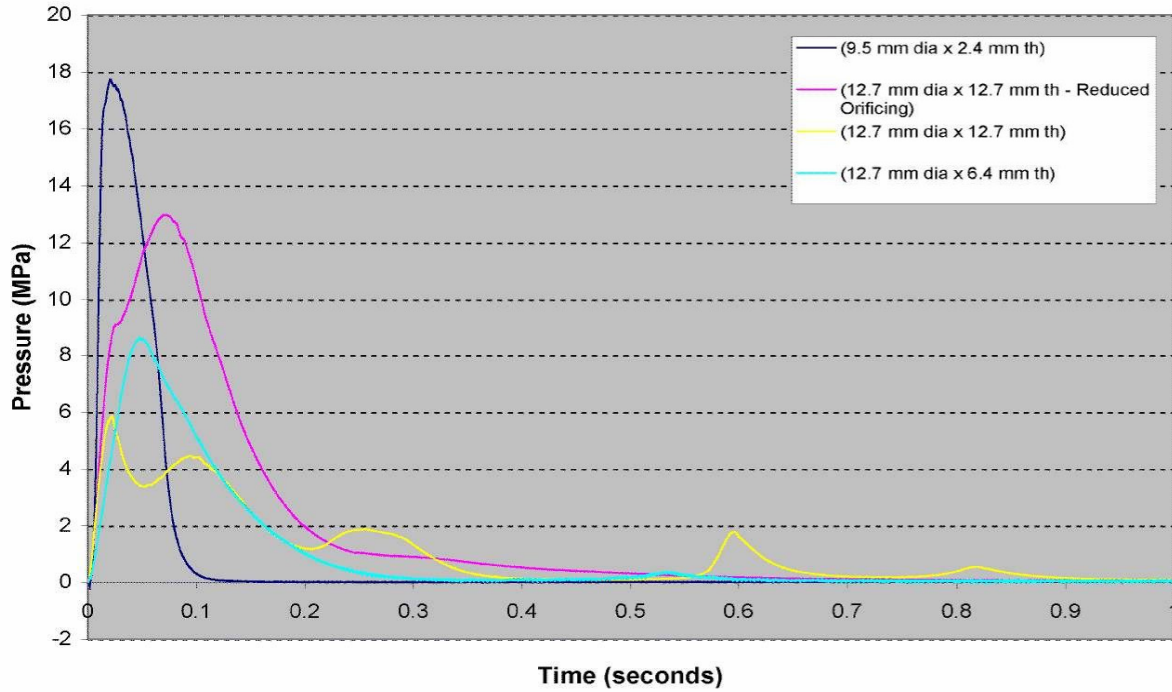


Figure 9–47. Chamber Pressure for Different Propellant Surface Areas (CA-04).

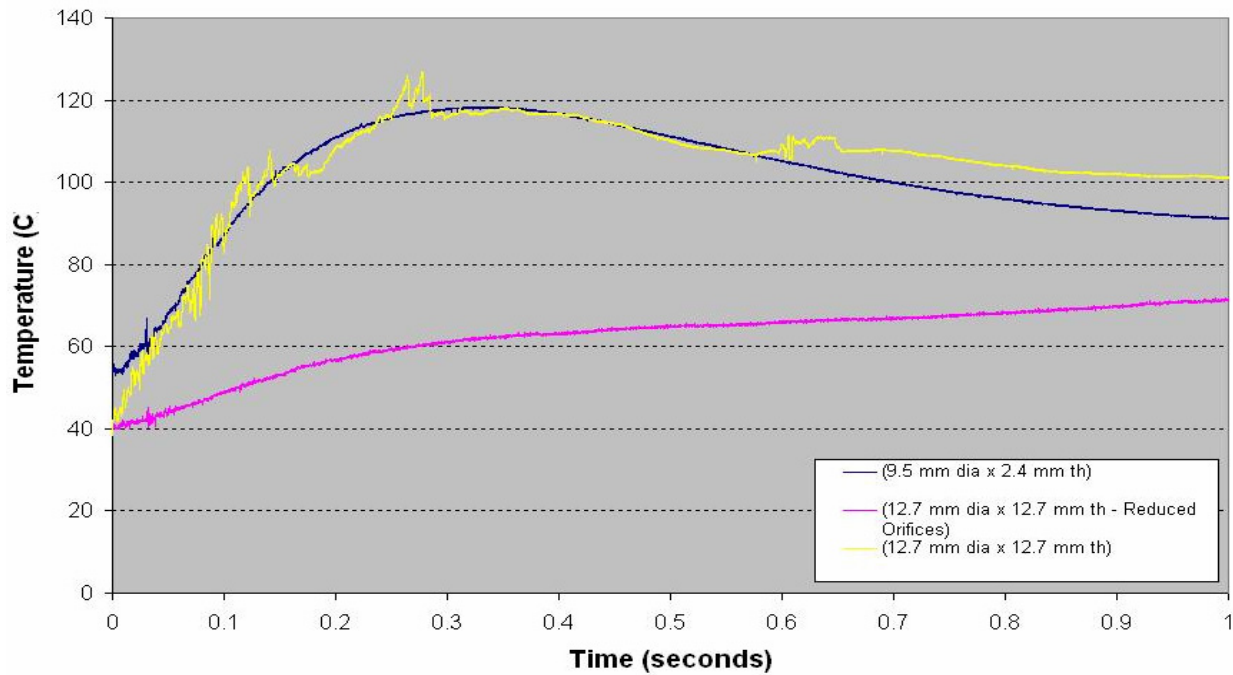


Figure 9–48. Housing Temperatures for Different Propellant Surface Areas (CA-04).

## Effects of Propellant Temperature on Burn Rate

Besides pressure, the burn rate is also dependent on the initial temperature at which the propellant is burned. Higher temperatures generally result in increased burn rates, as is typical for activated processes. Given that most propellant applications require functioning of the propellant device over temperature extremes as wide as  $-50\text{ }^{\circ}\text{C}$  to  $75\text{ }^{\circ}\text{C}$ , a low sensitivity of burning rate on temperature is desirable. Two parameters are typically used to describe this temperature sensitivity of burn rate, the derivative of the linear burn rate with respect to temperature at fixed pressure,  $\sigma_p$ , and the variation in combustion chamber pressure with temperature at fixed propellant geometry,  $\pi_k$ . These parameters are dependent on the nature of the propellant composition, its burn rate and the combustion mechanism of the given propellant, and are defined as follows:<sup>48</sup>

$$\sigma_p = \left( \frac{1}{r} \frac{r_1 - r_0}{T_1 - T_0} \right)_p = \left( \frac{\partial \ln r}{\partial T} \right)_p$$

and

$$\pi_k = \left( \frac{1}{P} \frac{P_1 - P_0}{T_1 - T_0} \right)_{K_n} = \left( \frac{\partial \ln P}{\partial T} \right)_{K_n},$$

where  $r$  is the linear burn rate,  $r_0$  and  $r_1$  are the burn rates at  $T_0$  and  $T_1$ , respectively, and  $K_n$  is defined as the ratio of burning surface area to exit orifice area,  $A_b/A_t$ . For conventional propellants,  $\sigma_p$  ranges between  $0.002/\text{K}$  to  $0.008/\text{K}$ ; for AP-based propellants,  $\sigma_p$  is typically  $\approx 0.0015$ , while for AN-based propellants,  $\sigma_p$  is often in the vicinity of  $0.002/\text{K}$ .

These two parameters can be related to each other through the pressure exponent defined previously,  $n$ .

$$\pi_k = \frac{1}{1-n} \sigma_p$$

Note that in the case of  $n$  approaching 1,  $\pi_k$  can become very large even for small  $\sigma_p$ ; i.e., large changes in chamber pressure can be expected with even small temperature variations.

Table 9–13 shows the measured burning rates at various initial temperatures for the baseline propellant composition used in the current study, along with the derived temperature sensitivity parameters and pressure exponent. These findings reveal that the burn rate increases with temperature in a predictable manner.

**Table 9–13. Temperature Dependence of Burn Rate for Baseline Propellant, FS-0140.**

T, °C	BR <sub>1000</sub> (mm/s)	P <sub>max</sub> (MPa)
-25	12.7	7.83
25	14.0	10.3
75	15.2	12.8
$\sigma_p = 0.13\text{ } \%/^{\circ}\text{C}$	$\pi_k = 0.48\text{ } \%/^{\circ}\text{C}$	$n = 0.73$

### 9.3.5 Results: Cooled Propellant Formulations

The hot exhaust gases of typical solid propellant compositions are not efficient suppressants for combustion reactions. Additionally, the quantity of gases required for suppression may result in over-pressurization conditions when released in enclosed bays, as well as resulting in greater concerns for materials compatibility for the structure surrounding the suppressor. For these reasons and others, cooler solid propellant fire extinguisher compositions are highly desired.

This research explored three different routes towards achieving cooler solid propellant fire extinguisher compositions:

- reducing the enthalpy of the combustion process through selection of various fuels/oxidizer blends;
- altering the stoichiometry and enthalpy of the propellant reactions through various fuel:oxidizer ratios; and
- seeking faster-burning solid propellant compositions, to which one could add coolant to reduce the overall exhaust gas temperature.

### Solid Propellant Combustion Thermodynamics

The impact of different fuels upon calculated adiabatic flame temperatures was explored. The selection of fuels focused on those with nitrogen-nitrogen bonding in the fuels' molecular structure. N–N bonding was considered to provide two distinct advantages: N–N molecular bonds are often kinetically labile and therefore susceptible to rapid reaction with an oxidant; and additional nitrogen atoms in the fuel increases the production of the molecular nitrogen in the exhaust.

Several high-nitrogen fuels were considered. (See Figure 9–49.) A more negative enthalpy of formation generally leads to cooler exhaust products; however, one must also consider the enthalpy of the equilibrium products that are formed. In particular, a higher N:C and N:H ratio in a fuel results in the formation of a greater proportion of N<sub>2</sub> vs. CO<sub>2</sub> and H<sub>2</sub>O gas; the lesser enthalpy associated with N<sub>2</sub> (vs. CO<sub>2</sub> or H<sub>2</sub>O) results in a cooler solid propellant exhaust composition.

Thermodynamic equilibrium calculations of the adiabatic flame temperature (typically conducted at 6.9 MPa) are precise and straightforward. On the other hand, predictive solid propellant kinetics modeling is very poorly developed and unreliable. Hence, characterization of viability of cooler propellant compositions requires complementary thermodynamic modeling together with experimental measurement of combustion kinetics, or burn rate.

The effect of different fuels upon exhaust gas temperatures was determined for a common oxidizer in a stoichiometric mixture. The calculations were performed using the NAWC PEP<sup>40</sup> computer code, and the results are shown in Table 9–14. A review of these data shows that all but the GAZT (bisguanidium azotetrazole)/strontium nitrate blend exhibit adiabatic combustion temperatures well in excess of 2000 K.

Among the fuels studied, 5-amino-tetrazole (5AT) is the most readily available; it and its derivatives are used in several commercially viable automotive airbag formulations. Many of the other fuels considered have limited commercial availability. Preliminary evaluations suggested that bis(5-aminotetrazolyl) tetrazine (BTATZ) would be an attractive candidate for further study because of its high nitrogen content.

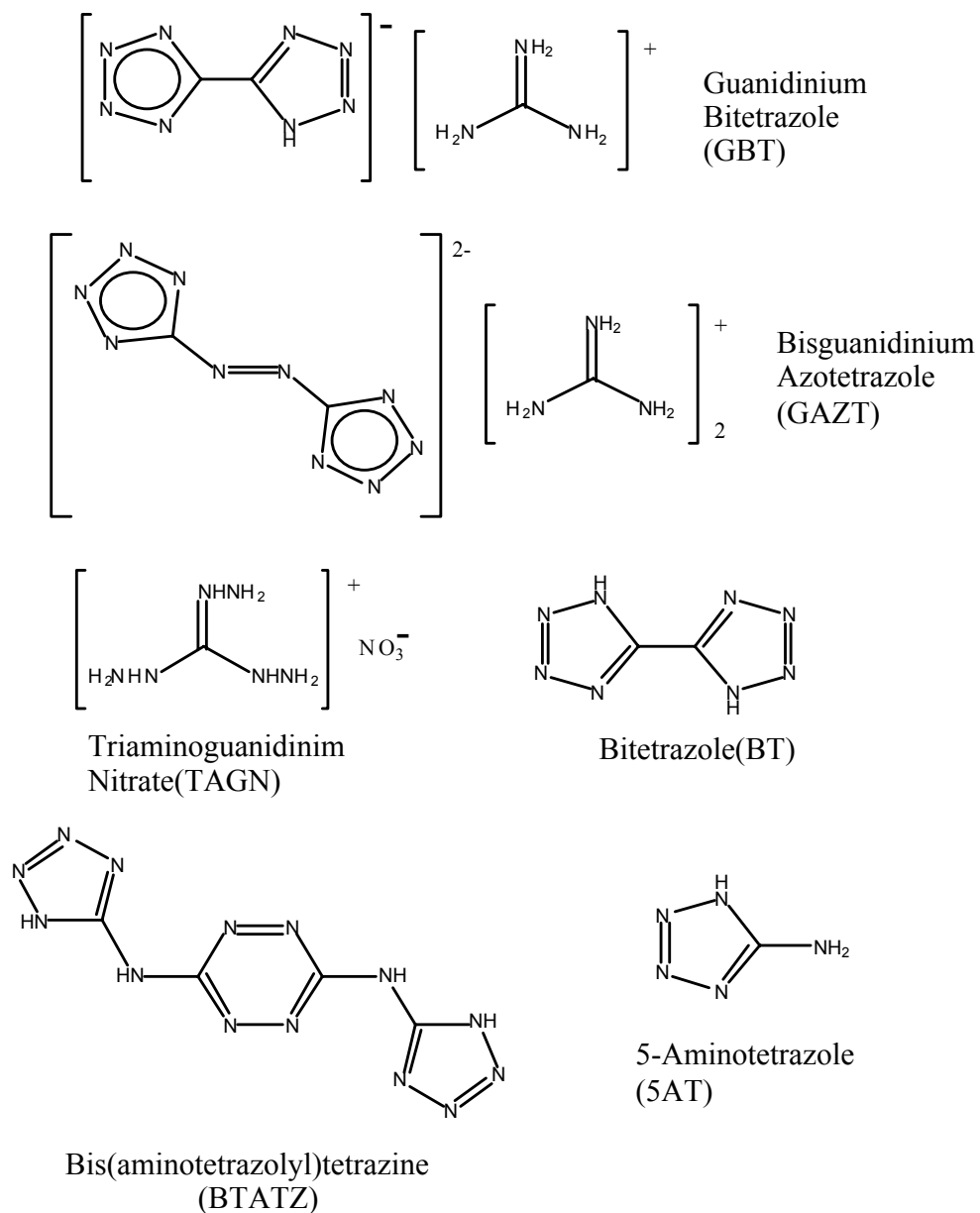


**Figure 9–49. High-nitrogen Fuels Used in China Lake/Aerojet Propellant Development.**

BTATZ was discovered recently by Hiskey et al.<sup>49,50</sup> at Los Alamos National Laboratory (LANL). Its promise as a high-nitrogen, highly reactive fuel led to an extensive NGP effort to explore its utility for solid propellant compositions, and to work to scale up synthesis of this material from the several gram, laboratory level to kilogram quantities.

**Table 9–14. Adiabatic Temperatures of High Nitrogen Propellant Fuels in Stoichiometric Mixtures with Sr(NO<sub>3</sub>)<sub>2</sub> Oxidizer.**

Fuel	Molecular Formula	$\Delta H$ (J/g)	Density (g/cm <sup>3</sup> )	T <sub>c</sub> (K)
5AT	CH <sub>3</sub> N <sub>5</sub>	2450	1.65	2650
BTATZ	C <sub>4</sub> H <sub>4</sub> N <sub>14</sub>	3560	1.74	2750
TAGN	CH <sub>9</sub> N <sub>7</sub> O <sub>3</sub>	-290	1.54	2680
BT	C <sub>2</sub> H <sub>2</sub> N <sub>8</sub>	3350	1.79	2750
GBT	C <sub>3</sub> H <sub>7</sub> N <sub>11</sub>	1540	1.57	2520
GAZT	C <sub>4</sub> H <sub>12</sub> N <sub>16</sub>	-1110	1.66	1930
GN	CH <sub>6</sub> N <sub>4</sub> O <sub>3</sub>	-3530	1.39	2250
NQ	CH <sub>4</sub> N <sub>4</sub> O <sub>2</sub>	-880	1.73	2720

BTATZ is synthesized from commercially available ingredients in a four-step procedure furnished by LANL and outlined in Figure 9–50.<sup>49,50</sup> Reaction of guanidine hydrochloride with three equivalents of hydrazine hydrate yields triaminoguanidine hydrochloride (TAG•HCl) in almost quantitative yield. Reaction of TAG•HCl with 2,4-pentanedione leads to dihydroDMPTZ which upon oxidation with N<sub>2</sub>O<sub>4</sub> gives DMPTZ. Very careful control of the reaction conditions is required for the final step. The solvent used for the reaction (sulfolane) is a solid at room temperature (melting point 28 °C). The solvent is heated to 40 °C and DMPTZ and 5AT are added. This temperature is maintained for 2 hours and then the temperature increased over a six-hour period to 135 °C and held at that temperature for 18 hours. BTATZ precipitates from the reaction mixture during this time. The reaction mixture is allowed to cool to 70 °C and ethanol is added to prevent the mixture from freezing upon further cooling. BTATZ is collected on a medium porosity glass frit and is washed with copious amounts of ethanol. The crude product is purified by trituration with dimethylformamide (DMF) or ethanol, with ethanol giving a higher recovery but providing slightly less pure material. The yield for this last step in a typical experiment is in the 70 % to 75 % range with ethanol purification versus  $\approx$  50% when DMF is employed. The synthesis of BTATZ was carried out initially at quantities of about 1 g for review by the safety committee, as is common for the synthesis of energetic materials. The results and procedures used were reviewed by a panel of experienced energetic materials researchers before any scaling up of the synthesis was permitted. Typically, if upon review, the procedures are deemed safe and the material itself has no hazardous properties that cannot be mitigated through the use of appropriate handling techniques, the reaction can be scaled up by a factor of five. Several results at each level were required for review.

Using these guidelines NSWC staff preceded through the 1 g, 5 g, 25 g, 100 g, 250 g and 450 g levels. All of these reactions were carried out in a laboratory fume hood. At this level, 6 L of solvent were used in a 12 L flask. On the 450 g scale, the product was collected by filtration on two 3 L medium porosity filter funnels. In order to carry out the syntheses described above we needed a large amount of the immediate precursor DMPTZ (C<sub>12</sub>H<sub>14</sub>N<sub>8</sub>). This material is not an energetic material and is not subject to the scale-up limitations described for the synthesis of BTATZ. NSWC staff used a published procedure to carry out the synthesis of approximately 4.5 kg of this material. A further 4.5 kg were supplied by the Los Alamos National Laboratory. Modifications to the purification process provided material with acceptable properties but in higher yield than that using the standard method.

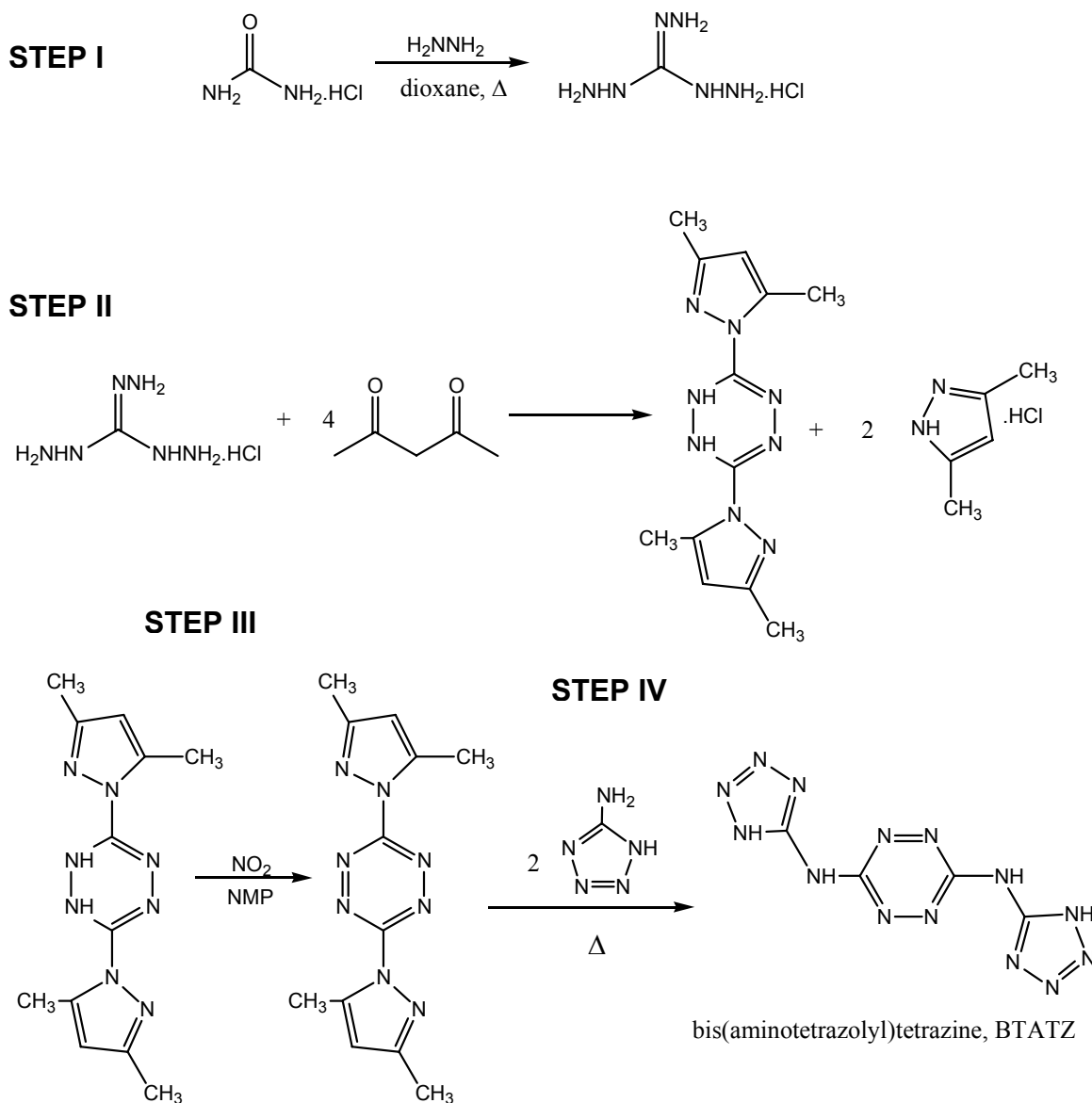


**Figure 9–50. Synthetic Route to BTATZ.**

Further safety data on BTATZ itself has been obtained. BTATZ shows acceptable friction and impact sensitivity but is somewhat sensitive to electrostatic initiation. When formulated into a molding powder with poly(ethyl acrylate) (3 % as a binder) electrostatic sensitivity is still a concern, even when 0.5 % carbon black is added; however when pressed into pellets or deposited as a thin layer the material meets the criteria set for routine handling of energetics. However, shipments of these new energetic materials is still limited to small quantities.

In order to assess the effect of the choice of oxidizer on exhaust gas temperatures, thermodynamic calculations were performed using the NAWC PEP<sup>40</sup> computer code, with different oxidizers and a common fuel (5-aminotetrazole, or 5AT) in stoichiometric proportions. Combustion was assumed to be complete. The results are compiled in Table 9–15.

Among the oxidizers considered, strontium nitrate and potassium perchlorate produced the hottest exhaust gases. The ammonium nitrate/5AT blend, while it produces a lower adiabatic flame temperature, has poor thermal stability, rendering it impractical for use in a fire extinguisher on DoD weapons platforms.

**Table 9–15. Adiabatic Temperatures of Oxidizers in Stoichiometric Mixtures with 5-aminotetrazole.**

Oxidizer	Molecular Formula	$\Delta H$ , J/g	Density, g/cc	Calculated $T_c$ , K
Strontium Nitrate	$\text{Sr}(\text{NO}_3)_2$	-4610	2.99	2650
Potassium Nitrate	$\text{KNO}_3$	-4880	2.12	2150
Potassium Perchlorate	$\text{KClO}_4$	-3210	2.52	2970
Ammonium Nitrate	$\text{NH}_4\text{NO}_3$	-4980	1.72	2390

### High Nitrogen Propellant Burning Characteristics

While fuel and oxidizer thermodynamic studies provide a useful means of predicting appropriate solid propellant compositions having cooler exhaust gases, actual use of a composition requires that it be kinetically robust; i.e., the composition must burn at an appropriate rate.

For different DoD fire suppression applications, agent discharge rates can be expected to extend over a broad range, from 50 ms to 500 ms for aircraft dry bay applications, to 0.5 s to 5 s for aircraft engine bay applications. The focus of this NGP research was the shorter timeframe associated with aircraft dry bays.

The chemical reaction proceeds with a rate that is directly proportional to the pressure raised to the  $n^{\text{th}}$  power. When taking place inside a closed vessel – e.g., a gas generator – pressures typically build to  $\approx 6.9$  MPa to 34 MPa in order to produce consistent performance. The burn rate at 6.9 MPa (1000 psi) is often used as a standard condition for comparison of different solid propellants; this  $\text{BR}_{1000}$  is typically in the range of 5 mm/s to 15 mm/s. For the sake of ease of manufacturability (of both the gas generator and enclosed propellant grains),  $n$  is preferred to be less than 0.6. Propellant compositions exhibiting pressure exponents greater than unity were not considered for further evaluation, as this pressure dependence is not suitable for practical applications.

For this project, several different combinations of fuels, oxidizers and coolants have been modeled and tested. A summary of several cooler propellant compositions is presented in Table 9–16. The baseline solid propellant fire extinguisher composition (FS-0140) can be seen to have a moderately high combustion temperature (1450 K), a moderate burn rate (1.27 cm/s), and a moderate pressure exponent ( $n \approx 0.5$ ). Most of these compositions contain, low levels of the processing/combustion aids including PBA (poly(butyl acetate) binder), C-black (carbon black combustion aid) and mica (a lubricant); oxidizers were typically KP (potassium perchlorate) or KN (potassium nitrate).

**Table 9–16. Development Propellant Compositions and Burning Parameters.**

Propellant Composition (wt %)	Exhaust Species, vol % @ $T_c$	Temperature (K)		Calculated Density (g/cm <sup>3</sup> )	Gas Output (mol/100 g)	Measured BR <sub>1000</sub> (cm/s)	Measured Pressure exponent, n
		$T_c$	$T_{exh}$				
<b>Baseline:</b> 5AT, 21.9, Sr(NO <sub>3</sub> ) <sub>2</sub> 19.1, MgCO <sub>3</sub> 60.0	N <sub>2</sub> 45, CO <sub>2</sub> 35, H <sub>2</sub> O 20	1450	1000	2.55	2	1.27	0.5
<b>5AT:</b> 5AT 86.0, KP 10.0, PBA 3.0, C-black 0.5, Mica 0.5	N <sub>2</sub> 61, H <sub>2</sub> 29, CO 3, CH <sub>4</sub> 3, KCl(s) 5.3 g	1667	874	1.68	4.41	0.43	0.80
<b>BTATZ-1:</b> BTATZ 97.0, PBA 2.0, C-black 0.5, Mica 0.5	N <sub>2</sub> 75, H <sub>2</sub> 24, CO, CH <sub>4</sub>	2349	1151	1.72	3.66	5.44	0.51
<b>BTATZ-2:</b> BTATZ 86.0, KP 10.0, PBA 3.0 C-black 0.5, Mica 0.5	N <sub>2</sub> 68, H <sub>2</sub> 23, CO 9	2290	1135	1.76	3.68	5.46	0.55
<b>BTATZ-3:</b> BTATZ 86.0, KN 10.0, PBA 3.0, C-black 0.5, Mica 0.5	N <sub>2</sub> 69, H <sub>2</sub> 23, CO 8	2085	1088	1.74	3.72	4.57	0.57
<b>5AT/BTATZ-1:</b> 5AT 48.0 BTATZ 48.0, PBA 3.0, C-black 0.5, Mica 0.5	N <sub>2</sub> 68, H <sub>2</sub> 29	1939	908	1.66	4.14	1.40	1.6 (3.45-6.89 MPa)
<b>5AT/BTATZ-2:</b> BTATZ 72.0, 5AT 24.0, PBA 3.0 C-black 0.5, Mica 0.5	N <sub>2</sub> 70, H <sub>2</sub> 28	2118	995	1.69	3.94	4.52	0.71
<b>5AT/BTATZ-3:</b> 5AT 43.0, BTATZ 43.0, KP 10.0, PBA 3.0, C-black 0.5, Mica 0.5	N <sub>2</sub> 63, H <sub>2</sub> 28, CO 6, KCl (s) 5.3 g	1961	967	1.72	4.01	3.85	0.7 (6.89-18.9 MPa)
<b>5AT/BTATZ-4:</b> 5AT 43.0, BTATZ 43, KN 10.0, PBA 3.0, C-black 0.5, Mica 0.5	N <sub>2</sub> 65, H <sub>2</sub> 29, CO 4 K <sub>2</sub> CO <sub>3</sub> (s) 5.3 g	1799	965	1.70	4.10	1.55	1.6
<b>GAZT:</b> GAZT 33.6, KP 62.4, PBA 3.0 C-black 0.5, Mica 0.5	N <sub>2</sub> 28, CO <sub>2</sub> 13, H <sub>2</sub> O 28 H <sub>2</sub> 26, CO 24, KCl(s) 32.6 g	1723	964	1.92	2.51	>6.4	ND
<b>BT:</b> BT 33.6, KP 62.4, PBA 3.0, C-black 0.5, Mica 0.5	N <sub>2</sub> 31, CO <sub>2</sub> 12, H <sub>2</sub> O 10, H <sub>2</sub> 13, CO 29, KCl(s) 32.6 g	2479	1761	1.92	2.13	>6.4	ND
<b>GBT:</b> GBT 33.6, KP 62.4, PBA 3.0, C-black 0.5, Mica 0.5	N <sub>2</sub> 28, CO <sub>2</sub> 10, H <sub>2</sub> O 9, H <sub>2</sub> 23, CO 29, KCl(s) 32.6 g	2000	1457	1.88	2.19	>6.4	ND
<b>TAGN:</b> TAGN 33.6, KP 62.4, PBA 3.0, C-black 0.5, Mica 0.5	N <sub>2</sub> 21, CO <sub>2</sub> 17, H <sub>2</sub> O 30, H <sub>2</sub> 11, CO 13, KCl(s) 32.6 g	2646	1421	1.86	2.44	>6.4	ND

In addition to its high nitrogen content, BTATZ has a high burn rate with a low pressure exponent and burns well even without any added oxidizer. This is attractive because addition of oxidizer leads to a much hotter effluent gas mixture as the product. In contrast, 5AT does not sustain combustion at atmospheric pressure and requires added oxidizer and significant pressure to a burn steadily.

BTATZ was included in several formulations in combination with 5AT in an attempt to increase the efficiency of combustion while keeping oxidizer content to a minimum. A composition with 10 % KP has a very low dependence of burn rate on pressure, with a calculated combustion temperature of approximately 1700 K, and yields over 4 mol gas/100 g, nearly 60 % of which is N<sub>2</sub>.

A concern in most of these compositions is the high fraction of un-oxidized gases in the exhaust. Hydrogen levels are typically in the 10 % to 30 % range, with CO levels 5 % to 10 %. Although these gases are always diluted in N<sub>2</sub>-dominated exhaust, their presence would seem to represent a challenge in suppression applications. The CO levels would render their use unattractive in occupied spaces.

Over the range 6.89 MPa to 18.9 MPa the pressure exponent for formulation 5AT/BTATZ-3 is 0.5 and decreasing. This formulation is a promising candidate as the burn rate is relatively high at low pressures and has a decreasing pressure dependence of the burn rate. Formulations BTATZ-2 and BTATZ-3 also exhibit ideal burning characteristics for gas generator applications with pressure exponents around 0.5 and with relatively high burn rates.

BTATZ and its blends offer the potential for SPGG formulations with higher gas output and cooler effluents at low pressure. Low-pressure operation offers the possibility of constructing hardware from lighter mass materials resulting in an overall significant reduction in mass of the system. Evaluation of these compositions did not result in truly applicable, cooler solid propellant fire extinguisher compositions. However, several of these compositions offered promise for applicability when additives are used to promote cooler exhaust gases.

### **Additives and Formulations for Cooler Exhausts**

The temperature of an otherwise hot solid propellant exhaust can be reduced if it is intermixed with a heat sink or cooling agent. This cooling agent can be included within the fuel-oxidizer blend, or it can be implemented externally to the combustion chamber. These two approaches are considered, in order, in this section.

Coolants are materials that undergo an endothermic reaction (or phase change) upon exposure to heat. Several endothermically active agents were considered, including MgCO<sub>3</sub>, Al(OH)<sub>3</sub>, CaCO<sub>3</sub> and hydrated clays. When dispersed within a propellant blend, these solids absorb heat and decompose endothermically, producing inert gases such as CO<sub>2</sub> and H<sub>2</sub>O. The combination of lower temperatures from heat absorption and inert gas production contributes directly to more effective fire suppression.

The effect of different coolants upon calculated adiabatic combustion temperature for fully-oxidized stoichiometric blends was calculated using the NAWSC PEP<sup>40</sup> thermodynamics code. The fuel-oxidizer blend (5AT- Sr(NO<sub>3</sub>)<sub>2</sub>) and mass fraction of coolant (40 %) were maintained constant for the different coolants. Relative effectiveness for heat absorption of the different coolants can be seen in Table 9–17 through the lowered adiabatic flame temperature. Magnesium carbonate was selected for the baseline propellant mixture because of its strong cooling performance. The benefits of other coolants are not

always realized in propellant formulation; aluminum hydroxide, for instance, while offering attractive cooling properties has the unattractive feature of excessive reduction in propellant burn rates. The calculated adiabatic flame temperature for calcium carbonate should be lower than that of  $\text{MgCO}_3$ ; this discrepancy suggests there are gaps in the thermodynamic reference data used in the PEP code. Note that relative heat absorption capabilities are less than the evaporative cooling from water, but can approach 80 % that of water in the case of calcium carbonate.

**Table 9–17. Effect of Different Coolants on Adiabatic Flame Temperature of 5AT-Sr(NO<sub>3</sub>)<sub>2</sub> Propellant Mixture.**

Coolant	Molecular Formula	Endothermic Process	$\Delta H$ , J/g	Density, g/cm <sup>3</sup>	T <sub>c</sub> , K
Magnesium carbonate	$\text{MgCO}_3$	decomposition to MgO	1390	3.05	1440
Aluminum Hydroxide	$\text{Al(OH)}_3$	decomposition to $\text{Al}_2\text{O}_3$	970	2.42	1480
Copper(II) Oxalate	$\text{Cu(C}_2\text{O}_4\text{)} \cdot 0.5\text{H}_2\text{O}$	decomposition to Cu	83	2.21	1910
Calcium Carbonate	$\text{CaCO}_3$	decomposition to CaO	1780	2.71	1440
Water	$\text{H}_2\text{O}$	evaporation	2260	1.00	not determined

The benefits of decreased exhaust temperatures are often offset by a decrease in the burn rate of the propellant, which in turn decreases the rate of suppressant delivery. This is illustrated in Figure 9–51, where  $\ln(\text{BR}_{1000})$  is plotted as a function of  $1/T_c$  for five proprietary formulations. The linear relationships indicate that an Arrhenius-type activated process is occurring, as might have been anticipated.

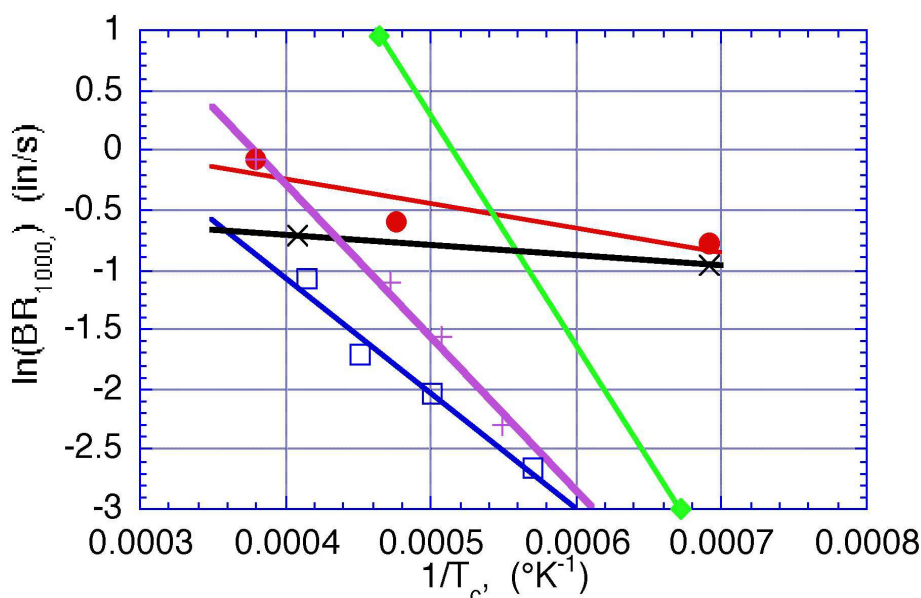


**Figure 9–51. Temperature Dependence of Propellant Burn Rates for Different FS01-40/additive Combinations.**

A number of high nitrogen component formulations based on BTATZ have been evaluated for their suitability in agent generation devices as a function of the amount of coolant added ( $\text{MgCO}_3$ ). The results are presented in Table 9–18 and in Figure 9–52. These data again illustrate the falloff in burn (agent generation) rate with decreased adiabatic combustion temperature.

**Table 9–18. High Nitrogen Content Developmental Propellants with MgCO<sub>3</sub> Coolant: Compositions and Burning Parameters.**

Propellant Composition (wt %)	Exhaust species (vol % @ T <sub>c</sub> )	Temperature (K)		Calculated Density (g/cm <sup>3</sup> )	Gas output (mol/100 g)	Measured BR <sub>1000</sub> (cm/s)	Measured Pressure exponent, n
		T <sub>c</sub>	T <sub>exh</sub>				
<b>Baseline:</b> 5AT, 21.9, Sr(NO <sub>3</sub> ) <sub>2</sub> 38.1, MgCO <sub>3</sub> 40.0	N <sub>2</sub> 45, CO <sub>2</sub> 35, H <sub>2</sub> O 20	1450	1000	2.55	2	1.27	0.5
<b>BTSN-00:</b> BTATZ 36.0, Sr(NO <sub>3</sub> ) <sub>2</sub> 63.0, PBA 3.0, C-black 0.5, Mica 0.5	N <sub>2</sub> 59, CO <sub>2</sub> 26, H <sub>2</sub> O 13	2770	1590	2.38	2.27	2.77	nd
<b>BTSN-10:</b> BTATZ 32.4, Sr(NO <sub>3</sub> ) <sub>2</sub> 56.6, PBA 3.0, C- black 0.5, Mica 0.5	N <sub>2</sub> 56, CO <sub>2</sub> 30, H <sub>2</sub> O 12	2560	1460	2.43	2.12	TBD	nd
<b>BTSN-20:</b> BTATZ 28.8, Sr(NO <sub>3</sub> ) <sub>2</sub> 50.3, PBA 3.0, C-black 0.5, Mica 0.5	N <sub>2</sub> 55, CO <sub>2</sub> 34, H <sub>2</sub> O 13	2260	1440	2.49	2.00	0.75	nd
<b>BTSN-30:</b> BTATZ 25.1, Sr(NO <sub>3</sub> ) <sub>2</sub> 43.9, PBA 3.0, C- black 0.5, Mica 0.5	N <sub>2</sub> 54, CO <sub>2</sub> 33, H <sub>2</sub> O 12	1890	1410	2.55	1.89	TBD	nd
<b>BTSN-40:</b> BTATZ 21.4, Sr(NO <sub>3</sub> ) <sub>2</sub> 37.6, PBA 3.0, C-black 0.5, Mica 0.5	N <sub>2</sub> 49, CO <sub>2</sub> 40, H <sub>2</sub> O 11	1500	1140	2.61	1.79	0.89	nd
<b>BTSN-50:</b> BTATZ 17.8, Sr(NO <sub>3</sub> ) <sub>2</sub> 31.2, PBA 3.0, C-black 0.5, Mica 0.5	N <sub>2</sub> 42, CO <sub>2</sub> 48, H <sub>2</sub> O 9	1444	964	2.67	1.54	0.38	nd

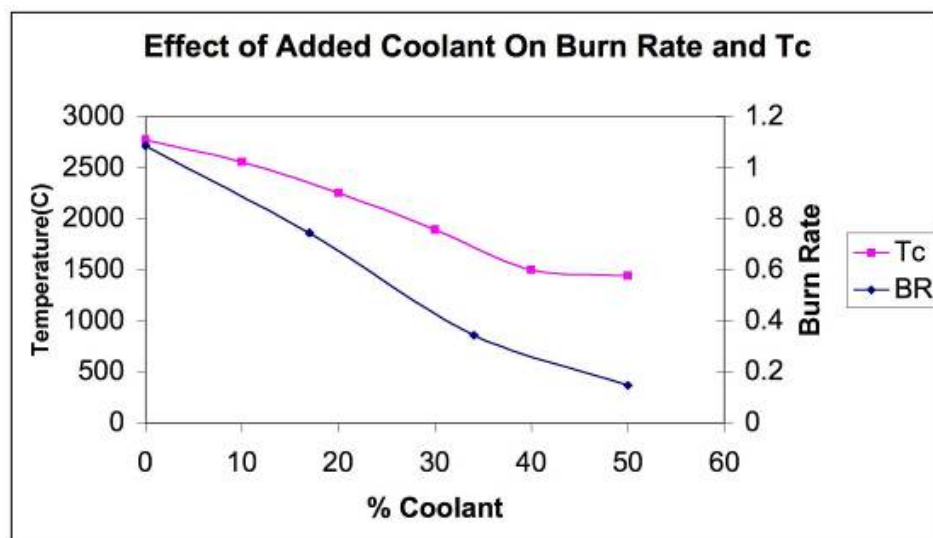


**Figure 9–52. Effect of Coolant Percentage on Burning Rate (in./s) and Adiabatic Temperature of High Nitrogen Propellants Listed in Table 9-18.**

The cooler, high gas output propellant compositions described in Table 9–18 represent an important step towards increased efficiency SPGG fire suppression devices. Gas temperatures were reduced in some

cases by up to 20 % when compared to the current baseline. The findings of increased burn rate compositions, while maintaining relatively low gas temperatures, provides a means for further increases in agent cooling when these compositions are further modified with endothermic chemical coolants. In general, the most successful energetic fuels were high in nitrogen, based upon BTAZ, with atomic N:C ratios of at least 3:1, as well as significant levels of unsaturation. These features combined to enable the cooler exhaust temperatures and N<sub>2</sub>-dominated exhaust gases at the expense of the more exothermic CO, CO<sub>2</sub>, and H<sub>2</sub>O.

The relative fire suppression effectiveness of some of these new, cooled solid propellant fire extinguisher compositions was not evaluated in this program due to excessive costs associated with addressing US Department of Transportation (DoT) restrictions on the shipping of energetic BTATZ materials from where they were prepared (China Lake, California) to where they were to be tested in the FTF (Redmond, Washington). A DoT classification requires several kg of propellant for testing, with its associated costs, plus the fees for DoT witnessing and licensing.

Further testing of BTATZ blends in the FTF is certainly warranted due to the potential of these materials to produce lower temperature products. In addition, it is necessary to confirm that, because of the relatively high hydrogen levels in the exhaust of some of these blends, the presence of H<sub>2</sub> does not diminish suppression effectiveness. China Lake presented calculations that the H<sub>2</sub> did not promote additional combustion; experiments to validate these have not yet been conducted.

### 9.3.6 Results: Chemically Active Fire Suppressants

#### Candidate Active Agents

The great fire suppression effectiveness of halon 1301 is due largely to its combination of high chemical activity and ease of dispersion (Chapter 8). Many other bromine- and iodine-containing compounds would have similar chemical effectiveness, but disperse less effectively due to significantly higher boiling points.

In addition, there are other compounds known to be effective fire suppressants, including some "superagents" which exhibit fire suppression effectiveness much greater than halon 1301 (Chapter 3).<sup>51</sup> The foremost example of these agents is iron pentacarbonyl, Fe(CO)<sub>5</sub>, but other examples include chromyl chloride, CrO<sub>2</sub>Cl<sub>2</sub>, and tetraethyl lead, Pb(C<sub>2</sub>H<sub>5</sub>)<sub>4</sub>. These agents have very high boiling points and are highly toxic, and so are not used in general suppression applications.

Solid propellant compositions offer a potent means of delivering such chemically active materials to a fire. These chemicals can be incorporated directly into the propellant composition. Upon combustion of the solid propellant, its product gases carry the additive and its radical-trapping reaction products into the fire zone. To enable testing of this concept in SPGG formulations, a broad review of potential candidates was undertaken in this project, including the examples presented in Table 9–19.

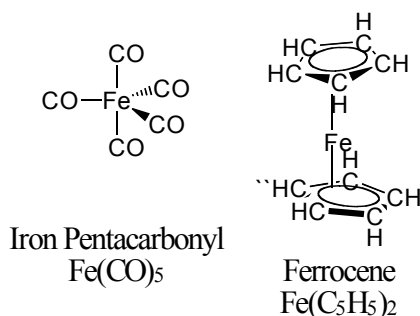
Among halide-containing species, Br- and I-containing compounds were considered to offer the most promise. Among these compounds, the alkali-metal salts offered appealing combinations of availability, and volatility; further, those potassium-based halides appeared to offer the most suitable levels of hygroscopicity – where low moisture-affinity is desired.

**Table 9–19. Candidate Chemically Active Agents.** (Data from References 52, 53)

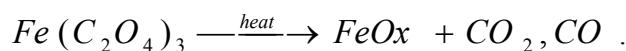
Compound	Active Species	MP (°C)	BP (°C)	Comments
<b>HALOGEN VEHICLES</b>				
NaI	I	660	1304	deliquescent powder
KI	I	681	1330	
KIO <sub>3</sub>	I	560		sometimes used as propellant oxidizer; partial decomposition at MP, releasing O <sub>2</sub>
NaBr	Br	747	1390	forms a dihydrate - NaBr·2H <sub>2</sub> O
KBr	Br	734	1435	
C <sub>12</sub> Br <sub>10</sub> O	Br	294	unknown	
NaCl	Cl	801	1413	
KCl	Cl	770	1500 sublimes	
KClO <sub>4</sub>	Cl	610 (controlled conditions)		used frequently as a propellant oxidizer; decomposes at 400 °C
<b>ALKALI VEHICLES</b>				
CaCl <sub>2</sub>	Ca	772 anhy	1935 anhy	forms mono-, di-, tetra-, & hexahydrates; highly hygroscopic
LiBr	Li	550	1265	forms mono-, di-, and trihydrates
LiCl	Li	605	1360	
LiI	Li	449	1180	forms mono-, di-, and trihydrates
RbBr	Rb	693	1340	
RbCl	Rb	718	1390	
RbI	Rb	647	1300	
Na <sub>2</sub> CO <sub>3</sub>	Na	851	decomposition	forms mono- and decahydrates; begins to loosen CO <sub>2</sub> well before melting
K <sub>2</sub> CO <sub>3</sub>	K	891	decomposition	
Li <sub>2</sub> CO <sub>3</sub>	Li	723	1310 (decomp.)	
Rb <sub>2</sub> CO <sub>3</sub>	Rb	837	900 (decomp.)	very hygroscopic; readily forms monohydrate
NaHCO <sub>3</sub>	Na	50 (decomp.)		begins to lose CO <sub>2</sub> at 50 °C; converts to Na <sub>2</sub> CO <sub>3</sub> at 100 °C
KHCO <sub>3</sub>	K	>100		Decomposition
LiHCO <sub>3</sub>	Li	no data	No data	
RbHCO <sub>3</sub>	Rb	no data	No data	
NaNO <sub>3</sub>	Na	308	380	
KNO <sub>3</sub>	K	334	400 (decomp.)	evolves O <sub>2</sub> at decomposition
LiNO <sub>3</sub>	Li	264	600 (decomp.)	hygroscopic
RbNO <sub>3</sub>	Rb	305		
NOAC	Na	58		decomposition, forms trihydrate
KAc	K	292		deliquescent crystals
LiAc	Li	70	decomposition	
RbAc	Rb	246		hygroscopic
Na <sub>2</sub> SO <sub>4</sub>	Na	884		forms a decahydrate; hygroscopic
K <sub>2</sub> SO <sub>4</sub>	K	1069	1689	
Li <sub>2</sub> SO <sub>4</sub>	Li	845 subl		forms a monohydrate

Compound	Active Species	MP (°C)	BP (°C)	Comments
Rb <sub>2</sub> SO <sub>4</sub>	Rb	1050		
<b>TRANSITION METAL (Iron) VEHICLES</b>				
FeO	Fe <sup>+2</sup>	1377		readily oxidizes to Fe <sub>3</sub> O <sub>4</sub> ; insoluble in H <sub>2</sub> O
Fe <sub>2</sub> O <sub>3</sub>	Fe <sup>+3</sup>	1565		insoluble in H <sub>2</sub> O
Fe <sub>3</sub> O <sub>4</sub>	Fe <sup>+2</sup>	1594		insoluble in H <sub>2</sub> O
Fe(C <sub>2</sub> H <sub>5</sub> ) <sub>2</sub>	“Fe”			ferrocene
Fe <sub>2</sub> (CO) <sub>9</sub>		100 (decomp.)		iron nonacarbonyl; toxic
Fe <sub>3</sub> (CO) <sub>12</sub>		140 (decomp.)		iron dodecacarbonyl; toxic
FeCl <sub>2</sub>	Fe <sup>+2</sup>	677	1023	forms di- and tetrahydrate; hygroscopic
FeCl <sub>3</sub>	Fe <sup>+3</sup>	306	315 (decomp.)	hygroscopic

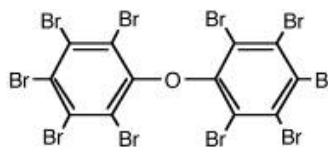
Fe(CO)<sub>5</sub> was considered too hazardous for handling in the Aerojet test fixture due to its toxicity and the large scale of the test fixture. Alternative vehicles for the iron atom were considered, including ferrocene, bis(cyclopentadienyl)iron, and Fe(C<sub>5</sub>H<sub>5</sub>)<sub>2</sub>, shown here:



Additional iron-containing compounds that were considered included several oxides and the oxalate. At elevated temperatures, the oxalate is known to decompose according to



Decabromodiphenyl ether (DBPE) was also investigated:



This material has been used in many plastic formulations as a flame inhibitor. On thermal degradation, C-Br bond breakage results in formation of volatile Br compounds.

### Suppression Effectiveness of Entrained Chemicals

Some of the candidate chemical agents were tested in the FTF to evaluate their effectiveness in fire suppression for a controlled JP-8 fire. The agents were delivered into the fire zone using the slow discharge SPGG displayed in Figure 9–40, whereby powdered candidate agents were entrained by high-

temperature exhaust gases produced by a neutral-burning solid-propellant gas generator producing a blend of CO<sub>2</sub>, N<sub>2</sub>, and H<sub>2</sub>O with constant discharge rate of exhaust gases to carry the candidates into the fire. Discharge rates for this testing were purposefully slow in order to minimize strain and mixing effects associated with rapid SPGG discharges. A representative discharge (pressure-time) profile for these tests is presented in Figure 9–53.

Initial tests of this type used a coolant bed to support the candidate agents. Aqueous solutions of the candidate were mixed with the coolant material (magnesite, 6 mesh to 10 mesh) and heated until the water had evaporated. This yielded loadings of ≈ 20 % candidate agent on magnesite. The fraction of agent carried to the fire could again be controlled by varying a downstream orifice leading to ambient.

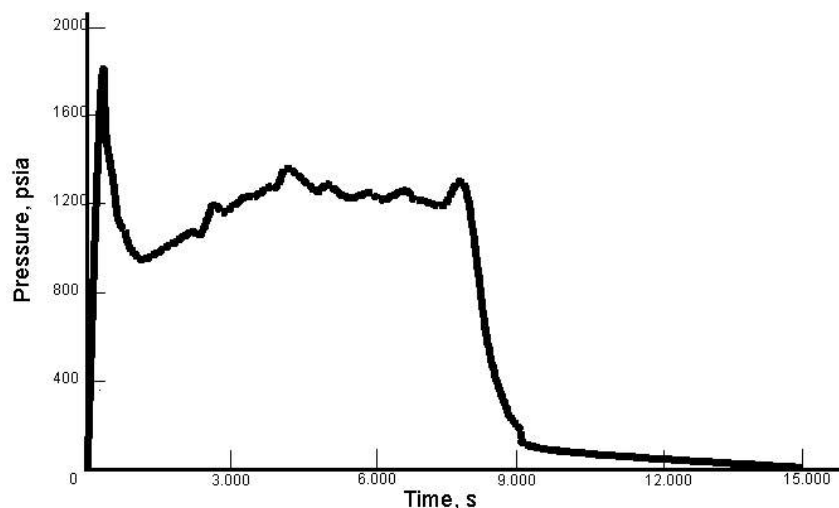


**Figure 9–53.**  
**Representative SPGG**  
**Pressure-time Curve**  
**Obtained During Delivery**  
**of Candidate Chemically**  
**Active Agents.**

An alternate approach gave more reproducible performance. In this case, powdered candidate agents were supported on a metal grid in the downstream chamber that formerly housed the coolant bed. Upon activation of the gas generator, the resultant exhaust would pass thru the chamber and entrain the powder and carry it to the fire. Test results using the latter method are shown in Table 9–20.

**Table 9–20. Summary of SPGG Fire Suppression Testing with Chemically Active Agents.**

Agent	Mass, g	Test No.	Result	Agent	Mass, g	Test No.	Result
<b>KI</b>	20	027-06	fire not out	<b>Fe<sub>2</sub>O<sub>3</sub></b>	40	038-01	fire not out
	40	027-07	fire not out		80	038-02	fire not out
	40	027-05	fire out				
	60	027-04	fire out				
<b>KBr</b>	40	032-02	fire not out	<b>Ferrocene</b>	40	039-01	fire not out
	60	032-03	fire not out		80	039-02r	fire not out
	60	032-01	fire not out				
<b>K<sub>2</sub>CO<sub>3</sub></b>	20	035-03	fire not out	<b>Iron Oxalate</b>	40	040-01	fire not out
	40	035-02r	fire out				
	60	035-01	fire out	<b>DBPE</b>	60	041-01	fire not out

The iron-based agents and DBPE were less effective than KI and K<sub>2</sub>CO<sub>3</sub>, at least within Aerojet's FTF. The results also indicated that K<sub>2</sub>CO<sub>3</sub> and KI were more effective than KBr. The threshold amount for

successful fire extinguishment seemed to be around 40 g of neat  $K_2CO_3$  or KI powder used in each solid propellant extinguisher.

The similarity in performance between the iodide and the carbonate reflects the observations in turbulent spray burner testing;<sup>54</sup> those data were interpreted as reflective of the greater role of the potassium ion in suppression effectiveness rather than the anion. A possible explanation for this trend is the more facile vaporization of the chemically relevant potassium species from the  $K_2CO_3$ . This is inconsistent with the higher melting point of  $K_2CO_3$  vs. KI (891 °C vs. 681 °C), but may be consistent at higher temperatures where  $K_2CO_3$  decomposes before boiling whereas KI melts without decomposing at 1330 °C. Another possibility is that there is an antagonistic interaction between the halogen and alkali metal species in the flame region.

Testing with ferrocene yielded some unexpected results. Based on its chemical similarity to iron pentacarbonyl, ferrocene would be expected to be a potent suppressant. However, multiple tests in which powdered ferrocene was swept into the hot solid propellant exhaust did not result in fire suppression when loads were increased to levels well in excess of the KI, KBr, or  $K_2CO_3$  suppression loads. Furthermore, ferrocene delivery was accompanied by growth of needles of ferrocene crystals on the exit port of the delivery tube. These findings imply that the ferrocene is quite stable in air/combustion conditions, and further that this material could not be entrained for a sufficient length of time into the flame zone. Iron oxide, likewise, was ineffective as an active suppressant. While only one test with iron oxalate was attempted with a 40 g load, the results did not indicate that this iron-containing compound could reach superagent status in this mode of operation.

The lesser performance of the iron- and decabromo-containing species, known to be excellent flame inhibitors in other circumstances, indicates that an adequate agent delivery mechanism needs to be carefully designed and implemented in the solid propellant fire extinguisher in order to fully utilize the chemical capabilities of such agents.

### **Burning Characteristics of Active Propellant Compositions**

Chemical additives selected from Table 9–19 were incorporated into formulations wherein the chemically active agent is liberated upon combustion of the solid propellant, the exhaust consisting of inert gases plus entrained additives. These additives (or their precursors) were blended directly into the propellant, or the additive (or precursor) was blended into a hybrid fluid. Several compositions were developed, such that a common composition family evolved having different levels of additive. Burning properties of several of these compositions are summarized in Table 9–21. Compositions incorporating combustion inhibitors were demonstrated to burn efficiently and were subsequently shown to be effective in fire suppression. The incorporation of species to suppress fires did not prevent combustion of the propellant.

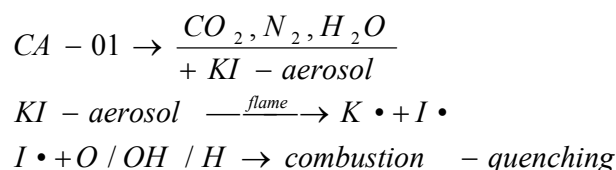
**Table 9–21. Chemically Active Developmental Propellants.**

Propellant Composition (wt %)	Exhaust species (vol % @ T <sub>c</sub> )	Temperature (K)		Calculated Density (g/cm <sup>3</sup> )	Gas output, mol/100 g	Measured BR <sub>1000</sub> (cm/s)	Measured Pressure exponent, n
		T <sub>c</sub>	T <sub>exh</sub>				
<b>Baseline:</b> 5AT, 21.9, Sr(NO <sub>3</sub> ) <sub>2</sub> 18.1, MgCO <sub>3</sub> 40.0	N <sub>2</sub> 45, CO <sub>2</sub> 35, H <sub>2</sub> O 20	1450	1000	2.55	2.00	1.27	0.5
<b>CA-01:</b> 5AT 17.2, Sr(NO <sub>3</sub> ) <sub>2</sub> 30.0, MgCO <sub>3</sub> 30.0, KI 21.3, Graphite 0.5	N <sub>2</sub> 47, CO <sub>2</sub> 31, H <sub>2</sub> O 22	1450	970	2.66	1.47	1.27	0.55
<b>CA-02:</b> 5AT 20.8, Sr(NO <sub>3</sub> ) <sub>2</sub> 36.2, MgCO <sub>3</sub> 38.0, K <sub>2</sub> CO <sub>3</sub> 5.0	N <sub>2</sub> 47, CO <sub>2</sub> 31, H <sub>2</sub> O 22 KI 21.3 g 0.13 mol K	1440	1200	2.54	1.67	1.40	0.48
<b>CA-03:</b> 5AT 20.0, Sr(NO <sub>3</sub> ) <sub>2</sub> 34.7, MgCO <sub>3</sub> 36.4, K <sub>2</sub> CO <sub>3</sub> 8.9	N <sub>2</sub> 47, CO <sub>2</sub> 31 H <sub>2</sub> O 22, <b>K<sub>2</sub>CO<sub>3</sub> 9.0 g</b> <b>0.13 mol K</b>	1450	1210	2.54	1.78	1.32	0.59
<b>CA-04:</b> 5AT 19.7 Sr(NO <sub>3</sub> ) <sub>2</sub> 34.3, MgCO <sub>3</sub> 36.0, K <sub>2</sub> CO <sub>3</sub> 10.	N <sub>2</sub> 47, CO <sub>2</sub> 32, H <sub>2</sub> O 22 K <sub>2</sub> CO <sub>3</sub> 10.0 g 0.15 mol K	1440	1110	2.54	1.75	1.27	0.44
<b>CA-05:</b> 5AT 17.52, Sr(NO <sub>3</sub> ) <sub>2</sub> 30.5, MgCO <sub>3</sub> 32.0, K <sub>2</sub> CO <sub>3</sub> 20.0	N <sub>2</sub> 47, CO <sub>2</sub> 31 H <sub>2</sub> O 22 K <sub>2</sub> CO <sub>3</sub> 20.0 g 0.30 mol K	1480	1180	2.52	1.55	0.64	0.77
<b>CA-06:</b> 5AT 22.1, Sr(NO <sub>3</sub> ) <sub>2</sub> 24.8, MgCO <sub>3</sub> 39.5, KNO <sub>3</sub> 13.1, Graphite 0.5	N <sub>2</sub> 47, CO <sub>2</sub> 31 H <sub>2</sub> O 22 K <sub>2</sub> CO <sub>3</sub> 9.0 g 0.13 mol K	1440	1100	2.44	1.61	1.04	0.66
<b>CA-07:</b> 5AT 22.1, Sr(NO <sub>3</sub> ) <sub>2</sub> 22.9, MgCO <sub>3</sub> 40.0, KNO <sub>3</sub> 15.0	N <sub>2</sub> 47, CO <sub>2</sub> 31, H <sub>2</sub> O 22 K <sub>2</sub> CO <sub>3</sub> 10.0g 0.15 mol K	1440	1090	2.42	1.78	1.62	0.52
<b>CA-08:</b> 5AT 22.1, Sr(NO <sub>3</sub> ) <sub>2</sub> 22.9, MgCO <sub>3</sub> 40.0, KNO <sub>3</sub> 30.0	N <sub>2</sub> 47, CO <sub>2</sub> 31 H <sub>2</sub> O 22 K <sub>2</sub> CO <sub>3</sub> 20.0 g 0.30 mol K	1470	990	2.30	1.79	.68	1.77
<b>CA-09:</b> 5AT 21.9, Sr(NO <sub>3</sub> ) <sub>2</sub> 38.1, MgCO <sub>3</sub> 34.5, Fe <sub>2</sub> O <sub>3</sub> 5.0 Graphite 0.5	N <sub>2</sub> 48, CO <sub>2</sub> 29, <b>H<sub>2</sub>O 33, Fe<sub>2</sub>O<sub>3</sub> 5g</b> <b>(0.06 mol Fe)</b>	1470	1100	2.59	1.88	1.62	0.62
<b>CA-10:</b> 5AT 81, KP 10, DBPE 5.0, PBA 3.0, C-black 0.5, Mica 0.5	N <sub>2</sub> 60, H <sub>2</sub> 28 CO 3, CH <sub>4</sub> 4 KCl(s) 2.0 g KBr(s) 5.4 g	1630	874	1.71	4.24	0.25	1.0
<b>CA-11:</b> 5AT 19.7, Sr(NO <sub>3</sub> ) <sub>2</sub> 34.3, MgCO <sub>3</sub> 36.0, DBPE 10.0	N <sub>2</sub> 42, CO <sub>2</sub> 30 H <sub>2</sub> O 11, H <sub>2</sub> 6	1440	853	2.57	1.76	nd	nd

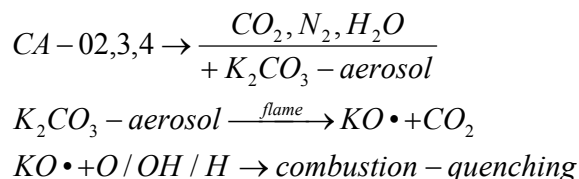
### Potassium-Containing Compositions

Three different approaches were used to incorporate potassium-containing species into propellant blends. These approaches built upon the agent testing efforts already described. The first blended potassium iodide directly into a propellant; the second blended potassium carbonate directly into a propellant, and the third used potassium nitrate blended into a propellant.

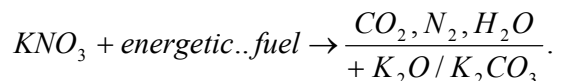
One potassium iodide-containing blend was made, labeled CA-01. This blend had an acceptable BR1000 and pressure exponent  $n$ . This composition was expected to obtain chemical activity by delivering KI aerosol, entrained in a  $CO_2$ ,  $N_2$ ,  $H_2O$  inert gas blend, to the fire, the KI then dissociating in the flame to produce combustion-radical-trapping  $I\bullet$  species according to:



Several potassium-carbonate-containing blends were made, where the mass of  $K_2CO_3$  in the blend was varied from 5 % to 20 %. The rationale for the varied levels of  $K_2CO_3$  was to probe this effect upon fire suppression effectiveness; i.e. varying the extent of chemically active agent within an otherwise nearly-common inert gas blend. All of these blends had acceptable burning properties, although at 20 %  $K_2CO_3$ , BR1000 was dropping to unattractively low levels at the same time that the pressure exponent,  $n$ , was increasing to unattractive levels. As such this propellant, as formulated, would not be ideally suited for commercial application. These compositions were expected to obtain chemical activity by delivering  $K_2CO_3$  aerosol, entrained in a  $CO_2$ ,  $N_2$ ,  $H_2O$  inert gas blend. The  $K_2CO_3$  would dissociate in the flame to produce combustion-radical-trapping  $I\bullet$  species according to:



In an attempt to counteract the fall-off in BR1000 observed in the 20 %  $K_2CO_3$ -containing blends, an alternative approach to potassium incorporation was investigated. Instead of direct incorporation of  $K_2CO_3$  into a propellant blend, we incorporated potassium nitrate ( $KNO_3$ , or KN). When blended into a propellant, KN is an oxidizer for fuels; the potassium product of this reaction is typically either the oxide,  $K_2O$ , or the carbonate,  $K_2CO_3$ :



For the cooled propellant blends under consideration here, the dominant K-containing species is expected to be  $K_2CO_3$ . Hence for K-containing blends based on KN,  $K_2CO_3$  aerosols can also be expected, with KN offering the possibility of circumventing the undesirable burn rates obtained in the higher percentage  $K_2CO_3$  blends. One caveat necessary to keep in mind when comparing the carbonate and the nitrate blends is that the use of KN requires that its oxidizing power be offset by a comparable amount of fuel in

order to maintain the desired CO<sub>2</sub>, N<sub>2</sub>, H<sub>2</sub>O inert gas exhaust blend; this offset is minimal and straightforward to achieve.

The KN-containing blends are listed as CA-6, CA-7, and CA-8 in Table 9–21. At lower levels, these KN blends yielded materials having suitable burning parameters. Unfortunately, attempts to obtain usable quantities of blends containing higher levels of KN (e.g., CA-8) were repeatedly thwarted by a combination of poor burning characteristics and/or poor processability.

### ***Iron-Containing Additives***

As mentioned previously, iron pentacarbonyl Fe(CO)<sub>5</sub>, was not blended into any propellant formulations because of its high toxicity. Ferrocene and its derivatives have been reportedly used in various propellants as burn rate modifiers with great success. However these formulations displayed unsuitable thermal stability. The ferrocene derivatives tended to migrate to the surface of the propellant, where they are oxidized to ferrocenium compounds. Ferrocenium derivatives in combination with propellant ingredients give friction sensitive materials. This limits the use of ferrocene derivatives to hybrid systems where the propellant and the additive are stored separately.

Iron oxide containing formulations do not have the drawbacks of iron pentacarbonyl and ferrocene mentioned above. Although definitive results were not obtained in this project, the routes explored to date involving iron oxide containing discharges have yielded burning characteristics that suggest further study is warranted.

### ***Decabromodiphenyl Ether***

Propellant compositions were formulated both with and without decabromodiphenyl ether (DBPE), added as a chemically active flame inhibitor, and these formulations underwent preliminary burning characterization. Composition CA-11 in Table 9–21 did not have suitable burning properties, with the effect of the DBPE to slow the burn rate and increase the pressure exponent. DBPE was also formulated into a 5AT-Sr(NO<sub>3</sub>)<sub>2</sub>-MgCO<sub>3</sub> blend (CA-11). These formulations were evaluated thermodynamically but not reduced to practice due to lack of resources and because of concerns with regard to DBPE handling during propellant processing and corrosivity during DBPE application.

## **Suppression Effectiveness of Chemically Active Propellant Compositions**

Chemically active propellant compositions were prepared in kilogram quantities to provide sufficient material for repeated testing. Propellant was typically pressed into 12.7 mm diameter x 6.4 mm thick tablets. The tablets were loaded into heavy mass, refurbishable gas generators, with some booster propellant ignition aid added, and then fitted with pyrotechnic initiators. Upon activation, the initiator ignites the booster propellant and then the main propellant. The internal pressure rises (Figure 9–54) until it exceeds the burst pressure of the material sealing the orifices of the device; this occurs at approximately 6.9 MPa. Internal pressures continue to rise, reaching a maximum of up to 10 MPa before the propellant completes its burn. Complete discharge of the agent from the SPGG is achieved within about 200 ms of initiation. Acceptable discharge times were achieved provided the pressures were maintained in the 6.8 MPa to 13.6 MPa range. Representative FTF pressure-time curves showing the impact of the SPGG discharge on the fixture pressure are shown in Figure 9–55 for two successful and one unsuccessful suppression event using the CA-04 propellant formulation.

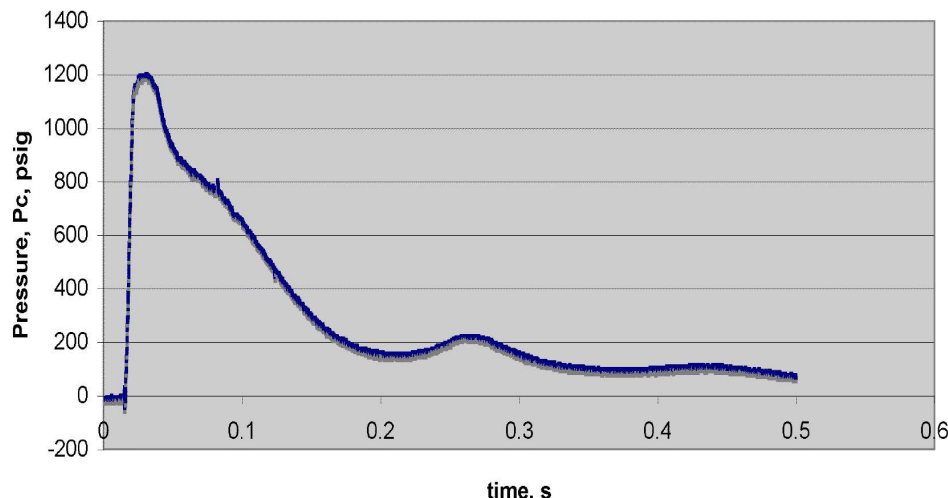


**Figure 9–54.**  
**Representative P-t**  
**Curve for SPGG**  
**Chamber**  
**Pressure.**

Peak SPGG chamber pressures below 6.8 MPa did not in general yield reproducible discharge behavior, and peak pressures much above 10.2 MPa in general yielded too rapid a discharge event and sometimes SPGG over pressurization (and rupture). The target peak pressure was 10.2 MPa, which yielded a discharge time of  $\approx 100$  ms. For ease of test turnaround, SPGG orifices for maintaining this sort of discharge rate were modeled after Aerojet proprietary designs used in the V-22/F-18 fire suppression systems. These designs use several different orifice diameters ranging from 2 mm to 4.8 mm with burst seal material consisting of 0.1 mm aluminum. Total orifice area was 168 mm<sup>2</sup> for a 210 g test SPGG. This total area is scalable to larger and smaller SPGG sizes.

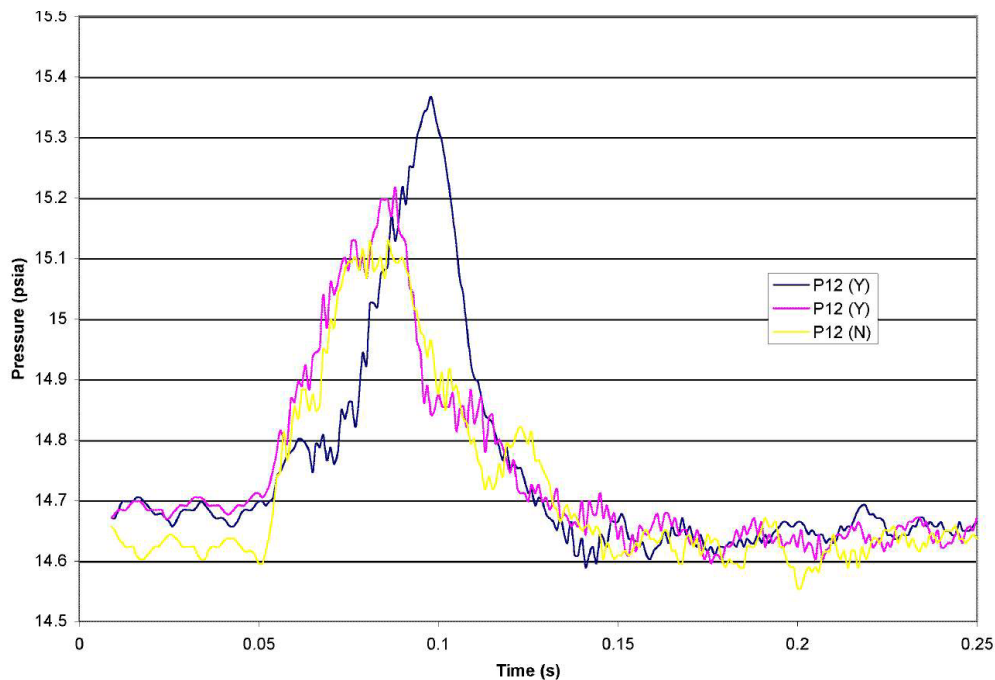


**Figure 9–55.**  
**Representative**  
**P-t Curve for**  
**Fire Test**  
**Fixture**  
**Pressure**  
**before, during,**  
**and after**  
**SPGG**  
**discharge.**

Figure 9–56 summarizes the test results and shows how the test configurations compare on a total agent mass basis and also on a K-molar basis. FTF testing with various inert and chemically active solid propellant compositions demonstrated that incorporation of 0.1 % additive (expressed as a fraction of the gaseous molar output) into inert fire suppressants has a dramatic positive effect on fire suppression

efficiency. The otherwise similar propellant compositions examined during this testing indicated a 50 % to 70 % (by mass) reduction of agent loading for suppression of identical fires when the propellant composition contained as little as 0.1 %. On an equimolar basis, potassium carbonate appears to be a more effective chemical additive than potassium iodide. Table 9–22 summarizes the threshold values of the most promising active agents. The threshold is defined as the amount of agent needed to extinguish the fire in the FTF at least two out of three times. Typically, three tests were conducted at the threshold amount and three additional tests were conducted at an agent load greater than the threshold amount.

The results indicate that  $K_2CO_3$  and KI yield significantly improved suppression effectiveness when compared to the inert propellant composition. For a composition containing 0.1 mole KI per 100 g propellant, the threshold propellant load was  $\approx$  45 % that of the baseline inert propellant composition, given similar discharge conditions and mass flows. A composition containing a similar amount of  $K_2CO_3$  (0.1 mole K per 100 g propellant) required only 30 % of the mass of the baseline propellant.

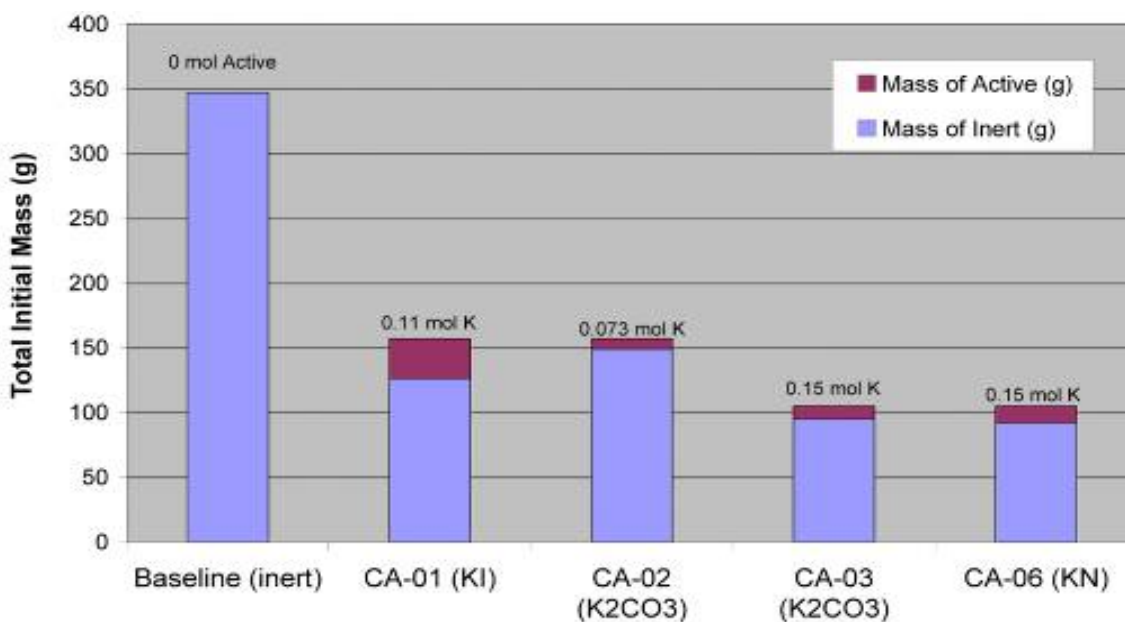


**Figure 9–56. Threshold Mass of Inert Propellant Plus Potassium Compound for Suppression in the FTF.**

The defined threshold level criterion of agent required for suppression (two out of three fires suppressed) was met for the baseline, CA-01, and CA-02 compositions; for CA-03 and CA-06, this criterion was exceeded and the fires were always suppressed, down to the minimum load capable for our equipment. This suggests that actual performance improvements for CA-03 and CA-06 were greater than a factor of three over the inert baseline propellant. A comparison of the suppression findings for CA-02 and CA-03 indicate that suppression effectiveness increased with higher levels of potassium content. CA-03 and CA-06, with comparable molar levels of potassium, appear to have similar suppression effectiveness. On the contrary, comparison of CA-01 with CA-02 suggests that the KI-containing composition (CA-01) may have some canceling contributions from the K and I portions of the additive.

**Table 9–22. Threshold Mass of Propellant and Potassium-based Additive for Fire Suppression in the FTF.**

Agent/Additive	Baseline/ none	CA-01/ KI	CA-02/ K <sub>2</sub> CO <sub>3</sub>	CA-03/ K <sub>2</sub> CO <sub>3</sub>	CA-06/ K <sub>2</sub> CO <sub>3</sub> (from KN)
Gas Fraction	50 %	50 %	50 %	50 %	50 %
MW, g/mole	30	30	30	30	30
Mole active (K)/100 g	0	0.127	0.073	0.145	0.145
Mole active (K) discharged	0	0.199	0.114	0.152	0.152
Threshold gas generator Load, g	347	157	157	105	105
Powder discharge mass, g (Threshold)	173.5	78.5	78.5	52.5	52.5

Table 9–22 and Figure 9–56 are subject to some uncertainty due to the nature of large-scale fire tests. The threshold quantity may not be a sharp line separating the regions between fire-out and fire-not-out, but more of a band due to variations in test parameters.

Larger pellets of the chemically active decabromodiphenyl ether formulation were burned and the temperature of the gaseous products measured. The SPGG outlet temperature was approximately 675 °C, which was in good agreement with the temperature predicted from thermochemical calculations. The chemically active formulation was found to be impact, friction and electrostatically insensitive. The PBDE formulations was able to successfully suppress a JP-8 pool fire in a small vented box, but was not able to suppress the JP-8 flame in the FTF at a loading of 60 g.

### 9.3.7 Results: Hybrid Fire Extinguishers

Hybrid Fire Extinguisher suppression effectiveness tests employed a set of re-usable “workhorse” generators, with size varying from 56 mL to 110 mL internal volume. A schematic of this test article is shown in Figure 9–57.

Exhaust orifices provided an outlet for the fluid; there were typically eight 3.1 mm to 3.4 mm orifices (oriented 90° apart on all four sides to ensure non-propulsive behavior) sealed with 0.05 mm thick Al 1100-T1 shim material. Propellant loads were typically 10 g to 20 g, and the nominal propellant:fluid mass loading ratio was 1:6 to 1:10.

The tests were conducted on combinations of the fluid suppressants listed in Table 9–23 with the following propellants: Baseline (FS-0140, inert); CA-01 (chemically active – KI); and CA-04 (chemically active – K<sub>2</sub>CO<sub>3</sub>). Halon 1301 was not tested, but is included in Table 9–23 for reference.

In order to ensure safe operation within the test fixture, all new propellant-fluid configurations underwent functional testing first to ensure proper performance of the propellant/fluid combination. These tests consisted of the assembly of the desired propellant/fluid combination, mounting the hybrid extinguisher unit in a vise anchored to a bench, and operating the hybrid extinguisher.

Accurate definition of threshold level loads for the hybrid extinguisher testing was found to be best accomplished using various combinations (single and/or different hybrid extinguisher sizes) mounted upstream of the flame in the test fixture, as shown in Figure 9–58. The results of hybrid extinguisher testing are presented in two separate categories: fluorocarbon systems and aqueous systems.

Hybrid Unit

Side View

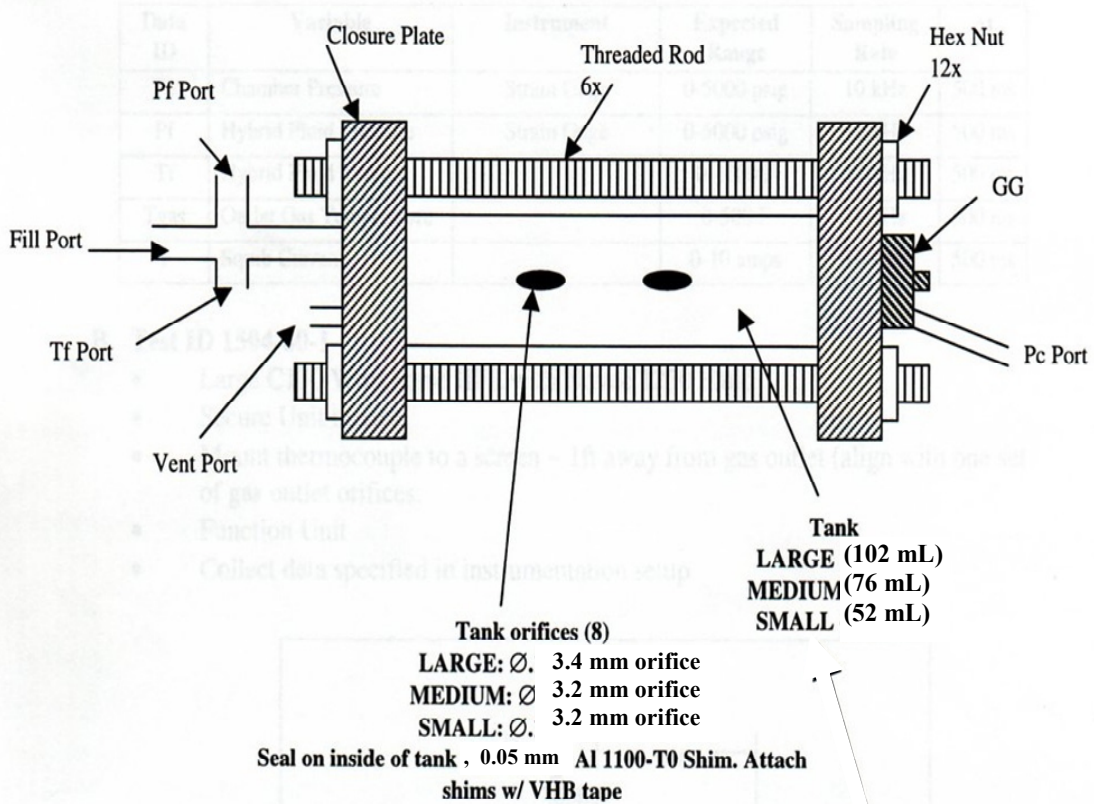


**Figure 9–57. Schematic of Hybrid Extinguisher Workhorse Hardware Configuration.**

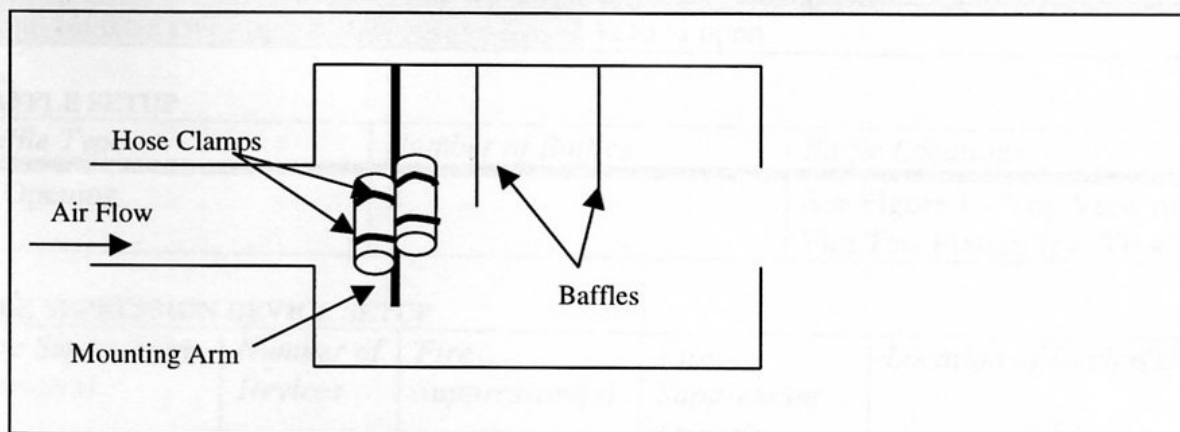


**Figure 9–58. Mounting Configuration of Multiple Hybrid Extinguishers Used to Bracket Threshold Levels.**

**Table 9–23. Properties of Hybrid Fluid Candidates.**

Property	Halon 1301	HFC-125	Water	HFC-227ea	HFE-7100	HFE-1230	CF <sub>3</sub> I
Chemical formula	CF <sub>3</sub> Br	C <sub>2</sub> F <sub>5</sub> H	H <sub>2</sub> O	C <sub>3</sub> F <sub>7</sub> H	C <sub>4</sub> F <sub>9</sub> OCH <sub>3</sub>	C <sub>6</sub> F <sub>12</sub> O	CF <sub>3</sub> I
Molecular wt.	149	120	18	170	250	316	196
Boiling pt.(°C)	-58	-48	100	-16	61	49	-21
Freezing point (°C)	-168	-102.8	0	-131	-135	-108	
Density @25° C (g/cm <sup>3</sup> )	1.55	1.19	1.00	1.4	1.52	1.6	2.1
Vapor pressure (kPa) @ 25° C	1510	1370	3	460	27	6	538
Specific heat (kJ/kg°C)		1.26	4.18	1.184		0.89	
(J/g) Heat of vaporization	117	113	2255	134	201	88	113
Cup-burner (vol %) fire extinguishing concentration	3.1	8.7	25 <sup>#</sup>	6.5	6	5	3.1
Fire extinguishing design concentration (g/m <sup>3</sup> )	305	516		590		776	401
Ozone depletion potential (relative to CFC-11)	12	0	0	0	0	0	0.0001
Global warming potential (relative to CO <sub>2</sub> )	5400	2800	0	2900	320	1	<5
Atmospheric lifetime (yr)	65	33	n/a	37	4.1	0.014	<0.005
Cardio-sensitization LOAEL (vol%)	10	10	n/a	10.5		10	0.4
Cardio-sensitization NOAEL (vol%)	7	7.5	n/a	9		10	0.2
EPA SNAP approved for unoccupied	No	Yes	Yes	Yes	Yes	Yes	Yes

# assumes full recovery of enthalpy of vaporization

### Fluorocarbon Hybrid Extinguishers

The fluorocarbon test results are listed in Table 9–24. The threshold values were determined for the hybrid extinguisher initially at ambient temperature. The baseline hybrid extinguisher against which the other propellant/fluids were compared consisted of the FS-0140 propellant (21.9 % 5AT, 38.1 % Sr(NO<sub>3</sub>)<sub>2</sub>, 40.0 % MgCO<sub>3</sub>) with HFC-227ea fluid. The threshold suppression level for this baseline hybrid extinguisher was 358 g. (The fire suppression number (FSN) reported in the table is the ratio of the threshold determined for the other hybrid extinguisher combinations normalized by the baseline mass.) Replacing the HFC-227ea with HFE-1230 led to a similar threshold level. Interestingly, this threshold level value is nearly identical to the value obtained for testing of the FS-0140 propellant alone in a standard SPGG.

Hybrid extinguisher tests with HFE-7100 and a total load of 358 g did not extinguish the fire. Further testing with this agent was suspended since the amount of agent needed would have been more than the base system, with no particular advantage. In addition, measurements in the test fixture revealed higher bay pressures than the norm and the flame seemed to be enhanced by the fluid discharge.

**Table 9–24. Hybrid Extinguisher Fluorocarbon System Data Summary.**

Agent	FS-0140/ HFC- 227ea	FS-0140/ HFE/ 1230	FS-0140/ HFE- 7100	CA-01/ HFC- 227ea	CA-04/ HFC- 227ea	FS-0140/ HFC-227ea + KHCO <sub>3</sub>	FS-0140/ HFC- 227ea + NaHCO <sub>3</sub>	FS- 0140/ CF <sub>3</sub> I
Active additive	-	-	-	K <sub>2</sub> CO <sub>3</sub>	K <sub>2</sub> CO <sub>3</sub>	KHCO <sub>3</sub>	NaHCO <sub>3</sub>	CF <sub>3</sub> I
MW, g/mol	170	316	250	170	170	170	170	196
Load, g	358	358	-	228	228	265	228	98 <sup>b</sup>
Discharge mass, g	340	340	-	217	217	252	220	93
Mole (K or I) discharged	0	0	-	0.040	0.046	0.040	0.052	0.429
FSN	1	1	>1 <sup>a</sup>	0.637	0.637	0.740	0.637	0.274

a. Tests conducted using 358 g (same agent mass as the FS01-40/HFC-227ea system) did not extinguish the fire.

Testing was suspended since the amount of agent needed would be more than the baseline system.

b. Anticipated threshold value: two tests were conducted using 130 g (both fires out) and two tests were conducted using 98 g (one fire out, one fire not out).

Several combinations of chemically active hybrid extinguishers were tested. Combinations of the chemically active propellants CA-01 and CA-04 with HFC-227ea were found to yield  $\approx 40\%$  enhancement in performance when compared to the baseline hybrid extinguisher. This finding indicates that significant reductions in hybrid extinguisher agent levels can be achieved by combining chemically active solid propellant compositions with inert fire suppression agents.

Chemically active hybrid extinguishers were also constructed using the FS-0140 propellant with HFC-227ea plus the chemically active powders KHCO<sub>3</sub> and NaHCO<sub>3</sub> (potassium bicarbonate and sodium bicarbonate, respectively). These systems exhibited performance enhancement of about  $\approx 40\%$ , similar to the results from the CA-01/HFC-227ea and CA-04/HFC-227ea tests. Note that each of these chemically active hybrid extinguisher combinations maintained similar levels of chemically active additive (0.04 mol to 0.05 mol), implying that in each case the benefit of this chemical activity is independent of the form in which that additive is delivered.

Testing of the inert FS-0140 propellant with the chemically active suppressant CF<sub>3</sub>I resulted in the most effective hybrid combination, with an approximate threshold value  $\approx 25\%$  of the baseline propellant/fluid combination. This represents an approximate threshold value since two tests were conducted using 130 g (both fires out) and two tests were conducted using 98 g (one fire out, one fire not out), as opposed to the standard two-out-of-three successful fire suppression events used to define the threshold. Fire extinction coincided with the formation of brilliant purple smoke exhausting from the test fixture, evidence of the formation of elemental iodine, I<sub>2</sub>, fumes during the suppression process.

Hybrid extinguisher testing with CF<sub>3</sub>I proved problematic because this agent tended to dissolve common adhesives not affected by other fluids like HFC-227ea. Because some leakage of agent around/through the Mylar burst tape occurred during these tests, the burst shims were moved to outside the hybrid extinguisher, thereby minimizing exposure of the adhesive to CF<sub>3</sub>I.

An additional test of the 130 g FS-0140 propellant/CF<sub>3</sub>I hybrid extinguisher was conducted after cold soaking; the fire was successfully extinguished. In this test the hybrid extinguisher was conditioned to -65 °C; however, the CF<sub>3</sub>I temperature rose to -27 °C before the extinguisher was operated.

### Aqueous Hybrid Extinguishers

The results of the aqueous-based hybrid extinguisher combinations are summarized in Table 9–25.

**Table 9–25. Hybrid Extinguisher Aqueous System Data Summary.**

Agent	CA-01/ Water	CA-04/ Water	Baseline/ Water:KOAc:Soap <sup>b</sup>
Active additive	KI	K <sub>2</sub> CO <sub>3</sub>	KC <sub>2</sub> H <sub>3</sub> O <sub>2</sub>
MW, g/mol	18	18	30
Load	-	-	228
Discharge mass, g	-	-	217
Mole (K) discharged	-	-	0.96
FSN (Baseline/HFC-227ea)	>1 <sup>a</sup>	>1 <sup>a</sup>	0.637

a. Testing conducted using 358 g (same agent mass as the FS01-40/HFC-227ea system) did not extinguish the fire. Testing was suspended since the amount of agent needed would be more than the baseline system.

b. 48:48:4 mass ratio of water:potassium acetate:soap.

Tests conducted at ambient temperature using pure water with a total load of 358 g (same agent mass as the FS-0140/HFC-227ea system) did not extinguish the fire. Testing of hybrid extinguishers charged with chemically active CA-01 and CA-04 propellants in conjunction with pure water also did not successfully extinguish the fire with agent loads up to the baseline mass. Substituting a water-potassium acetate-soap (surfactant) blend (48:48:4 mass ratio) for pure water, and pressurizing with the CA-04 chemically active propellant did yield successful flame extinction at levels approximately 60 % that of the Baseline hybrid extinguisher. Potassium acetate, KO<sub>2</sub>CCH<sub>3</sub>, or “KOAc,” is a well known freezing point suppressant for aqueous solutions, and as it contains potassium ions, also contributes a chemically active agent to the suppressant mix. The improved performance of these KOAc blends vs. pure water is presumably due to the chemical activity contributed by the potassium; assuming this is the case, one would expect to see a range of performance thresholds for this hybrid extinguisher given variations in KOAc levels. However, testing of different levels of KOAc in water was not attempted in this effort as the focus was on KOAc loadings suitable for meeting typical low temperature performance requirements of -40 °C.

Testing of aqueous hybrid extinguishers was often plagued by poor performance/distribution of the agent. A frequent occurrence was the collection of puddles of water upstream of the flame zone in the FTF. While this means that flame suppression was accomplished with less than the full hybrid extinguisher load, it also means that the given test articles would benefit from design modifications to yield improved distribution, e.g., through use of screens to improve mixing of the SPGG exhaust with the fluid, or by varying the ratio of propellant to fluid.

### Summary of Hybrid Extinguisher Results

A summary of the hybrid extinguisher testing is presented in Figure 9–59. On a mass-to-mass basis, the inert hybrid extinguisher and SPGG systems appear to provide similar suppression protection, requiring

≈ 360 grams to suppress the 1 MW FTF fire. The higher molar efficiency of the hybrid testing reflects the higher molecular mass of the HFC-227ea. As in the pure SPGG, incorporation of chemically active species into the propellant improves the suppression efficiency for the hybrid extinguisher configuration. Testing conducted with  $\text{KHCO}_3$  added into the hybrid fluid of the system produced results similar (based on moles of K) to results with active agents (KI,  $\text{K}_2\text{CO}_3$ ) added into the propellant. This indicates that active additives in the hybrid fluid may be just as effective as active additives in the propellant.

Testing hybrid extinguishers with HFE-7100 and HFE-1230 did not lead to reductions in total propellant-plus-fluid mass (when compared to HFC-227ea), but it did demonstrate that higher boiling point fluids could be successfully discharged when pressurized by a solid propellant gas generator. This opens opportunities for alternate suppression fluids that, on the basis of vapor pressure alone, would not appear to be desirable candidates as fire suppressants.

The lowest hybrid extinguisher agent loads were found when using  $\text{CF}_3\text{I}$  as the hybrid fluid. Coupling this agent with a solid propellant gas generator also overcame the low temperature dispersion problem encountered in previous testing with conventional pressurized fire bottles.<sup>55</sup>

Hybrid extinguisher testing with aqueous agents provided additional insight into necessary levels of active agent required for suppression. Tests using an inert propellant configuration with pure water were found to require agent loads in excess of threshold levels of inert propellants and HFC-227ea. Similar findings were obtained when the active CA-04 propellant was used in conjunction with pure water. This relatively poor performance of the water hybrids is likely a function of insufficient distribution of the hybrid stream into the fire compartment of the FTF. However, while poor dispersion in the case of water-based hybrid extinguishers probably resulted in their lackluster performance, this effect was found to be offset by blending in potassium acetate.

The improvement found from the addition of chemically active species to the propellant mixture in the hybrid extinguisher systems (an approximate 36 % reduction in suppressant mass) appears to be less than that found in the SPGGs (70 %). Note, however, that the propellant is 100% of the total agent mass for the SPGG configuration, but only 14 % of the total agent mass for the hybrid extinguisher configuration, thus limiting the molar fraction of chemically active additive to ≈ 2 volume %. It is likely that if the amount of active additive in the hybrid extinguisher systems were optimized, these systems would show a mass reduction similar to the SPGG systems.

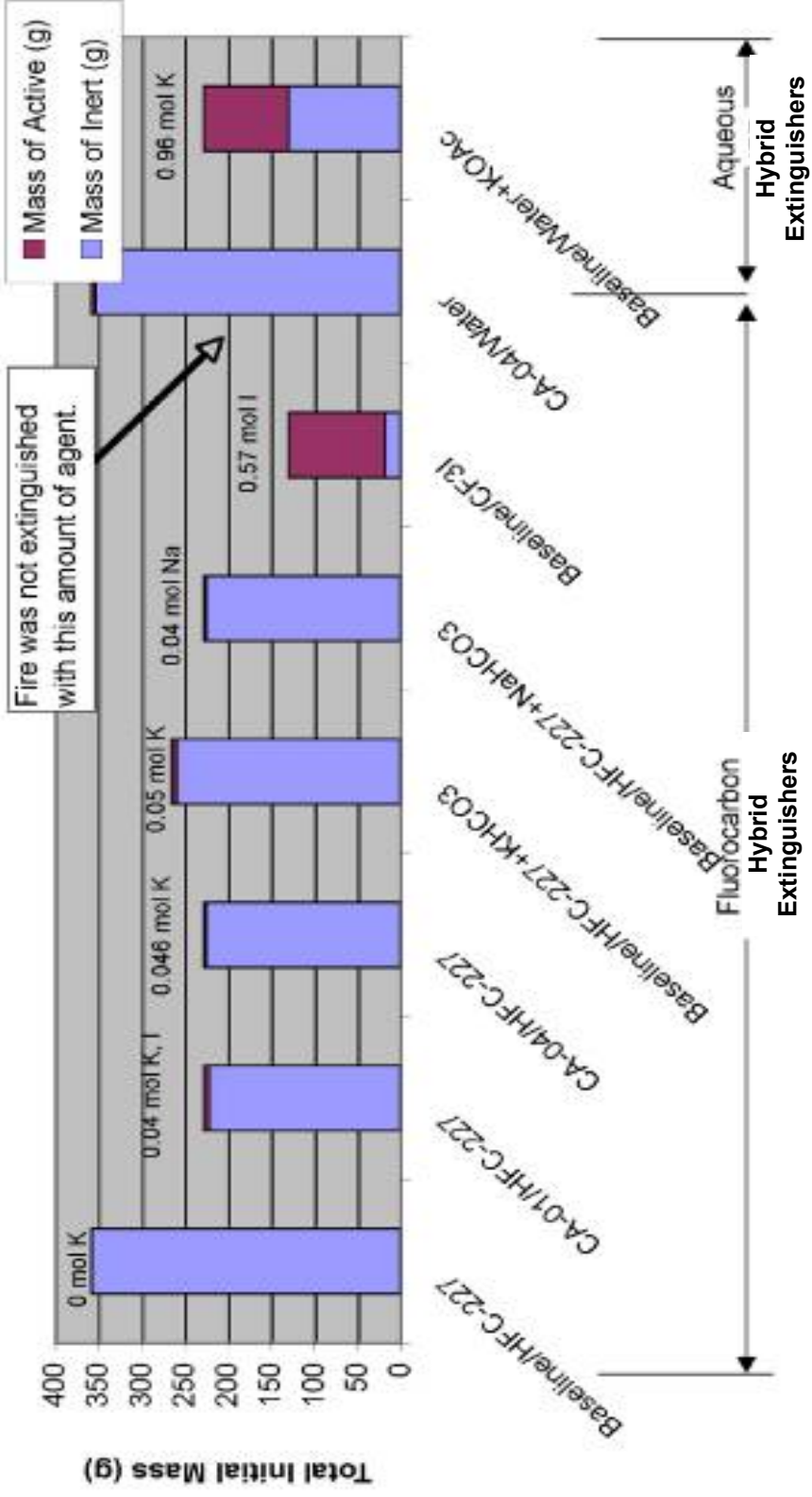


Figure 9-59. Effectiveness of Various Hybrid Extinguisher Propellant/fluid Combinations.

### 9.3.8 Summary of Solid Propellant Gas Generator Research

The Aerojet/NAWSC/NGP advances in solid propellant-based fire suppression technology include:

- Developing a methodology for screening candidate propellants.
- Developing a medium scale Fire Test Facility to evaluate alternative SPGG fire suppression technologies for a cluttered space such as a dry bay or engine nacelle.
- Scaling up the production of the high nitrogen propellant fuel, BTATZ, to half kilogram quantities.
- Calculating exhaust temperature and composition of new, high nitrogen propellants.
- Measuring burning rate and pressure exponent for these new, high nitrogen propellants.
- Tabulating the effect of different coolants on the effect of propellant burning rate and exhaust temperature.
- Examining the effect of various halogen, alkali, and iron compounds on fire suppression effectiveness of SPGG fire extinguishers.
- Determining the effectiveness of SPGG hybrid fire extinguishers using fluorocarbon and aqueous fluids.

Three different paths to cooler propellant compositions were demonstrated: by reducing the enthalpy of the combustion process through selection of various fuels/oxidizer blends; by altering the stoichiometry of the propellant reactions; and by seeking faster-burning solid propellant compositions, to which one could add coolant to reduce the overall exhaust gas temperature. Cooler propellant compositions have been used in conjunction with chemically active additives, or combustion radical scavengers. Adding radical traps to the exhaust provides means for cooling, dilution and chemical termination of the combustion process, hence increasing the overall effectiveness of the fire suppressant.

Propellant formulations incorporating the new high nitrogen compound BTATZ ( $C_4H_4N_{14}$ ) appear to provide increased means for reducing propellant combustion temperatures. The preparation of BTATZ has progressed to the half kilogram scale. This increased production capability plus the attractive burn rate and pressure sensitivity of BTATZ formulations make them good candidates for future work, including re-formulation with additional chemical coolants, as well as suppression effectiveness testing in the FTF. Direct incorporation of coolant species into the propellant composition reduced exhaust temperatures by as much as 30 % vs. current baselines.

Testing of propellant compositions containing potassium iodide and potassium carbonate as chemically active additives demonstrated enhanced effectiveness in the FTF as compared to chemically inert compositions. FTF testing with various inert and chemically active solid propellant compositions demonstrated that incorporation of 0.1 mole % additives into inert fire suppressants can have a dramatic effect upon suppression efficiency. The otherwise similar propellant compositions examined during this testing indicated a 50 % to 70 % reduction (by mass) of agent loading for suppression. On an equimolar basis, potassium carbonate appears to be a more effective chemical additive than potassium iodide. The greater effectiveness of potassium carbonate (vs. potassium iodide) may be related to more facile vaporization of the carbonate-based species after melting, or to an antagonistic interaction between the halogen and alkali metal species in the flame region.

Fire testing with chemically active compositions indicate that the CA-04 composition (20 % 5AT, 34 %  $\text{Sr}(\text{NO}_3)_2$ , 36 %  $\text{MgCO}_3$ , 10 %  $\text{K}_2\text{CO}_3$ ) is the most effective. This composition is three times more effective per unit mass than the inert baseline propellant (22 % 5AT, 19 %  $\text{Sr}(\text{NO}_3)_2$ , 60 %  $\text{MgCO}_3$ ), with no  $\text{K}_2\text{CO}_3$ . Testing with compositions of lower active-agent loading resulted in less effective performance. This indicates that the additive loading in CA-04 is below (or at) the saturation level reported in sub-scale testing with numerous other chemically active suppressants.

Testing of hybrid SPGGs with HFE-1230 indicates that high boiling point, low vapor pressure agents can be delivered efficiently to the fire zone by heating and pressurizing the liquid with an SPGG. Suppression tests with HFE-7100 were not as encouraging, and in fact resulted in flashback in fire tests. Both the HFE-1230 and HFC-227ea gave comparable results (on a mass basis) in fire suppression tests. Incorporation of  $\text{CF}_3\text{I}$  into a hybrid extinguisher proved convenient for overcoming poor cold-temperature dispersion. The water-based hybrid extinguishers did not perform as well as the fluorocarbon-based hybrid extinguishers; however, blending potassium acetate into the water was shown to significantly improve suppression effectiveness in the FTF.

On a mass basis, the inert hybrid extinguisher and SPGG systems appear to provide similar suppression protection. Incorporation of chemically active species into the hybrid extinguisher propellant improves the suppression efficiency. Testing conducted with additives incorporated into the hybrid fluid of the system produced results similar to results with active agents added into the propellant. This indicates that active additives in the hybrid fluid may be just as effective as active additives in the propellant.

Since initiation of this research in 1999, when inert SPGGs were installed in the first V-22 and F/A-18 dry bay fire protection systems, gas generator devices using advanced propellants and advanced additives have been demonstrated, developed and manufactured for three new platforms.<sup>56,57</sup> Developments in improved, chemically active SPGGs are being implemented over the course of 2005-2008 on the JSF F-35 dry bay fire protection system. Testing in 2005 validated the effectiveness of chemically active HFC-227ea hybrid devices in suppressing fires from ballistic events upon the US Army's M1114 HMMWV.

Figure 9-60 summarizes how the performance of SPGGs, as measured by suppression effectiveness, has improved over this period. This research has enabled system mass reductions by over a factor of two, with still greater reductions possible by optimizing the findings.

Finally, SPGG technology has also crossed over from military to civilian applications. Devices using chemically active, water-based hybrid extinguishers have moved from development to production and integration in commercial automobiles manufactured for the Ford Motor Company's Crown Victoria Police Interceptor.<sup>58</sup> A conceptual flow of this evolution and application is presented in Figure 9-61. (Note that in Figure 9-60 and Figure 9-61, the term "SPFE" for Solid Propellant Fire Extinguisher is used to distinguish these systems from a Hybrid Fire Extinguisher or "HFE.")

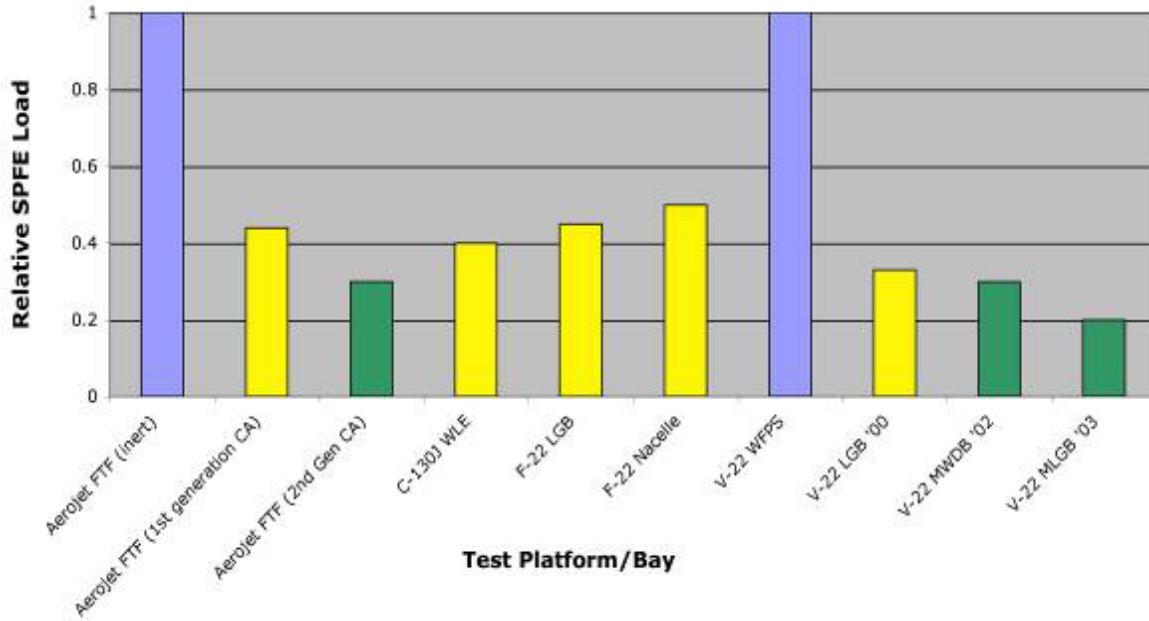


Figure 9–60. Relative Effectiveness of Various SPGG Fire Extinguishers over the Span of the NGP Research. Blue bars: inert effluent; yellow bars: 1<sup>st</sup> generation Chemically Active Systems; green bars: 2<sup>nd</sup> generation Chemically Active Systems.

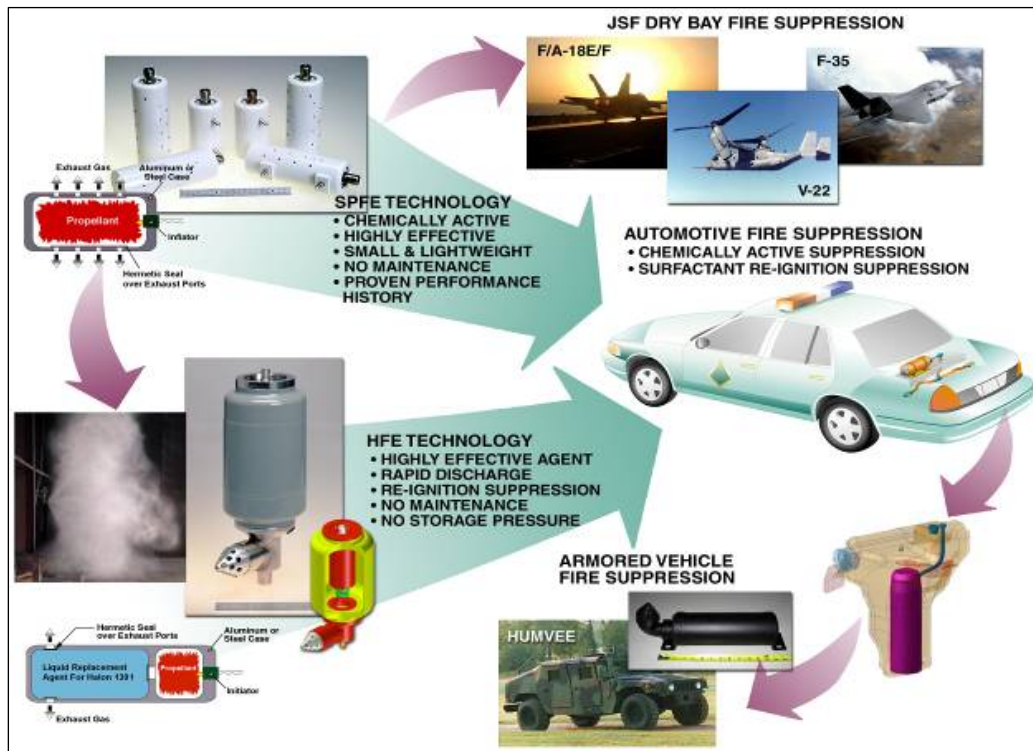


Figure 9–61. Evolution of SPGG Fire Suppression Application Technologies.

## 9.4 REFERENCES

1. Cyphers, D.C., *Enhanced Powder Panels: Final Technical Report*, report SKY-03-01, Skyward, Ltd, Dayton OH, December 2003.
2. Cyphers, D.C., Frederick, S.A., and Haas, J.P., "Enhanced Powder Panels," 2002, in Gann, R.G., Burgess, S.R., Whisner, K.C., and Reneke, P.A., eds., *Papers from 1991-2006 Halon Options Technical Working Conferences (HOTWC)*, CD-ROM, NIST SP 984-4, National Institute of Standards and Technology, Gaithersburg, MD, (2006).
3. Cyphers, D.C., Frederick, S.A., and Haas, J.P., "Demonstrating Enhanced Powder Panels," 2003, in Gann, R.G., Burgess, S.R., Whisner, K.C., and Reneke, P.A., eds., *Papers from 1991-2006 Halon Options Technical Working Conferences (HOTWC)*, CD-ROM, NIST SP 984-4, National Institute of Standards and Technology, Gaithersburg, MD, (2006).
4. Seymour, T.J. and Ellenwood, P.S., *Powder Pack Fire Protection for Aircraft Dry Bays*, AFWAL-TR-84-3119, June 1985.
5. Pascal, A., *B-1B LFT&E Dry Bay Fire Test Series Data Analysis*" (U), Enthalpy Corporation, June 1997.
6. Finnerty, A.E., Vande Kieft, L.J., and Drysdale, A., *Physical Characteristics of Fire-Extinguishing Powders*, ARL-TR-1450, Army Research Laboratory, August 1997.
7. Ewing, C.T., Highes, J.T., and Carhart, H.W., "The Extinction of Hydrocarbon Flames Based on the Heat-absorption Processes That Occur in Them," *Fire and Materials* **8**, 148-156, (1984).
8. Dolan, J.E., "The Suppression of Methane/Air Ignitions by Fine Powders," *Proceedings of the Combustion Institute* **6**, 787-801, (1957).
9. Altman, R.L., Teng, A.C., Mayer, L.A. and Myronuk, D.J., *Development and Testing of Dry Chemicals in Advanced Extinguishing Systems for Jet Engine Nacelle Fires*, Report JTCG/AS-82-T-002, Joint Technical Coordinating Group for Aircraft Survivability, 1983.
10. Finnerty, A.E., and Vande Kieft, L.J., "Powders as Halon Replacements," 1997, in Gann, R.G., Burgess, S.R., Whisner, K.C., and Reneke, P.A., eds., *Papers from 1991-2006 Halon Options Technical Working Conferences (HOTWC)*, CD-ROM, NIST SP 984-4, National Institute of Standards and Technology, Gaithersburg, MD, (2006).
11. Fischer, G., and Leonard, J.T., *Effectiveness of Fire Extinguishing Powders Based on Small Scale Suppression Tests*, NRL/MR/6180-95-7778, Naval Research Laboratory, October 19, 1995.
12. Jagers, Jerry F., *Development of Powder-Filled Structural Panels for AH-1S Fuel Fire Protection*, USAAVRADCOTR-81-D-32, Bell Helicopter Textron, October 1981.
13. Peregino II, P.J., Finnerty, A.E., Adkins, T., McGill, R., Cline, T., Gault, W., and Saunders, D., *Fire Protection for External Fuel Cells*, ARL-MR-413, U.S. Army Research Laboratory, October 1998.
14. Finnerty, A.E. and Polyanski, S., *Powder Packs – A Passive Approach to Extinguishing Fire in Combat Vehicles*, Technical Report BRL-TR-3191, U.S. Army Ballistic Research Laboratory, January 1991.
15. Finnerty, A.E., and Dehn, J.T., *Alternative Approaches to Fuel-Fire Protection for Combat Vehicles*, ARL-TR-377, U.S. Army Research Laboratory, April 1994.
16. Finnerty, A.E., McGill, R.L., Slack, W.A., and Saunders, D.M., *Fuel Cells in a Composite Armored Vehicle*, ARL-TR-1911, March 1999.

17. Pedriani, C.M., Ballistic Testing of Advanced Fire Suppression Systems Designed to Protect Helicopter Fuel Tanks from 23mm High Explosive Incendiary-Tracers (HEI-T), USAAVRADCOTM 80-D-3, February 1980.
18. Jagers, J. Fox, R., Johnson, J., and Liardon, D., *Development of Survivability and Vulnerability Improvement Modifications (SAVIM) for the AH-1S Helicopter, Appendix C – Vulnerability Analysis and Crew Protection*, USAAVRADCOTR-81-D-29, Bell Helicopter Textron, May 1982, CONFIDENTIAL.
19. Kiser, B. L., *Helicopter SAVIM Advanced Development Program*, USAAVSCOM TR-84-D-14, Bell Helicopter Textron Inc., October 1984.
20. Keane, C.A., *Vulnerability Reduction Technology for Rotary Wing Aircraft*, Master's Thesis, Naval Postgraduate School, June 1998.
21. Robaidek, M.F., *Aircraft Dry Bay Fire Protection*, AFWAL-TR-87-3032, Boeing Military Airplane Company, July 1987.
22. Pedriani, C.M., *Testing of Powder Packs and Powder-Filled Structures for Aircraft Fire Protection*, USAAVRADCOTR-82-D-12, JTCG/AS-81-T-002, July 1982.
23. Mercer, M., *A Ballistic Evaluation of Lightmass Void Fillers*, JTCG/AS-87-T-004, Naval Weapons Center, September 1987.
24. Finnerty, A.E., *Preliminary Evaluation of Powder Packs*, Memorandum Report BRL-MR-3641, Army Research Laboratory, December 1987.
25. Kolleck, M.L., *Halon Fire Protection Systems for Aviation - Existing System Configuration and Operational Environment Specifications*, Preliminary Report, prepared for Halon Replacement Program for Aviation Team, December 1992.
26. Manchor, J.A., *Reactive Powder Panel Ballistic Demonstration*, briefing, JTCG-AS Project V-1-04, NAVAIR (NAWCWD Code 418300D), January 2001.
27. Manchor, J.A., *V-1-04 Reactive Powder Panels*, briefing, JTCG-AS Project V-1-04, NAVAIR, September 2002.
28. Lundin, S.J., *Uncontained Engine Debris Tests - Fuselage Fire - Advanced Powder Panel Data CD-ROM*, NAVAIR and FAA, October 28, 2002.
29. Haas, J.P., Murphy, Jr., J.J., *C-130 Vulnerability Reduction Program/C-130J Live Fire Test Program Test Report, Phase IA - Wing Leading Edge Dry Bay Testing, (U)*, AAC TR 00-14, February 2001 (SECRET).
30. Fallis, S., Reed, R., McCormick, J.L., and Holland, G.F., "Advanced Propellant/Additive Development for Fire Suppressing Gas Generators: Development + Test," 2002, in Gann, R.G., Burgess, S.R., Whisner, K.C., and Reneke, P.A., eds., *Papers from 1991-2006 Halon Options Technical Working Conferences (HOTWC)*, CD-ROM, NIST SP 984-4, National Institute of Standards and Technology, Gaithersburg, MD, (2006).
31. *Advanced Propellant/Additive Development for Gas Generators*, Report Number D03008, Aerojet, Redmond, WA, March 2006.
32. Reed, R., Chan, M. L., and Moore, K. L., "Pyrotechnic Fire Extinguishing Method," U.S. Patent No. 4,601,344; 1986.
33. Galbraith, L. D., Holland, G. F., Poole, D. R., and Mitchell, R. M., "Apparatus for Suppressing a Fire," U.S. Patent No. 5,423,384; 1995.

34. Galbraith, L.D., "Apparatus & Method for Suppressing a Fire," U.S. Patent No. 5,449,041, 1995.
35. Galbraith, L.D., Holland, G.F., Poole, D.R., and Mitchell, R.M., "Apparatus for Suppressing a Fire," U.S. Patent No. 5,613,562, 1997.
36. Holland, G.F., Wilson, M.A., "Chemically Active Fire Suppression Composition," U.S. Patent No. 6,024,889, 1998.
37. Wucherer, E.J., and Holland, G.F., "Chemically Active Fire Suppressants and Device," U.S. Patent No. 6,217,788, 2001.
38. Williams, B., Wheatley, B., Neidert, J., Lynch, R., and Martin, R., "Fire Suppressant," U.S. Patent No. 6,045,726, 2000.
39. Scheffe, R., Neidert, J., Black, R., Lynch, R., and Martin, R., "Fire Suppressant Compositions," U.S. Patent No. 6,277,296, 2001.
40. Cruise, D.R., *Theoretical Computations of Equilibrium Compositions, Thermodynamic Properties, and Performance Characteristics of Propellant Systems*, NWC TP-6037, Naval Weapons Center, China Lake, CA, 1979.
41. Holland, G., Aerojet Report 98-R-2134, 1998.
42. Grosshandler, W., Gann, R., and Pitts, W., eds, "Evaluation of Alternative In-flight Fire Suppressants for Full-scale Testing in Simulated Aircraft Engine Nacelles and Dry Bays," NIST SP 861, National Institute of Standards and Technology, Gaithersburg, MD, April 1994.
43. Grosshandler, W., Donnelly, M., Charagundla, S.R., and Presser, C., "Suppressant Performance Evaluation in a Baffle-stabilized Pool Fire," 1999, in Gann, R.G., Burgess, S.R., Whisner, K.C., and Reneke, P.A., eds., *Papers from 1991-2006 Halon Options Technical Working Conferences (HOTWC)*, CD-ROM, NIST SP 984-4, National Institute of Standards and Technology, Gaithersburg, MD, (2006).
44. Grosshandler, W., Hamins, A., Charagundla, S.R., and Presser, C., "Suppression Effectiveness Screening for Impulsively Discharged Agents," 2000, in Gann, R.G., Burgess, S.R., Whisner, K.C., and Reneke, P.A., eds., *Papers from 1991-2006 Halon Options Technical Working Conferences (HOTWC)*, CD-ROM, NIST SP 984-4, National Institute of Standards and Technology, Gaithersburg, MD, (2006).
45. Fallis, S., Reed, R., McCormick, J.L., Wilson, K.A., and Holland, G.F., "Advanced Propellant/Additive Development for Fire Suppressing Gas Generator: Hybrids," 2001, in Gann, R.G., Burgess, S.R., Whisner, K.C., and Reneke, P.A., eds., *Papers from 1991-2006 Halon Options Technical Working Conferences (HOTWC)*, CD-ROM, NIST SP 984-4, National Institute of Standards and Technology, Gaithersburg, MD, (2006).
46. Manchor, J., "Aerojet Active Chemical Gas Generator (ACGG) Testing (August 4-7, 2003)," Internal White Paper, Naval Air Systems Command Survivability Division, 2003.
47. Manchor, J., "Aerojet Chemical Gas Generator Mid-Wing Testing (September 22-24, 2003)," Internal White Paper, Naval Air Systems Command Survivability Division, 2003.
48. Sutton, G., and Biblarz, O., *Rocket Propulsion Elements*, 7th ed. John Wiley & Sons, Inc. New York 2001.
49. Chavez, David E.; Hiskey, Michael A., "1,2,4,5-Tetrazine-based Energetic Materials," *Journal of Energetic Materials* **17**(4), 357-377 (1999)..
50. Chavez, David E.; Hiskey, Michael A.; Naud, Darren L., "Tetrazine Explosives," *Propellants, Explosives, Pyrotechnics*, **29**(4), 209 -215, (2004).

51. Linteris, G.T., Rumminger, M.D., and Babushok, V.I., "Premixed Carbon Monoxide-Nitrous Oxide-Hydrogen Flames: Measured and Calculated Burning Velocities with and without  $\text{Fe}(\text{CO})_5$ ," *Combustion and Flame* **122**, 58-75 (2000).
52. Patnaik, P., *Handbook of Inorganic Chemicals*, Knovel.com, 2003.
53. Lide, David R. ed. *Handbook of Chemistry and Physics*, 73rd edition, Taylor & Francis, New York, 1993.
54. Aerojet Internal Research and Development Report, H00016 (Proprietary to Aerojet)
55. Yang, J.C., Nyden, M.R., and Manzello, S.L., "Cold Discharge of  $\text{CF}_3\text{I}$  in a Simulated Aircraft Engine Nacelle," 2001 in Gann, R.G., Burgess, S.R., Whisner, K.C., and Reneke, P.A., eds., *Papers from 1991-2006 Halon Options Technical Working Conferences (HOTWC)*, CD-ROM, NIST SP 984-4, National Institute of Standards and Technology, Gaithersburg, MD, (2006).
56. Wierenga, P.H., and Holland, G.F., "Developments in and Implementation of Gas Generators for Fire Suppression," 1999, in Gann, R.G., Burgess, S.R., Whisner, K.C., and Reneke, P.A., eds., *Papers from 1991-2006 Halon Options Technical Working Conferences (HOTWC)*, CD-ROM, NIST SP 984-4, National Institute of Standards and Technology, Gaithersburg, MD, (2006).
57. Wierenga, P.H., "Further Advances in the Development of Hybrid Fire Extinguisher Technology," 2000, in Gann, R.G., Burgess, S.R., Whisner, K.C., and Reneke, P.A., eds., *Papers from 1991-2006 Halon Options Technical Working Conferences (HOTWC)*, CD-ROM, NIST SP 984-4, National Institute of Standards and Technology, Gaithersburg, MD, (2006).
58. Dierker, J.B., Jr., Thompson, R.H., Wierenga, P.H., and Schneider, M.A., "Fire Suppression System Development for the Ford Crown Victoria Police Interceptor," 2005, in Gann, R.G., Burgess, S.R., Whisner, K.C., and Reneke, P.A., eds., *Papers from 1991-2006 Halon Options Technical Working Conferences (HOTWC)*, CD-ROM, NIST SP 984-4, National Institute of Standards and Technology, Gaithersburg, MD, (2006).